(4)

RADC-TR-89-91
Interim Report
June 1989

PERFORMANCE OF FOUR RAKE MODEMS OVER THE NON-DISTURBED WIDEBAND HF CHANNEL

MITRE Corporation

Dr. Phillip A. Bello

ROME AIR DEVELOPMENT CENTER
Air Force Systems Command
Griffiss Air Force Base, NY 13441-5700

UNCLASSIFIED

SECURITY CLASSIFICATION OF THIS PAGE

REPORT DOCUMENTATION PAGE

Form Approved OMB No 0704-0188

1a. REPORT SECURITY CLASSIFICATION UNCLASSIFIED	1b. RESTRICTIVE MARKINGS N/A
2a. SECURITY CLASSIFICATION AUTHORITY N/A	3. DISTRIBUTION/AVAILABILITY OF REPORT Approved for public release; distribution unlimited.
2b. DECLASSIFICATION/DOWNGRADING SCHEDULE N/A	
4. PERFORMING ORGANIZATION REPORT NUMBER(S) MTR 10445	5. MONITORING ORGANIZATION REPORT NUMBER(S) RADC-TR-89-91
6a. NAME OF PERFORMING ORGANIZATION MITRE Corporation 6b. OFFICE SYMBOL (If applicable) D-90	7a. NAME OF MONITORING ORGANIZATION Rome Air Development Center (DCCD)
6c. ADDRESS (City, State, and ZIP Code) Bedford MA 01730	7b. ADDRESS (City, State, and ZIP Code) Griffiss AFB NY 13441-5700
8a. NAME OF FUNDING/SPONSORING ORGANIZATION Electronic Systems Division 8b. OFFICE SYMBOL (If applicable) XP	9. PROCUREMENT INSTRUMENT IDENTIFICATION NUMBER F19628-86-C-0001
8c. ADDRESS (City, State, and ZIP Code) Hanscom AFB MA 01731-5000	10. SOURCE OF FUNDING NUMBERS PROGRAM ELEMENT NO: 62702F; PROJECT NO: MOIE; TASK NO: 77; WORK UNIT ACCESSION NO: 90

11. TITLE (Include Security Classification)

PERFORMANCE OF FOUR RAKE MODEMS OVER THE NON-DISTURBED WIDEBAND HF CHANNEL

12. PERSONAL AUTHOR(S)
Dr. Phillip A. Bello

13a. TYPE OF REPORT	13b. TIME COVERED	14. DATE OF REPORT (Year, Month, Day)	15. PAGE COUNT
Interim	FROM Oct 87 TO Aug 88	June 1989	106

16. SUPPLEMENTARY NOTATION

This work was originally presented by Dr. Bello at MILCOM '88.

17. COSATI CODES			18. SUBJECT TERMS (Continue on reverse if necessary and identify by block number)
FIELD	GROUP	SUB-GROUP	Spread spectrum communications, Rake modems, LPI communications, wideband HF radio
25	02		

19. ABSTRACT (Continue on reverse if necessary and identify by block number)

The Rake Modem technique was proposed some thirty years ago by R. Price and P. Green as a means for combating multipath when direct sequence spread spectrum signals are transmitted. This report presents performance evaluations for four Rake modems used to communicate over the wide band (e.g., 1-MHz) HF channel. Attention is confined in this paper to performance for the non-disturbed HF channel. Consideration is given to the impact of mode Doppler shift and multipath spread due to dispersion. The effects of additive noise, self noise, and imperfect channel measurements are included. Results are presented for decision-directed, parallel-probe, serial-probe, and DPSK Rake modems. With a suitable codec, performance to within 1-3 dB of the additive white Gaussian noise channel at 10^{-5} error rate is predicted, depending upon the modem and the channel dispersion, if Doppler shifts of modes can be tracked to within 0.1 Hz.

20. DISTRIBUTION/AVAILABILITY OF ABSTRACT ☒ UNCLASSIFIED/UNLIMITED ☐ SAME AS RPT ☐ DTIC USERS	21. ABSTRACT SECURITY CLASSIFICATION UNCLASSIFIED
22a. NAME OF RESPONSIBLE INDIVIDUAL James B. McEvoy	22b. TELEPHONE (Include Area Code) (315) 330-3224 22c. OFFICE SYMBOL RADC (DCCD)

DD Form 1473, JUN 86 *Previous editions are obsolete.*

SECURITY CLASSIFICATION OF THIS PAGE
UNCLASSIFIED

TABLE OF CONTENTS

LIST OF ILLUSTRATIONS

LIST OF TABLES

SECTION 1
INTRODUCTION

A recent paper [1] considered various trade-offs in the use of spread spectrum communications over the wide band (e.g., 1-MHz) HF channel. It was concluded that direct sequence pseudo-noise (DSPN) spreading, with interference excision and adaptive matched filtering at the receiver, can provide an efficient communication technique, with links in the 1000–3000 km range being particularly favorable.

This report examines the effectiveness of four different Rake techniques as a means to achieve adaptive matched filtering of DSPN signals received over the wide band HF channel. The Rake technique was conceived by R. Price and P. Green over thirty years ago [2] as a means of combating multipath and was, in fact, built and tested over a narrowband (10 kHz) HF channel. Current technology makes viable the application of the Rake technique to the wide band HF channel.

The presence of strong narrowband interfering signals throughout the HF band requires that any DSPN wide band HF communication system employ a narrowband interference excisor preceding the data demodulation. Based upon actual interference measurements, it is shown in [3] that only a relatively small percentage of a 1-MHz band may need to be excised to achieve large improvements in signal-to-noise ratio (SNR). As long as the percentage of the band excised is small, the effect of the excisor on the DSPN signal is a small reduction in amplitude plus the creation of a small amount of self noise. However, this self noise will be negligible compared to the noise at the Rake combiner output. The performance analysis presented here does not include the effect of the excisor per sé, since it expresses performance in terms of the value of E_b/N_o (energy/bit/noise power density) at the input to the Rake processor. Any self noise due to the excisor is neglected and, in addition, the residual noise at the excisor output is assumed white. The validity of this latter assumption has not yet been established, although measurements at The MITRE Corporation, Bedford, MA facility do show an essentially white noise behavior at the excisor output.

Prediction of modem performance over the HF channel, wide band or not, is a difficult task due to the random and unpredictable nature of various HF channel parameters and to the lack of definitive statistical characterization of these parameters. As discussed further in section 2, we sidestep these issues by confining our performance calculations to non-overlapping, purely dispersive propagation modes and conditioning our calculations on specified mode strengths and Doppler shifts. Nonetheless, these results are useful in providing comparative modem performance results. In addition, once an adequate statistical description of mode strengths and Doppler shifts is available, the conditional results presented here may be *unconditioned* by averaging over these parameters.

Section 2 summarizes the wide band HF model used in the performance analysis and section 3 briefly describes the four Rake modems analyzed. Some performance results are presented in section 4. The detailed analysis supporting the results is presented in the appendix.

SECTION 2
CHANNEL MODEL

The HF propagation medium can be represented as a linear, randomly time-variant operation. From innumerable measurements and propagation analyses, it is known that the received HF signal can be expressed closely as the sum of contributions from one or more propagation modes (e.g., see [4]). Each propagation mode itself may be regarded as a time-variant linear operation. This linear operation will have different statistical structures, depending upon the ionospheric conditions in the corresponding layer. Thus, if the percentage change in electron density is small enough, the propagation is called *quiet* or *normal*, and a mode acts over a MHz bandwidth approximately like an all-pass filter with a somewhat nonlinear group delay vs. frequency, a slowly-changing mean time delay, complex amplitude, and Doppler shift. For path lengths in the 1000–3000 km range, and operations somewhat below the maximum useable frequency (MUF), the group delay is nearly linear vs. frequency and dispersions are usually not greater than 100 μs/MHz. Although Doppler shifts can be of the order of 1 Hz, this usually occurs at dawn or dusk. For shorter path lengths these numbers increase. When the electron density fluctuations become sufficiently large, the mode acts like a scatter-type channel with an associated Doppler spread and a multipath spread caused by random fluctuations of received energy over a range of path delays. The mode may then be called *disturbed.* Doppler spreads of tens of Hz and multipath spreads of tens of milliseconds may occur in extreme cases. Such variations in mode properties with the degree of electron density fluctuations have been discussed by Booker et al [5][6] for the F layer.

For the purpose of our analysis, the channel per sé must be regarded as a composite filter consisting of the cascade of all transmitter filtering operations, the HF propagation medium, and all receiver filtering operations. This view makes clear that the ability to resolve propagation modes depends not only on how close these modes are in propagation delay, but also on the impulse response duration of the transmitter and receiver filters. In evaluating the performance of the Rake modem, it is useful to place the wide band HF channel into one of the following categories:

(a) non-overlapping, purely dispersive propagation modes

(b) partially overlapping, purely dispersive propagation modes

(c) scatter type or combination scatter/dispersive propagation modes.

Case (a) is the category that corresponds, ideally, to the use of wide band HF under normal, i.e., non-disturbed HF propagation conditions. All modes are resolvable and have complex amplitudes that vary very slowly and do not fade deeply (e.g., time constants exceeding 10 seconds and a few dB fade depth). However, Doppler shifts exist with values that may be as large as 1 Hz for long paths, particularly close to evening

or daybreak. Error correction coding can be used with great benefit for this case.* Also, Doppler shift correction of individual modes is a distinct possibility, allowing long averaging times in the Rake processor and a resulting performance improvement at high Doppler shifts.

Case (b) applies to the non-disturbed HF channel also, but includes the likelihood that some mode overlap may occur under special propagation conditions. E.g., the 2-hop E layer may come close to the 1-hop F_2 layer on summer afternoons. For those multipath components in which the modes overlap, fluctuation in the impulse response will occur at the Doppler difference between modes. If the energy in these fluctuating components is small compared to the non-overlapping components, little performance loss will result for a system designed as if Case (a) applied. However, the use of interleaving in addition to coding would provide some protection in the event that the fading energy is high. Doppler shift correction would have limited benefit for the overlap paths.

Case (c) applies to the disturbed HF channel. Interleaving and coding can provide benefits here. The statistical model for the mode is quite different from that of Cases (a) and (b). A useful model here would be the complex Gaussian WSSUS (wide-sense-stationary uncorrelated scattering) model [7].

In the performance analysis it was assumed that the transmitter filter limited the transmission bandwidth W to a value of $1/\Delta$, where $1/\Delta$ is the chip rate and Δ is the chip duration. This degree of filtering stretches the impulse response of the composite channel filter slightly, but does not degrade the performance of the system due to the Rake processor. With this bandwidth limitation, it is possible to represent the composite channel by means of a tapped delay line with taps spaced Δ apart [7]. This representation is shown in figure 1. The transmitted signal is represented as an impulse train with areas $a_q m_q$ transmitted at the rate $1/\Delta$, where a_q is the chip modulation and m_q is the data modulation. In this paper we confine our attention to binary phase shift keying (BPSK) data and chip modulation. The i-th complex weight in figure 1 is given by

$$b_i(t) = h(t, i\Delta) \tag{2-1}$$

where $h(t, \xi)$ is the time variant impulse response of the composite channel. A maximum delay of $M\Delta$ is shown (M+1 taps) to accommodate the multipath spread of the channel. The model in figure 1 is applicable to Cases (a), (b), and (c) discussed above, the difference appearing in the behavior of the complex tap weights $\{b_i(t)\}$. At the channel output a sampler is shown representing a (complex) A/D conversion operation at a rate of $1/\Delta$.

*A phenomenon called *twinkling* by Booker et al. [5] [6] can occur in the transition from Cases (a) and (b) to Case (c). Then the shallow fading becomes modified by the introduction of a superimposed slow random modulation with occasional deep fades. Interleaving may make the use of coding effective during twinkling.

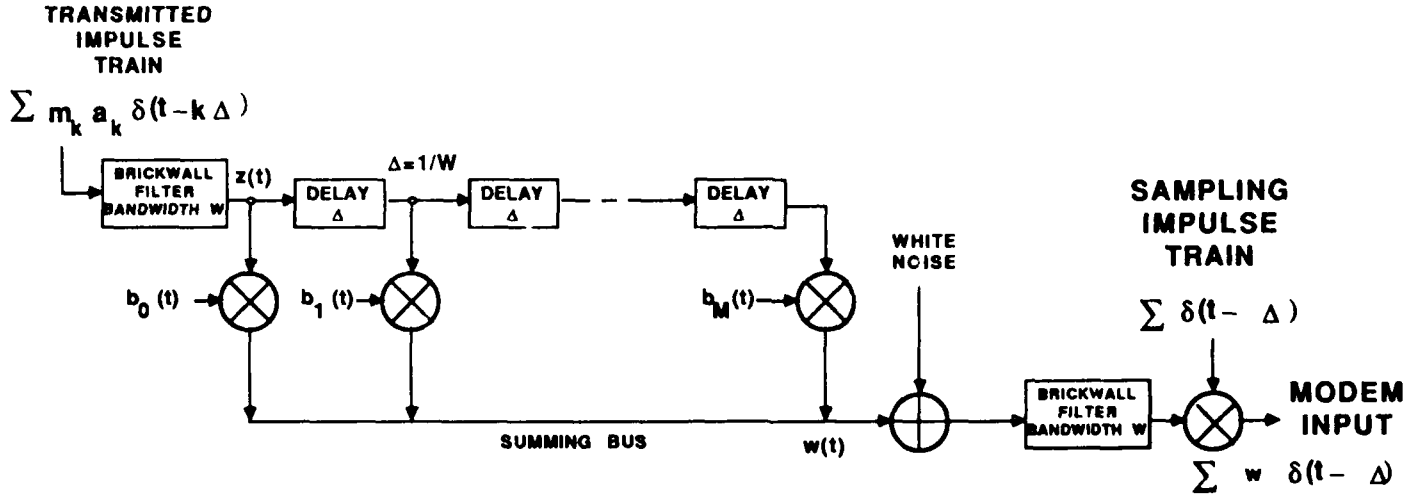

Figure 1. Formulation of Modem Input Using Tapped Delay Line Model of Composite Channel

SECTION 3
RAKE MODEMS

The transmitted signal consists of a sequence of spread spectrum data symbols containing ± 1 (BPSK) modulation according to the output of the binary encoder. Each symbol is random appearing, being spread in bandwidth with ± 1 chip modulation at the rate $1/\Delta$. If we ignore intersymbol interference and assume that the fading is slow compared to the sum of the multipath spread of the channel and the data symbol time duration, a matched filter for the received symbol followed by a sampler provides a minimum error probability demodulator for white Gaussian noise (e.g., see [8]). Ignoring intersymbol interference will cause little error since the spread spectrum processing gain reduces this interference to negligible proportions. The slow fading assumption will be assumed valid in this analysis. It is not known whether the residual noise at the excisor output may be modeled as Gaussian. However, in any case, the matched filter maximizes the output SNR even when the noise is non-Gaussian but white.

The Rake technique attempts to construct a filter matched to each received symbol. This matched filter can be decomposed into the cascade of a filter matched to the transmitted symbol and a filter matched to the channel. In addition, the matched filter/sampler operation can be re-interpreted as a correlation operation. Moreover, various signal processing elements may be rearranged to simplify processing. Because of these variations, there are a large number of versions of the Rake technique. In this paper we examine that particular subclass of Rake techniques which appears in the form of a multipath diversity combiner. This structure can be shown to be a rearranged version of a Rake modem consisting of the cascade of tapped delay line channel-matching operation with a correlator-implemented signal-matching operation. The four techniques examined differ in the way the channel is measured to provide weights for the diversity combiner.

Figure 2 presents a block diagram of the decision-directed coherent Rake modem. In this version* the (complex) sampled input process is passed through a (shift-register) tapped delay line with R incremental delays of Δ. Then the input plus the R delayed versions of the input are correlated with a locally-generated, unmodulated PN sequence. The correlation operation involves conjugate multiplication followed by an integrate and dump (I&D) over successive groups of $N = T/\Delta$ samples, where T is the transmitted symbol duration. Each I&D output is multiplied by a complex tap weight and the results summed to produce the Rake complex combiner output (i.e., the channel matched filter output).

*Alternate versions exist in which the complex digital input and the local pseudo-noise (PN) sequence exchange positions or in which the input signal and reference are both delayed. See [9] for another version of a decision-directed modem in which the signal matching is done with a matched filter rather than a correlator.

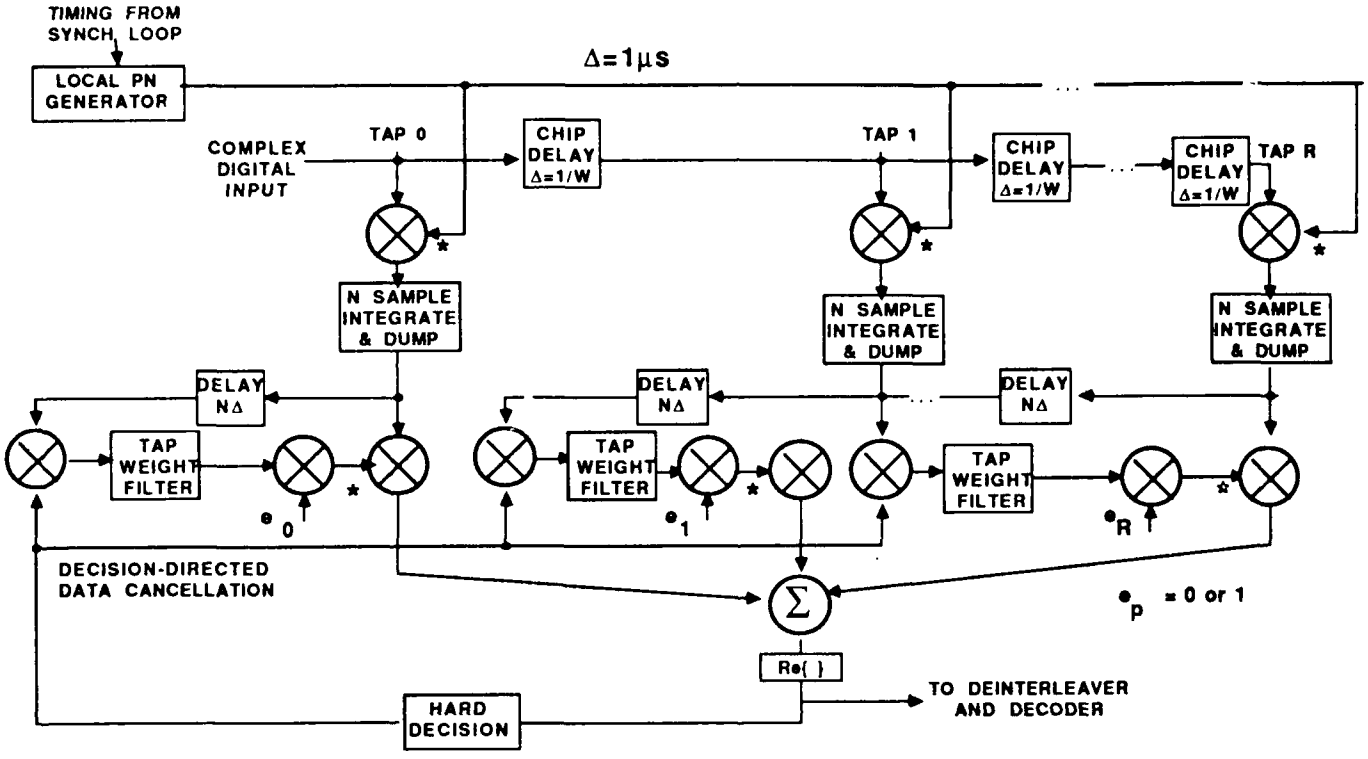

Figure 2. A Decision-Directed Coherent Rake Processor. No Delay Compensation

The real part is taken for BPSK demodulation. This output is fed to a hard decision device and also to a deinterleaver and decoder. The hard decisions are used in the tap weight processing as discussed below.

The tap weight measurement circuit shown in figure 2 is a decision-directed procedure in which an attempt is made to cancel the data modulation on the I&D output through feedback of hard data decisions (with a delay to compensate for an assumed decision delay of T). If the data modulation were cancelled, the noise-free component left would be proportional to the optimal weight for predetection diversity combining. Averaging with a long time constant digital filter can reduce the noise level sufficiently to make the combining effective. The tap weight filter output is shown multiplied by a factor e_p equal to 0 or 1. This factor is used to eliminate tap contributions which contain such weak signals that they will degrade output SNR. The processing to determine e_p is not shown.

Because of the existence of a group delay in the tap weight filter, plus the delay of T shown in the tap weight branch, Doppler shift produces a spurious phase shift in the tap weight that does not exist on the signal at the I&D output. This phase error will produce an SNR degradation at the coherent detector output. If a compensating delay could be introduced in the signal path ahead of the tap weight multiplication, the same spurious phase shift would be introduced on the signal component. Then the weighting process will remove the phase shift effect since the I&D output is multiplied by the complex conjugate of the tap weight. Figure 3 shows a method for introducing such a delay compensation in a decision-directed coherent Rake modem. Separate weighting and combining circuits are necessary for decision-directed data cancellation and delay-compensated data combining.

In the parallel-probe Rake modem, both a non-data modulated probe DSPN sequence and a statistically-independent, data-modulated DSPN sequence are transmitted. The received DSPN probe is used to estimate the tap weights for the Rake combiner. Figure 4 presents a block diagram of a parallel-probe Rake demodulator processor.* Two local PN generators are used to correlate against the received signal at each tap of the delay line. The probe correlator and the data correlator produce outputs at the I&D rate. A digital filter averages the probe I&D output to produce the tap weight as shown in figure 4. Note that because of the absence of the decision-directed operation, the compensating delay for minimizing the Doppler shift degradation can be inserted between the data I&D and the tap weighting.

The block diagram of a serial-probe coherent Rake demodulator is shown in figure 5. For this modem every P-th transmitted symbol is part of a data symbol subsequence known at the receiver. The tap gain measurement is conducted only with this subsequence, thus avoiding the use of decision-directed operation. Both the normal data

*An alternate version of a parallel-probe Rake modem was presented in [10].

symbol and the subsequence symbol epochs are obtained from the known starting state of the local PN generator in the same way they are obtained from the PN generator at the transmitter. An optional compensating delay is shown inserted in the signal path to minimize the phase error in the complex tap gain produced by mean Doppler shift. Not shown is the fact that the data subsequence must be inserted after the coding and interleaving and deleted prior to de-interleaving and decoding.

The serial-probe coherent modem requires little additional hardware compared to the decision-directed coherent modem. In contrast, the parallel-probe modem requires a substantial increase in hardware. Moreover, the analyses show that the serial-probe modem performance is essentially identical to that of the parallel-probe modem when parameters are set properly.

The differential phase shift keying (DPSK) Rake modem processing is shown in figure 6. For this version of the Rake, the tap weights are simply the previous I&D outputs. No decision-directed data cancellation is necessary since the coded binary data at the transmitter modulates a binary phase change $(0°, 180°)$ onto the carrier. The analysis of this modem may be seen to be identical to a decision-directed Rake modem in which there are no decision errors and there is no tap gain filtering. Because of the noisier tap weights, the DPSK Rake will have additional SNR degradation. However, due to the small group delay in the tap weight path, the DPSK Rake technique will be less susceptible to Doppler shift and for high enough Doppler shift will be superior to the other modems.

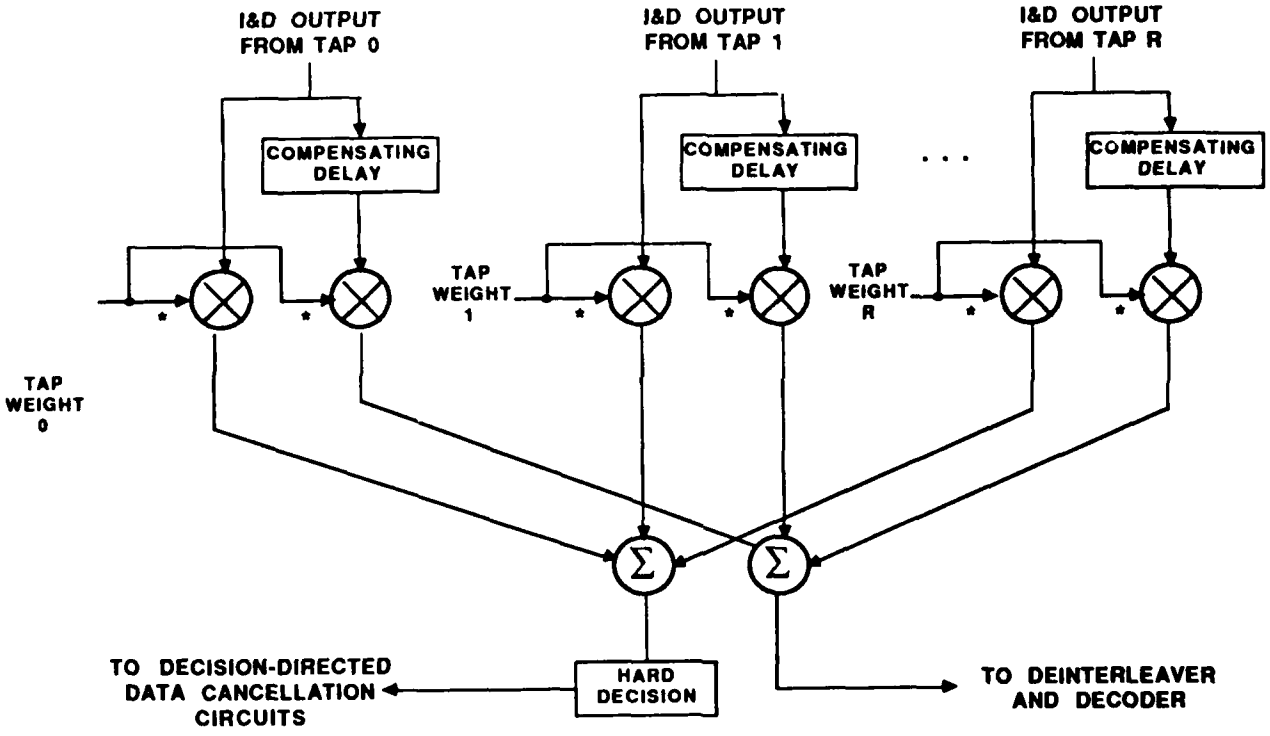

Figure 3. Use of Compensating Delay in Decision-Directed Coherent Rake Operation

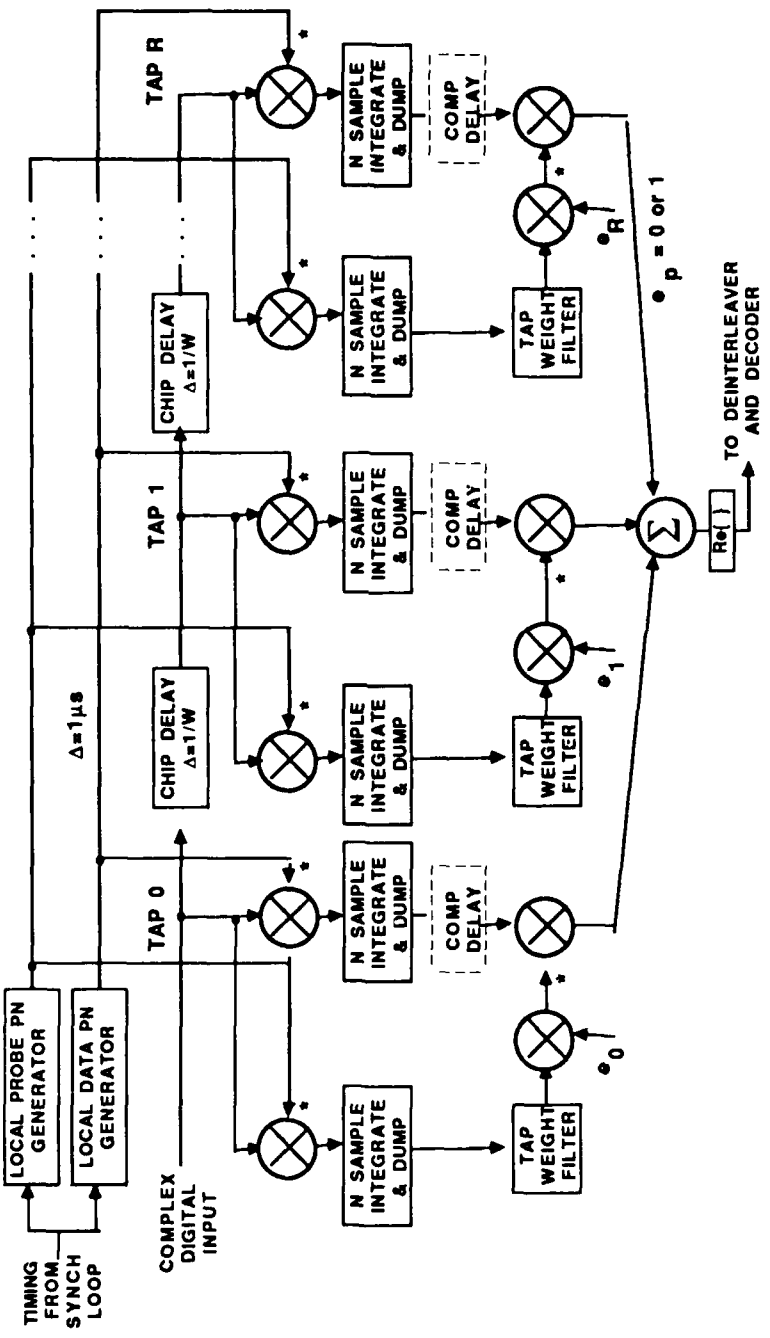

Figure 4. A Parallel-Probe Coherent Rake Processor

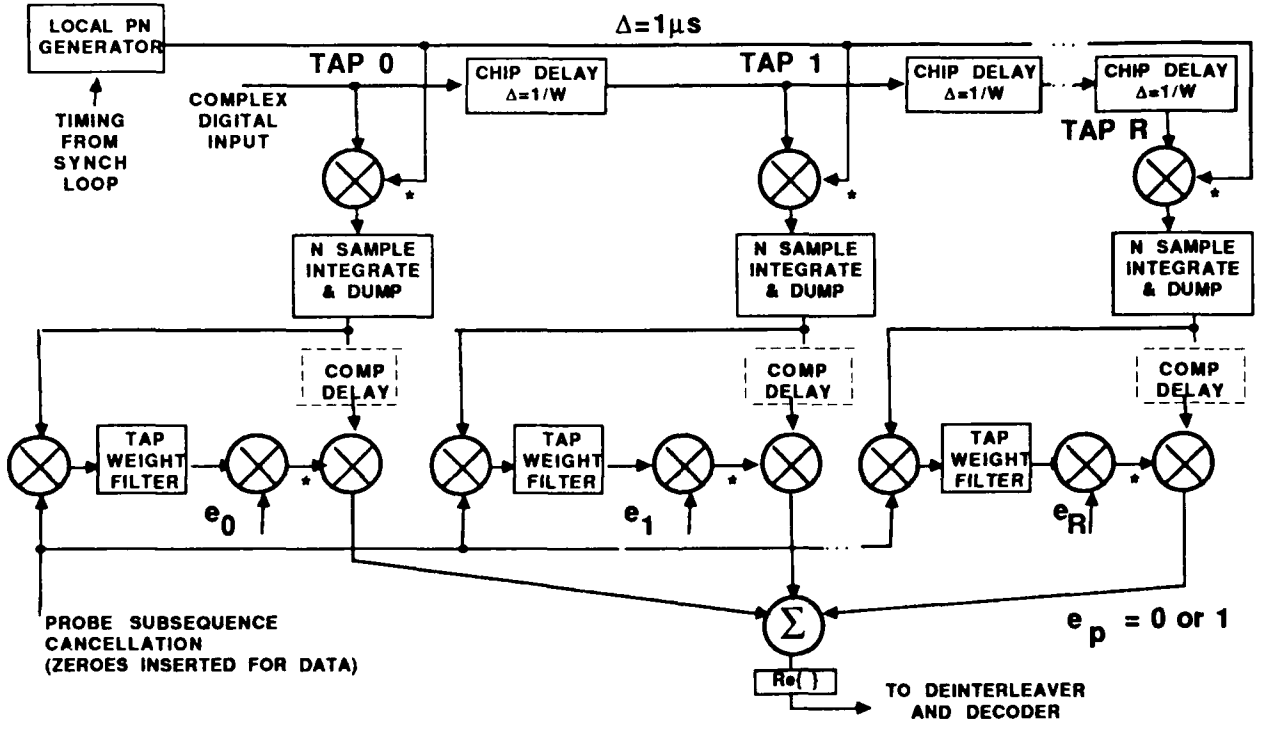

Figure 5. A Serial-Probe Coherent Rake Processor

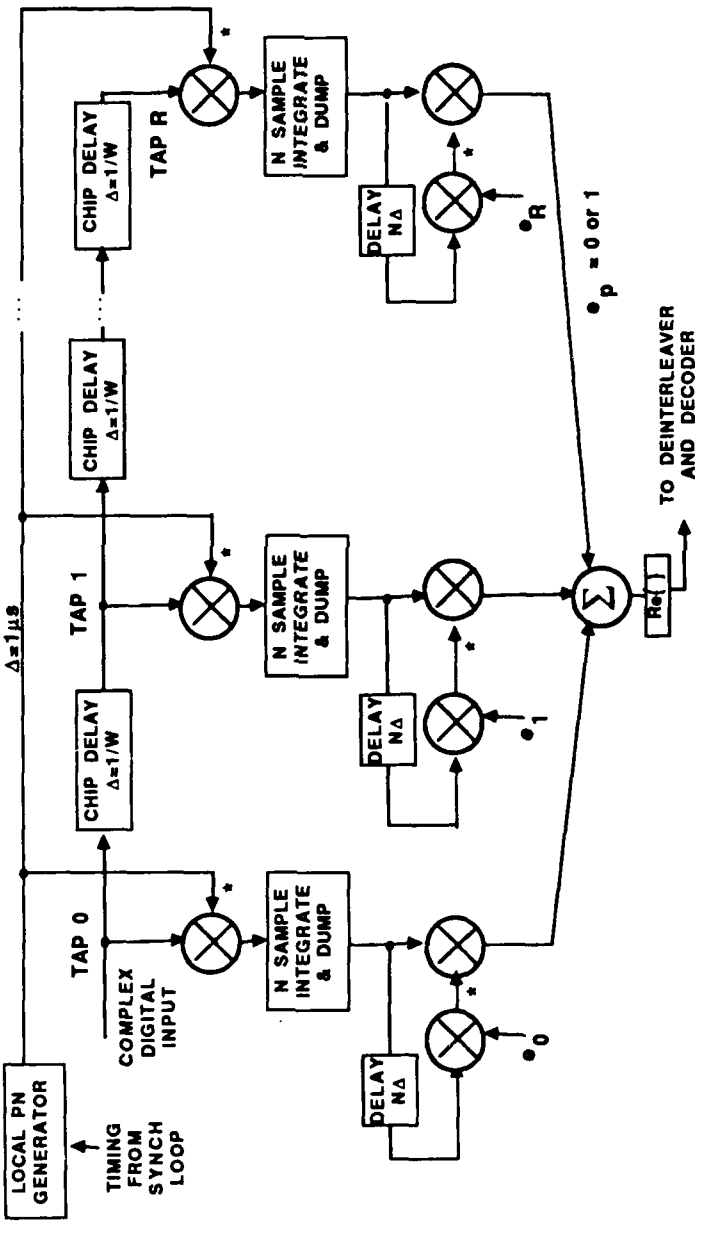

Figure 6. A DPSK Rake Processor

SECTION 4
PERFORMANCE

As mentioned in section 1, the performance analysis is confined here to the case of non-overlapping, purely dispersive propagation modes with the performance conditioned on the strengths and Doppler shifts of the modes. The analysis includes the effects of non-ideal tap weight measurements. Aside from the degrading effects of Doppler shifts, the tap weights are degraded by additive noise and by multipath-produced *self noise*. The correlation operation at the output of each delay line tap ideally selects the contribution from one multipath component (i.e., tap weight) of the tapped delay line channel model in figure 1 Due to the finite averaging time of the correlator, contributions appear from all other multipath components, but at a reduced level, producing a self noise.

In section A.4.3 of the appendix, an analysis is conducted to evaluate multipath self noise. It is found that if the Rake processor input SNR, ρ_i is small enough, the self noise can be neglected at the Rake combiner output in relation to the additive noise contributions. Specifically, it is shown that if

$$\rho_i \ll w/2 \tag{4-1}$$

self noise may be neglected, where the parameter

$$w = \frac{R_o}{\sum_s |R_s|^2} \tag{4-2}$$

in which R_s is the discrete autocorrelation function of the composite channel sampled impulse response (see (2-1) and figure 1)

$$R_s = \sum_p b_p^*(t)\, b_{p+s}(t) = \sum_p h^*(t, p\Delta)\, h(t, p\Delta + s\Delta)\ . \tag{4-3}$$

The parameter w may also be expressed in the frequency domain as

$$w = \frac{\left[\frac{1}{W}\int_{-W/2}^{W/2} |H(f,t)|^2\, df\right]^2}{\frac{1}{W}\int_{-W/2}^{W/2} |H(f,t)|^4\, df} \tag{4-4}$$

where $H(f,t)$ is the composite channel transfer function (Fourier transform of $h(t,\xi)$). As may be seen from (4-2), w is upper-bounded by 1. For a single purely dispersive

propagation mode, w will be very nearly unity because the propagation medium will have a nearly constant magnitude over the 1-MHz transmission band. Multiple modes will cause w to become smaller than unity. Detailed numerical evaluations of w have not been carried out as of the writing of this report, but it does appear, based upon preliminary calculations, that w will not be very much less than unity for the wide band HF channel. Thus, if $\rho_i <<< 1$, it appears self noise may be neglected. The calculations presented here assume that inequality (4-1) is satisfied and self noise may be neglected.

In order to simplify the error rate calculations, it was assumed that the number of taps in the Rake combiner is much bigger than 1 so that one may use the Central Limit Theorem to justify normally distributed statistics for the combiner output. With such statistics, the SNR is the fundamental parameter in the determination of error rate. Thus, the hard decision error rate q (no decoding) is given by

$$q = \phi(\sqrt{\rho}) \tag{4-5}$$

where ρ is the combiner output SNR and

$$\phi(y) = \int_y^\infty \frac{1}{\sqrt{2\pi}} exp(-\frac{x^2}{2})\, dx \tag{4-6}$$

As shown in the appendix, for the decision-directed Rake with no decision errors and for the other three Rake techniques, the SNR at the Rake combiner output can be expressed in the generic form

$$\rho = \frac{(E_b/N_o)\, A^2}{B(\frac{C}{E_b/N_o} + 1) + D} \tag{4-7}$$

where E_b/N_o is the energy/bit/noise power density at the Rake processor input. See table 1 for a list of these parameters for the four Rake techniques and the definition of some fundamental system parameters ($Q, N_T, p_n, \nu_n, \gamma, P, T, g$, and $G(f)$).

Decision errors produce two kinds of degrading effects: a suppression of signal level and an introduction of additional noise. An approximate analysis of these effects (see A.4.4) yields the following expression for combiner output SNR

$$\rho = \frac{(E_b/N_o)\, A^2}{B(\frac{C}{E_b/N_o} + 1) + (\sigma^2 + (1-2q)^2)\, D + \sigma^2 (E_b/N_o)\, A^2} \tag{4-8}$$

where

$$\sigma^2 = 4 \sum \gamma_m (P_m - q^2) \tag{4-9}$$

and γ_m is the autocorrelation function of the discrete impulse response $\{\alpha_m; m = 0, 1, \ldots\}$ and P_m is the probability that a pair of hard decision errors occur spaced m symbols apart. It appears (4-8) will be most accurate for long integration times. Note that q, the hard decision error rate, is a function of ρ so that (4-8) is a nonlinear equation in ρ (or q). The values of ρ (and q) are solved first with no delay compensation ($g = 0$). Then (4-8) is evaluated using the appropriate value of g and the previously calculated value of q for $g = 0$, to obtain the combiner output SNR with delay compensation. The missing element in the above formulation is P_m. Calculations presented here assumed independent bit errors. However, it is expected that the decision feedback will produce error bursts. As a result the calculations will be optimistic.

Tables 2–4 present calculations of performance for the four Rake processors based upon (4-7) and (4-8). To simplify the presentation, the propagation modes were assumed to have the same Doppler shift. A constraint length 7 convolutional code with three-bit quantized soft decision Viterbi decoding was assumed with an information rate of 75 bits/second. The tables show the required value of E_b/N_o to achieve 10^{-5} decoded error rate for three values of Rake taps $N_T = 100, 50, 20$ and six values of Doppler shift $\nu = 0.1, 0.2, 0.4, 0.6, 0.8$ and 1.0 Hz. Since only as many Rake taps are used as are necessary to extract the significant multipath energy, one may regard the corresponding multipath spreads as not exceeding N_T μsec (assuming $\Delta = 1$ μsec).

The digital tap gain filter chosen was a boxcar shape. The memory or integration time of this filter was adjusted to minimize the required SNR at each Doppler shift, and for the parallel- and serial-probe cases, it was necessary to jointly optimize the probe power and the filter memory. For reference purposes, note that $E_b/N_o \approx 4.3$ dB is required to achieve 10^{-5} error rate for the codec with BPSK over the additive white Gaussian noise (AWGN) channel. In the case of the decision-directed modem, differential encoding and decoding were assumed to counteract the possible $(0°, 180°)$ ambiguity produced by the decision-directed operation. In this case $E_b/N_o \approx 4.6$ dB is required for 10^{-5} error rate over the AWGN channel.

It is interesting to note that the performances of the parallel and serial-probe modems are virtually identical. In fact, at the end of section A.5.2 it will be shown that when the relative power in the two probes and the time constant of the two tap weight filters are made the same, the resulting values of combiner output SNR will be nearly the same, assuming slow enough fading. The DPSK Rake modem is quite inefficient at the low Doppler shifts and even at 1 Hz it is 1.7 to 2.7 dB worse than the probe type modems, depending on the number of Rake taps. The decision-directed Rake shows somewhat better performance than the probe type modems (e.g., 0.7 to 1.5 dB depending upon the number of Rake taps and the Doppler shift). However this result is provisional until the impact of assuming independent decision errors is determined. The tables show that the potential benefits of correcting for mode Doppler shift are 2–3 dB, with the greatest benefit associated with the largest number of Rake taps. SNR

improvement can also be obtained by applying techniques for reducing the dispersion of individual modes and thus reducing the required number of Rake taps (i.e., 1.3–2.3 dB for the probe cases if a reduction from 100 to 20 μs dispersion were possible). The benefits of delay compensation are greater for the probe systems (1.0–1.5 dB) than the decision-directed system (0.3–0.7 dB). This is because of the increased degradation due to decision errors when the system attempts to operate at a larger value of q.

The optimum values of integration time are relatively insensitive to the number of Rake taps, N_T. Although the integration times are long for the low Doppler shifts (seconds), the curves of E_b/N_o vs. integration time have a broad minima at low Doppler shifts. Thus, a substantial decrease in integration time is possible without significantly increasing the required E_b/N_o.

TABLE 1

**PARAMETERS IN RAKE COMBINER OUTPUT SNR FOR FOUR RAKE MODEMS.
NON-OVERLAPPING, PURELY DISPERSIVE PROPAGATION MODES.
RAKE TAPS SELECTED TO ACCOMMODATE ALL SIGNIFICANT MULTIPATH.**

RAKE TECHNIQUE	A	B	C	D
DECISION-DIRECTED RAKE MODEM	$\sum_{n=1}^{Q} p_n \, Re\{G(\nu_n)\, e^{j2\pi\nu_n T(g-1)}\}$	$\sum \alpha_m^2$	$2\,N_T$	$\sum_{n=1}^{Q} p_n \, \lvert G(\nu_n)\rvert^2$
PARALLEL-PROBE RAKE MODEM	$\frac{1}{1+\gamma} \sum_{p=1}^{Q} p_r \, Re\{G(\nu_n)\, e^{j2\pi\nu_n Tg}\}$	$\frac{\sum \alpha_m^2}{\gamma}$	$2\,N_T(1+\gamma)$	$\sum_{n=1}^{Q} p_n \, \lvert G(\nu_n)\rvert^2$
SERIAL-PROBE RAKE MODEM	$\frac{P-1}{P} \sum_{p=1}^{Q} p_r \, Re\{G\big((P-1)\nu_n\big)\, e^{j2\pi\nu_n T\frac{P-1}{P}(g-P+1)}\}$	$\sum \alpha_m^2$	$2\,N_T\frac{P}{(P-1)}$	$\sum_{n=1}^{Q} p_n \, \lvert G\big((P-1)\nu_n\big)\rvert^2$
DPSK RAKE MODEM	$\sum_{n=1}^{Q} p_n \cos 2\pi\nu_n T$	1	$2\,N_T$	1

Q = number of modes
N_T = number of taps in Rake combiner
p_n = relative strength of r-th mode ($\sum_{n=1}^{Q} p_n = 1$)
ν_n = Doppler shift of n-th mode
γ = power in parallel probe relative to data power
P = subsequence period (in symbols) of serial probe
T = duration of integrate and dump for decision-directed system
gT = compensating group delay in data path
$G(f) = \sum \alpha_m \, e^{-j2\pi mfT}$, transfer function of discrete tap weight filter for decision-directed system

NOTE: THE VALUE OF g AND THE TAP GAIN FILTER TIME CONSTANT MUST BE SEPARATELY OPTIMIZED FOR EACH SYSTEM.

TABLE 2

MINIMUM REQUIRED VALUES FOR Eb/No AND CORRESPONDING OPTIMUM TAP WEIGHT FILTER MEMORY FOR 10^{-5} DECODED* BIT ERROR RATE (AT 75 BITS/SEC) VERSUS CHANNEL DOPPLER SHIFT. CALCULATIONS FOR DECISION-DIRECTED, PARALLEL-PROBE, SERIAL-PROBE, AND DPSK RAKE MODEMS

20 TAPS USED IN RAKE COMBINER

DOPPLER (Hz)	DECISION-DIRECTED RAKE MODEM		PARALLEL-PROBE RAKE MODEM			SERIAL-PROBE RAKE MODEM			DPSK RAKE MODEM
			JOINTLY OPTIMIZED			JOINTLY OPTIMIZED			
	OPTIMUM TAP WEIGHT INTEGRATION TIME (SEC)	Eb/No IN DB FOR 10^{-5} BIT ERROR PROBABILITY	PROBE STRENGTH RELATIVE TO DATA	TAP WEIGHT INTEGRATION TIME (SEC)	Eb/No IN DB FOR 10^{-5} BIT ERROR PROBABILITY	PROBE STRENGTH RELATIVE TO DATA	TAP WEIGHT INTEGRATION TIME (SEC)	Eb/No IN DB FOR 10^{-5} BIT ERROR PROBABILITY	Eb/No IN DB FOR 10^{-5} BIT ERROR PROBABILITY
1.0	† 0.21 0.13	6.69 7.45	0.42 0.48	0.37 0.14	8.07 9.40	0.50 0.50	0.37 0.13	8.10 9.50	11.27
0.8	0.27 0.15	6.41 7.16	0.39 0.45	0.47 0.17	7.79 9.11	0.33 0.50	0.46 0.16	7.82 9.19	11.27
0.6	0.35 0.19	6.08 6.82	0.36 0.42	0.62 0.22	7.45 8.74	0.33 0.50	0.62 0.21	7.46 8.82	11.27
0.4	0.55 0.27	5.70 6.40	0.31 0.37	0.93 0.31	7.01 8.25	0.33 0.33	0.92 0.32	7.02 8.32	11.27
0.2	0.65 0.46	5.36 5.84	0.24 0.30	1.85 0.57	6.37 7.51	0.25 0.33	1.87 0.56	6.37 7.54	11.27
0.1	0.98 0.77	5.11 5.43	0.18 0.24	3.71 1.04	5.86 6.87	0.17 0.25	3.72 1.01	5.86 6.89	11.27

* CONSTRAINT LENGTH SEVEN CONVOLUTIONAL CODE WITH THREE-BIT QUANTIZED SOFT DECISION VITERBI DECODING.

† THE UPPER ENTRY DENOTES PARAMETERS AND PERFORMANCE WITH DELAY COMPENSATION; THE LOWER ENTRY INDICATES THE SAME WITHOUT DELAY COMPENSATION.

TABLE 3

MINIMUM REQUIRED VALUES FOR Eb/No AND CORRESPONDING OPTIMUM TAP WEIGHT FILTER MEMORY FOR 10^{-5} DECODED* BIT ERROR RATE (AT 75 BITS/SEC) VERSUS CHANNEL DOPPLER SHIFT. CALCULATIONS FOR DECISION-DIRECTED, PARALLEL-PROBE, SERIAL-PROBE, AND DPSK RAKE MODEMS

50 TAPS USED IN RAKE COMBINER

DOPPLER (Hz)	DECISION-DIRECTED RAKE MODEM		PARALLEL-PROBE RAKE MODEM			SERIAL-PROBE RAKE MODEM			DPSK RAKE MODEM
	OPTIMUM TAP WEIGHT INTEGRATION TIME (SEC)	Eb/No IN DB FOR 10^{-5} BIT ERROR PROBABILITY	JOINTLY OPTIMIZED: PROBE STRENGTH RELATIVE TO DATA	JOINTLY OPTIMIZED: TAP WEIGHT INTEGRATION TIME (SEC)	Eb/No IN DB FOR 10^{-5} BIT ERROR PROBABILITY	JOINTLY OPTIMIZED: PROBE STRENGTH RELATIVE TO DATA	JOINTLY OPTIMIZED: TAP WEIGHT INTEGRATION TIME (SEC)	Eb/No IN DB FOR 10^{-5} BIT ERROR PROBABILITY	Eb/No IN DB FOR 10^{-5} BIT ERROR PROBABILITY
1.0	† 0.21 0.14	7.79 8.54	0.53 0.57	0.37 0.15	9.25 10.64	0.50 0.50	0.51 0.15	9.26 10.75	12.86
0.8	0.27 0.17	7.44 8.14	0.50 0.54	0.47 0.19	8.93 10.30	0.50 0.50	0.47 0.19	8.93 10.39	12.86
0.6	0.37 0.22	7.02 7.78	0.46 0.51	0.62 0.24	8.52 9.89	0.50 0.50	0.61 0.24	8.53 9.95	12.86
0.4	0.55 0.31	6.49 7.25	0.41 0.46	0.93 0.35	7.99 9.33	0.33 0.50	0.92 0.33	8.02 9.37	12.86
0.2	1.13 0.55	5.79 6.50	0.32 0.38	1.85 0.64	7.19 8.45	0.33 0.33	1.86 0.64	7.19 8.49	12.86
0.1	1.99 0.95	5.30 5.93	0.25 0.31	3.71 1.17	6.52 7.68	0.25 0.33	3.71 1.14	6.52 7.64	12.86

* CONSTRAINT LENGTH SEVEN CONVOLUTIONAL CODE WITH THREE-BIT QUANTIZED SOFT DECISION VITERBI DECODING.

† THE UPPER ENTRY DENOTES PARAMETERS AND PERFORMANCE WITH DELAY COMPENSATION; THE LOWER ENTRY INDICATES THE SAME WITHOUT DELAY COMPENSATION.

TABLE 4

MINIMUM REQUIRED VALUES FOR Eb/No AND CORRESPONDING OPTIMUM TAP WEIGHT FILTER MEMORY FOR 10^{-5} DECODED* BIT ERROR RATE (AT 75 BITS/SEC) VERSUS CHANNEL DOPPLER SHIFT. CALCULATIONS FOR DECISION-DIRECTED, PARALLEL-PROBE, SERIAL-PROBE, AND DPSK RAKE MODEMS

100 TAPS USED IN RAKE COMBINER

DOPPLER (Hz)	DECISION-DIRECTED RAKE MODEM		PARALLEL-PROBE RAKE MODEM			SERIAL-PROBE RAKE MODEM			DPSK RAKE MODEM
	OPTIMUM TAP WEIGHT INTEGRATION TIME (SEC)	Eb/No IN DB FOR 10^{-5} BIT ERROR PROBABILITY	JOINTLY OPTIMIZED: PROBE STRENGTH RELATIVE TO DATA	JOINTLY OPTIMIZED: TAP WEIGHT INTEGRATION TIME (SEC)	Eb/No IN DB FOR 10^{-5} BIT ERROR PROBABILITY	JOINTLY OPTIMIZED: PROBE STRENGTH RELATIVE TO DATA	JOINTLY OPTIMIZED: TAP WEIGHT INTEGRATION TIME (SEC)	Eb/No IN DB FOR 10^{-5} BIT ERROR PROBABILITY	Eb/No IN DB FOR 10^{-5} BIT ERROR PROBABILITY
1.0	† 0.21 0.15	8.81 9.53	0.61 0.64	0.37 0.16	10.30 11.71	0.50 0.50	0.37 0.16	10.33 11.85	14.16
0.8	0.27 0.19	8.42 9.15	0.58 0.61	0.47 0.19	9.94 11.35	0.50 0.50	0.47 0.19	9.95 11.46	14.16
0.6	0.37 0.24	7.94 8.69	0.54 0.58	0.62 0.25	9.49 10.89	0.50 0.50	0.61 0.25	9.50 10.97	14.16
0.4	0.55 0.34	7.32 8.08	0.49 0.53	0.93 0.37	8.89 10.28	0.50 0.50	0.93 0.36	8.89 10.32	14.16
0.2	1.13 0.62	6.43 7.19	0.40 0.45	1.85 0.69	7.96 9.30	0.33 0.50	1.86 0.67	7.99 9.32	14.16
0.1	2.21 1.09	5.75 6.46	0.32 0.38	3.71 1.27	7.17 8.42	0.25 0.33	3.71 1.28	7.21 8.45	14.16

* CONSTRAINT LENGTH SEVEN CONVOLUTIONAL CODE WITH THREE-BIT QUANTIZED SOFT DECISION VITERBI DECODING.

† THE UPPER ENTRY DENOTES PARAMETERS AND PERFORMANCE WITH DELAY COMPENSATION; THE LOWER ENTRY INDICATES THE SAME WITHOUT DELAY COMPENSATION.

LIST OF REFERENCES

1. B. D. Perry, E. A. Palo, R. P. Haggarty, and E. L. Key, "Trade-Off Considerations in the Use of Wide Band HF Communications," *Proc. IEEE International Conference on Communications* (June 1987), 930–940.

2. R. Price and P. Green, "A Communication Technique for Multipath Channels," *Proc. IRE* **46** (March 1958), 555–570.

. *See also Chapter 2 of* M. K. Simon, J. K. Omura, R. A. Sholtz, and B. K. Levitt, in *Spread Spectrum Communications*, Computer Science Press, 1985.

3. B. D. Perry and R. Rifkin, "Interference and Wide Band HF Communications," *Proc. of Fifth Ionospheric Effects Symposium at Springfield, VA* (May 1987).

4. K. Davies, "Ionospheric Radio Propagation," *National Bureau of Standards Monograph 80* (April 1, 1965).

5. H. G. Booker and J. Tao, "A Scintillation Theory of the Fading of HF Waves Returned from the F Region: Receiver Near Transmitter," *Journal of Atmospheric and Terrestrial Physics* **49, No. 9** (1987), 915–938.

6. H. G. Booker, J. Tao, and A. B. Behroozi-Toosi, "A Scintillatio[illegible]y of Fading in Long Distance HF Ionospheric Communications," *Journal of Atmospheric and Terrestrial Physics* **49, No. 7** (1987), 939–958.

7. P. A. Bello, "Characterization of Randomly Time-Variant Linear Channels," *IEEE Trans. on Comm. Systems* . **CS-11, No. 4** (December 1963), 360–393.

8. J. M. Wozencroft and I. M. Jacobs, in *Principles of Communication Engineering*, John Wiley and Sons, 1965, p. 235.

9. S. M. Sussman, "A Matched Filter Communication System for Multipath Channels," *IEEE Trans. on Info. Theory* **IT-6** (June 1960), 367–373.

10. P. A. Bello and H. Raemer, "Performance of a Rake System Over the Orbital Dipole Channel," *Utica National Communication Symposium Record* (October 1962), 46–53.

APPENDIX A
PERFORMANCE ANALYSIS

A.1 INTRODUCTION

This appendix presents the performance analysis of the Rake modems described in the body of this report. Section A.2 formulates the input to the modems, including the effect of the propagation medium. Section A.3 characterizes the Rake combiner output for the decision-directed Rake modem, neglecting the effect of decision errors. The approach to error rate evaluation is developed in section A.4. This latter section includes an examination of the impact of self noise (A.4.3) and the effect of decision errors (A.4.4). Section A.5 considers the other three Rake modems.

A.2 SAMPLED SIGNAL AT MODEM INPUT

Assuming that the noise samples at the excisor output are uncorrelated and stationary and that the percentage of the band excised is sufficiently small to model the signal output as proportional to the sampled signal input, the channel model, from the transmitter to excisor output, may be represented as shown in figure A.1. Without loss of generality, the transmitted signal is conveniently represented by an impulse train with areas $a_q m_q$ transmitted at the rate of $W = 1/\Delta$ per second, where Δ is the DSPN (direct sequence pseudo-noise) signal chip duration, a_q is the q-th DSPN chip modulation, and m_q is the data modulation superimposed on the q-th DSPN chip. The data modulation is at a much slower rate than the chip modulation,

$$m_{q+kN} = d_k; \quad 0 \leq q \leq N-1 \tag{A.1}$$

where d_k is the data modulation for the k-th data symbol. Each symbol spans a sequence of N DSPN chips $\{a_{q+kN}; \quad 0 \leq q \leq N-1\}$. The time duration of a data symbol is

$$T = N\Delta \tag{A.2}$$

Starting with an impulse train input signal, the received signal may be regarded as being formed by passing the input through four filters in cascade: a chip pulse-forming filter, a transmitter filter which attempts to confine the transmitted signal to a bandwidth of W Hz (say 1 MHz), an HF propagation medium "filter", and a receiver anti-alias filter. These four filtering operations may be combined, for analysis purposes, into one composite filter. Since we assume the transmitted signal to be limited to a

bandwidth W Hz, this composite filter, in turn, may be represented by a tapped delay line with taps spaced $\Delta = 1/W$ (say 1 μs) apart and with complex weights equal to sampled values of the composite channel impulse response [A.1]. This representation is shown in figure A.1 in which the i-th complex weight

$$b_i(t) = h(t, i\Delta) \tag{A.3}$$

where $h(t, \xi)$ is the composite channel time variant impulse response. A maximum delay of $M\Delta$ is shown ($M + 1$ taps) to accommodate the multipath spread of the channel.

The tapped delay line filter output plus white noise are passed through a brickwall filter of bandwidth W and then sampled at a rate W/sec to generate the modem input samples. The k-th sample is given by

$$w_k = c_k + n_k \tag{A.4}$$

where c_k is the signal sample and n_k is the noise sample.

We now relate the sampled signal values $\{c_\ell\}$ to the input chip modulation sequence $\{m_k a_k\}$ and to the composite channel tap multipliers $\{b_j(t)\}$. Let $z(t)$ represent the output of the brickwall filter, then

$$z(t) = \sum m_k a_k \ \operatorname{sinc} W(t - k\Delta) \tag{A.5}$$

where

$$\operatorname{sinc} x = \frac{\sin \pi x}{\pi x} \tag{A.6}$$

The composite channel filter output $w(t)$ is then given by

$$w(t) = \sum_{i=0}^{M} b_i(t) z(t - i\Delta) \tag{A.7}$$

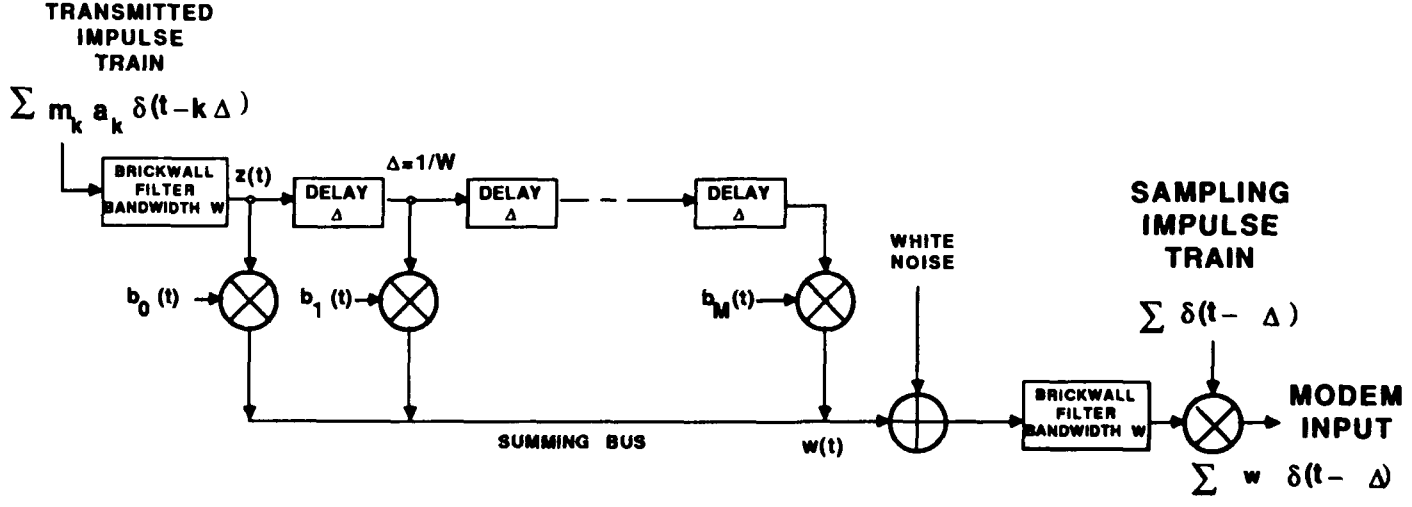

Figure A.1. Formulation of Modem Input Using Tapped Delay Line Model of Composite Channel

Using (A.5) in (A.7)

$$w(t) = \sum_{j=0}^{M} \sum_{k} a_k b_j(t) \ \mathrm{sinc}\, W(t - i\Delta - k\Delta) \tag{A.8}$$

Changing summation indices

$$q = i + k, \tag{A.9}$$

equation (A.8) becomes

$$w(t) = \sum_{q} \left(\sum_{k} a_k b_{q-k}(t) \right) \ \mathrm{sinc}\, W(t - q\Delta) \tag{A.10}$$

Thus, after sampling at $t = \ell\Delta$, we find

$$c_\ell = \sum_{k} m_k a_k b_{\ell-k}(\ell\Delta) = \sum_{k=0}^{M} b_k(\ell\Delta)\ m_{\ell-k}\ a_{\ell-k} \tag{A.11}$$

which is a discrete convolution.

Note that in figure A.1 the noise samples $\{n_k\}$ are formed by passing white noise through a brickwall filter of bandwidth W and sampling the result at W/sec. This construction produces uncorrelated noise samples.

A.3 RAKE COMBINER OUTPUT

Figure A.2 presents a block diagram of the decision-directed coherent Rake modem. In this version the (complex) sampled input process is passed through a (shift-register) tapped delay line with R incremental delays of Δ.* Then the input plus the R delayed versions of the input are correlated with a locally-generated, unmodulated PN sequence. The correlation operation involves conjugate multiplication followed by an integrate and dump (I&D) over successive groups of N input samples. Each I&D output is multiplied by a complex tap weight and the results summed to produce the Rake combiner output. This output is fed to a deinterleaver and decoder and also to a hard decision device. The hard decisions are used in the tap weight processing as discussed below.

As the analysis will show, ideally, each integrate and dump output suppresses all multipath components except one of the $M + 1$ shown in figure A.1 and, as a result,

*Alternate versions exist in which the complex digital input and the local PN sequence exchange positions or in which the input signal and reference are both delayed.

produces an output identical to that for a hypothetical channel having only one of the composite channel tapped delay line outputs. Thus, the successive I&D outputs for a particular correlator contain a data signal proportional to one of the composite channel impulse response samples. A tap weight measurement circuit attempts to measure this complex impulse response sample. Multiplication of each I&D output by the conjugate of the corresponding tap weight measurement followed by summation of all products then approximates predetection or coherent combining of multipath components.

The tap weight measurement circuit shown in figure A.2 is a decision-directed procedure in which an attempt is made to cancel the data modulation on the I&D output through feedback of hard data decisions (with a delay to compensate for an assumed decision delay of T). If the data modulation were cancelled, the noise-free component left would be proportional to the desired impulse response sample. Averaging with a long time constant digital filter can reduce the noise level sufficiently to make the predetection combining effective. The tap weight filter output is shown multiplied by a factor e_p equal to 0 or 1. This factor is used to eliminate tap contributions which contain such weak signals that they will degrade output SNR.

The block diagrams for the other non-decision-directed Rake modems differ from figure A.2 primarily in the method used to generate the tap weights. In the serial probe Rake modem, a percentage of the symbols are modulated with a known data sequence. Correlation is carried out only with the known data subsequence. Thus, decision-directed operation is unnecessary as is the delay, T, shown in figure A.2 used to compensate for decision delays. In the parallel-probe Rake modem, a separate uncorrelated unmodulated DSPN signal is transmitted in parallel with the data modulated DSPN sequence. A separate correlation operation with the probe sequence provides the complex tap gain values for weighting the data I&D outputs. The DPSK Rake modem is the simplest of all and has a block diagram that differs from figure A.2 in that the decision-directed operation is removed. Then the previous I&D output is used as the complex tap weight. However, DPSK modulation is required at the transmitter and DPSK demodulation is produced by the tap weight conjugate-multiply operation. In practice, the decision-directed coherent Rake modem would employ differential encoding at the transmitter and differential decoding at the receiver, since the decision-directed operation can produce 180° phase ambiguities.

The detailed analysis presented is for the decision-directed coherent Rake modem, first assuming no decision errors and then, in section A.4.4, including the effect of decision errors. Section A.5 extends the analysis to the other three Rake modems.

In this section we will develop analytic expressions for the combiner output which include the nonidealities associated with tap weight measurement (excluding decision errors) and the basic correlation operation. These nonidealities include additive noise,

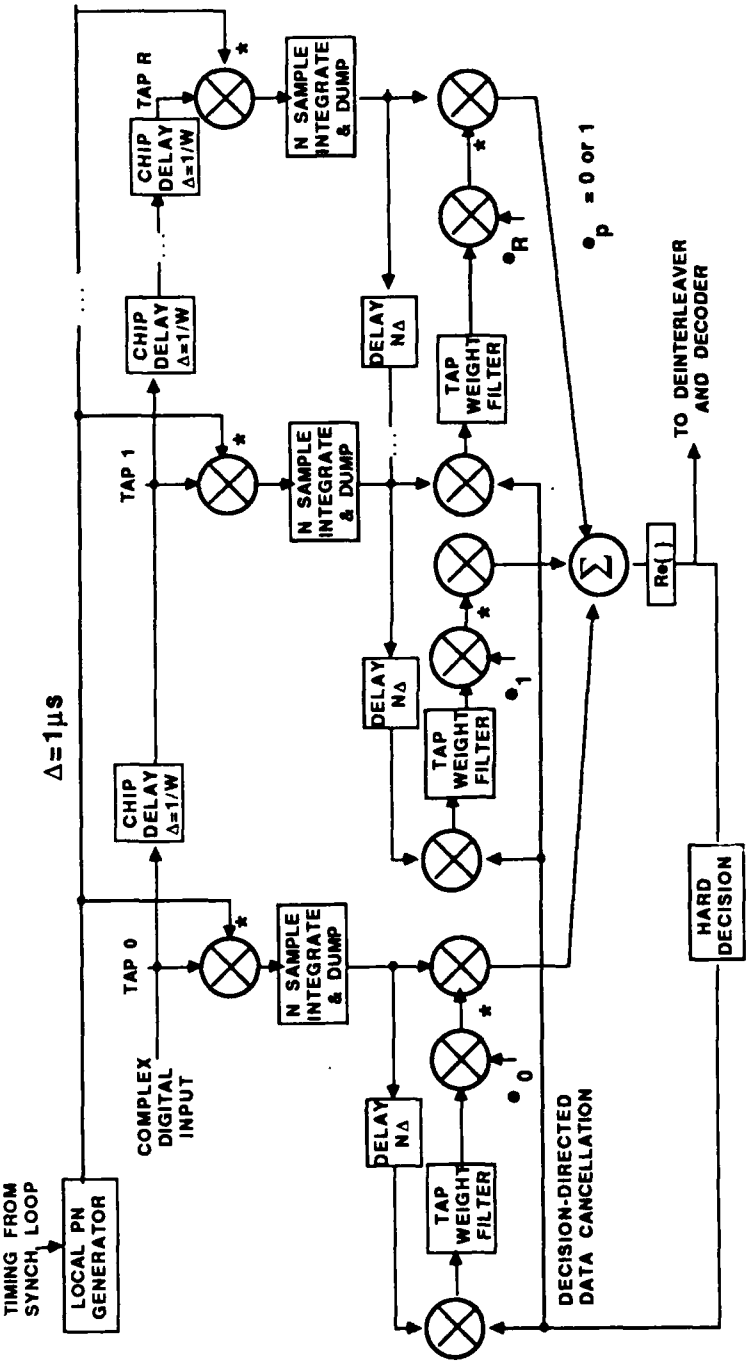

Figure A.2. Decision-Directed Coherent Rake Modem, Delayed Signal Version

phase errors due to Doppler shift, and "self noise", but do not include decision errors. Self noise is due to the residual signal components at an I&D output due to undesired multipath components. These cannot be suppressed completely due to the random nature of the PN sequence and the finite integration time of the I&D.

The local PN sequence $\{\hat{a}_m\}$ fed in parallel to all correlators is given by

$$\hat{a}_m = a_{m-R} \tag{A.12}$$

Then each correlator will ideally select only that multipath component synchronized with a_{m-R}, the $R\Delta$-delayed component from the channel. We examine the quantity y_{pk}, the I&D output due to a correlator input delayed by $p\Delta$, assuming integration over the k-th symbol time interval

$$y_{pk} = \frac{1}{N} \sum_{m=kN+R}^{(k+1)N-1+R} w_{m-p} a^*_{m-R} = \frac{1}{N} \sum_{q=0}^{N-1} w_{q+kN+R-p} a^*_{q+kN} \tag{A.13}$$

This I&D output has a signal component s_{pk} and a noise component n_{pk}

$$y_{pk} = s_{pk} + n_{pk} \tag{A.14}$$

where, using (A.4),

$$s_{pk} = \frac{1}{N} \sum_{q=0}^{N-1} c_{q+kN+R-p}\ a^*_{q+kN} \tag{A.15}$$

$$n_{pk} = \frac{1}{N} \sum_{q=0}^{N-1} n_{q+kN+R-p}\ a^*_{q+kN} \tag{A.16}$$

The noise correlations are

$$\overline{n^*_{pk} n_{r\ell}} = \frac{1}{N^2} \sum_{q=0}^{N-1} \sum_{s=0}^{N-1} \overline{n^*_{q+kN+R-p}\ n_{s+\ell N+R-r}}\ \overline{a_{q+kN}\ a^*_{s+\ell N}} \tag{A.17}$$

Since, by hypothesis,

$$\overline{n^*_{q+kN+R-p}\ n_{s+\ell N+R-r}} = \delta_{(q+kN-p)(s+\ell N-r)}\ \overline{|n|^2} \tag{A.18}$$

$$\overline{a_{q+kN}\ a^*_{s+\ell N}} = \delta_{(q+kN)(s+\ell N)}\ \overline{|a|^2} \tag{A.19}$$

where

$$\delta_{ab} = \begin{cases} 1\ ; & a = b \\ 0\ ; & \text{otherwise} \end{cases} \tag{A.20}$$

it follows that

$$\overline{n^*_{pk}\, n_{r\ell}} = \begin{cases} I/N; & p = r,\ k = \ell \\ 0\ ; & \text{otherwise} \end{cases} \tag{A.21}$$

where we have defined the excisor output complex noise strength

$$\overline{|n|^2} = I \tag{A.22}$$

and the PN sequence strength,

$$\overline{|a|^2} = 1 \tag{A.23}$$

Thus, the noise components at the I&D outputs are uncorrelated and of equal strength. Since we assume the input noise to be zero mean, it also follows that the I&D output noises are zero mean. One may argue, by application of the Central Limit Theorem, that the noises are very nearly complex Gaussian variables when N is large.

Consider now the use of the sampled received signal representation (A.11) in (A.15),

$$s_{pk} = \frac{1}{N} \sum_{q=0}^{N-1} \sum_{r=0}^{M} b_r(\Delta[q + kN + R - p]) m_{q+kN+R-p-r}\, a_{q+kN+R-p-r}\, a^*_{q+kN} \tag{A.24}$$

By separating out the term for which $r = R - p$, we obtain

$$s_{pk} = \frac{1}{N} \sum_{q=0}^{N-1} b_{R-p}(\Delta[q + kN + R - p])\ m_{q+kN} + x_{pk} \tag{A.25}$$

Then, upon using (A.1) in (A.25),

$$s_{pk} = d_k\, \frac{1}{N} \sum_{q=0}^{N-1} b_{R-p}\,(\Delta[q + kN + R - p]) + x_{pk} \tag{A.26}$$

where d_k is the k-th data symbol complex modulation, and

$$x_{pk} = \frac{1}{N} \sum_{q=0}^{N-1} \sum_{\substack{r=0 \\ r \neq R-p}}^{M} b_r(\Delta[q + kN + R - p])\ m_{q+kN+R-p-r}\, a_{q+kN+R-p-r}\, a^*_{q+kN} \tag{A.27}$$

If the channel changes negligibly over a time duration equal to the sum of the data symbol and impulse response durations, then

$$b_{R-p}(\Delta[q+kN+R-p]) \approx b_{R-p}(kT); \quad 0 \leq q \leq N-1 \tag{A.28}$$

and (A.26), (A.27) simplify to

$$s_{pk} = d_k \; b_{R-p}(kT) + x_{pk} \tag{A.29}$$

$$x_{pk} = \sum_{s \neq 0} b_{R-p+s}(kT) \; R_{ks} \tag{A.30}$$

where

$$R_{ks} = \frac{1}{N} \sum_{q=0}^{N-1} m_{q+kN-s} \; a_{q+kN-s} \; a^*_{q+kN} \tag{A.31}$$

Equation (A.29) shows that for slow fading the signal component at each I&D output for the k-th symbol time contains a desired signal term equal to the product of the k-th data symbol by a particular impulse response sample, plus a term we shall call "self" noise. In (A.30) this term is shown to be equal to a weighted sum of contributions proportional to each of the other multipath components, where the weights are random variables as given in (A.31). These random variables are finite cross-correlations between the locally-generated PN sequence and the transmitted modulated PN sequence. If the averaging time were infinite, ($N = \infty$), then the cross-correlation would be zero and the self noise would vanish. Unfortunately, N is finite and it is necessary to evaluate the effect of this self noise on system performance. Assuming $N >> 1$ and using Central Limit Theorem arguments, one may show that the self noise terms have real and imaginary parts which are nearly normally distributed.

We analyze now the complex tap weight process. Since this process is a discrete filtered version of the corresponding I&D output, it will also be representable in terms of a desired signal component, a self noise component, and an additive noise component. In the case of decision-directed operations it will contain an additional perturbation due to decision errors fed back to the data cancellation circuit. This effect will not be considered until section A.4.4. However, one may determine that hard decision error rates in figure A.2 of 10^{-2} or less will not degrade performance perceptibly, while hard decision error rates of 10^{-1} will cause significant degradation. Thus it is necessary that the SNR be sufficient to keep the error rate at the hard decision device in figure A.2 not much less than 10^{-2} in order to achieve the performance predicted in sections A.4.1–A.4.3. Section A.5 discusses some alternate Rake concepts in which a transmitted probe, either in parallel or in series (time-multiplexed), is used. These techniques avoid

the degradations caused by decision-directed errors at the expense of an increase in transmitter power to achieve the same error rate performance as a decision-error-free decision-directed modem.

Using (A.29) and (A.30) in (A.14), the typical I&D output for slow fading can be represented by

$$y_{pk} = d_k\, b_{R-p}(kT) + x_{pk} + n_{pk} \tag{A.32}$$

Assuming perfect decision-directed data cancellation, the tap weight process is given by (see figure A.2)

$$g_{pk} = \sum_{m=0}^{\infty} \alpha_m\, d^*_{k-m-1}\, y_{p,k-m-1} \tag{A.33}$$

where the impulse response of the discrete tap weight filter is

$$g(t) = \sum_{m=0}^{\infty} \alpha_m\, \delta(t - mT) \tag{A.34}$$

Two frequent choices of impulse responses are the exponential impulse response,

$$\alpha_m = (1-\alpha)\,\alpha^m\,; \quad \alpha < 1 \tag{A.35}$$

corresponding to a first-order recursive filter, and the boxcar filter response,

$$\alpha_m = \begin{cases} \frac{1}{N_F}; & 0 \le m \le N_F - 1 \\ 0\ ; & \text{elsewhere}\ . \end{cases} \tag{A.36}$$

Both cases have been normalized to unity dc gain,

$$\sum_{m=0}^{\infty} \alpha_m = 1 \tag{A.37}$$

Using (A.32) in (A.33)

$$g_{pk} = \hat{b}_{R-p}(kT - T) + \hat{x}_{pk} + \hat{n}_{pk} \tag{A.38}$$

where the signal component of the tap weight is given by

$$\hat{b}_{R-p}(kT) = \sum_{m=0}^{\infty} \alpha_m\ b_{R-p}(kT - mT) \tag{A.39}$$

and the self noise and additive noise components by

$$\hat{x}_{pk} = \sum_{m=0}^{\infty} \alpha_m \; d^*_{k-m-1} \; x_{p,k-m-1} \tag{A.40}$$

$$\hat{n}_{pk} = \sum_{m=0}^{\infty} \alpha_m \; d^*_{k-m-1} \; n_{p,k-m-1} \tag{A.41}$$

The Rake combiner complex output for the k-th symbol is given by

$$C_k = \sum_{p=0}^{R} e_p \; g^*_{pk} \; y_{pk} \tag{A.42}$$

where, as noted previously, we have assumed that the Rake combiner has $R+1$ taps and e_p is 1 or 0 depending upon whether or not the tap output is included in the summation. The term e_p is included in the analysis to model the operation of "thresholding" to eliminate taps containing little signal in order to improve the combiner output SNR. A number of algorithms are possible for determining e_p. For example, e_p could be determined by comparing a long-term average over k of $|g_{pk}|^2$ with a threshold and setting $e_p = 0$ when this average is below the threshold. Using (A.38), (A.14), and (A.29) in (A.42),

$$C_k = \sum_{p=0}^{R} e_p\big(\hat{b}^*_{R-p}(kT-T) + \hat{x}^*_{pk} + \hat{n}^*_{pk}\big)\;\big(d_k b_{R-p}(kT) + x_{pk} + n_{pk}\big) \tag{A.43}$$

For coherent demodulation and BPSK data and chip modulation, only the real part of C_k is used. This real part can be separated into a signal and a noise part

$$Re(C_k) = S_k + N_k \tag{A.44}$$

where

$$S_k = d_k \; Re\Big\{ \sum_{p=0}^{R} e_p \hat{b}^*_{R-p}(kT-T) b_{R-p}(kT) \Big\} \tag{A.45}$$

$$N_k = Re\Big\{ \sum_{p=0}^{R} e_p \Big(\hat{x}^*_{pk} x_{pk} + \hat{n}^*_{pk} n_{pk} + \hat{b}^*_{R-p}(kT-T)(x_{pk} + n_{pk}) + x_{pk}\hat{n}^*_{pk} + n_{pk}\hat{x}^*_{pk} + d_k b_{R-p}(kT)(\hat{x}^*_{pk} + \hat{n}^*_{pk}) \Big) \Big\} \tag{A.46}$$

and $d_k = \pm 1$.

When the number of terms in the summation in (A.46) is sufficiently large, the sum of the real parts of the noise product terms may be assumed normally distributed due to the application of the Central Limit Theorem. We have already pointed out that the noise and self noise terms may be modeled as normally distributed. Thus, for purposes of evaluating error rates, we can model N_k as a normally distributed random variable. Since the noise and self noise terms are zero mean and uncorrelated, N_k will also be zero mean. Then the basic parameter for determination of error rate performance is the SNR

$$\rho_k = \frac{S_k^2}{N_k^2} \tag{A.47}$$

Assuming that the input noise is stationary, the variation of ρ_k with k will be due to time variations in the channel. One must consider, then, whether error rate predictions should be on a quasi-stationary basis where the SNR is fixed for the error rate computation and allowed to vary afterward, or whether the predictions should include averages over the channel fluctuations.

A.4 ERROR RATE EVALUATION FOR DECISION-DIRECTED MODEM

In this section we concentrate on the performance evaluation for the decision directed Rake modem. In sections A.4.1–A.4.3, we assume no decision errors and, for much of the analysis, BPSK data and chip modulation. Section A.4.4 presents an approximate analysis of the effect of decision errors.

A.4.1 Ideal Operation

Consider first the ideal situation in which the tap weight measurement is perfect and self noise is negligible, i.e.,

$$\hat{b}_{R-p}(kT - T) = b_{R-p}(kT) \tag{A.48}$$

$$\hat{x}_{pk} = x_{pk} = \hat{n}_{pk} = 0 \tag{A.49}$$

Then,

$$S_k = d_k \sum_{p=0}^{R} e_p \, |b_{R-p}(kT)|^2 \tag{A.50}$$

$$N_k = Re\Big\{ \sum_{p=0}^{R} e_p \; b^*_{R-p}(kT) \; n_{pk} \Big\} \tag{A.51}$$

and, using (A.21) in calculating $\overline{N_k^2}$,

$$\rho_k = \frac{2N}{I} \sum_{p=0}^{R} e_{R-p} \; |b_p(kT)|^2 \equiv \rho_{ok} \tag{A.52}$$

where we have used the following identity for a complex Gaussian variable, z,

$$\overline{Re^2\{z\}} = \frac{1}{2} \; \overline{|z|^2} \tag{A.53}$$

and ρ_{ok} has been defined as the value of ρ_k for perfect channel measurement.

The input SNR in the bandwidth W is (see equation (A.41))

$$\rho_{ik} = \frac{\frac{1}{2} \; \overline{|c_k|^2}}{\frac{1}{2} \; \overline{|n_k|^2}} \tag{A.54}$$

Since (see (A.11))

$$\overline{|c_k|^2} = \sum_p \sum_q \; \overline{a_p a_q^*} \; b_{k-p} b^*_{k-q} \tag{A.55}$$

we see from (A.19), (A.20), and (A.23), that

$$\overline{|c_k|^2} = \sum_{p=0}^{M} |b_p(kT)|^2 \tag{A.56}$$

Thus, using (A.23),

$$\rho_{ik} = \frac{1}{I} \sum_{p=0}^{M} |b_p(kT)|^2 \tag{A.57}$$

so that

$$\rho_{ok} = \rho_{ik} \, 2N \; \frac{\sum_{p=0}^{R} e_{R-p} \, |b_p(kT)|^2}{\sum_{p=0}^{M} |b_p(kT)|^2} \leq \rho_{ik} \, 2N \tag{A.58}$$

where equality occurs on the extreme right when $e_p = 1$ and $R = M$, i.e., when no Rake tap outputs are excised and the number of Rake taps equals the number of taps on the composite channel model.

Error rate performance curves are frequently presented as a function of E_b/N_o, the ratio of energy/bit to noise power density, or, equivalently, the SNR, where the noise is measured in a bandwidth equal to the bit rate. For a rate 1/2 code and binary PSK transmissions, the bandwidth equal to the bit rate is $1/2T$ where T is the symbol duration. The effective real (one-sided) noise power density at the excisor output is

$$N_o = \frac{I}{2W} \tag{A.59}$$

so that E_b/N_o in the vicinity of the k-th I&D is given by

$$\left(\frac{E_b}{N_o}\right)_k = \frac{2N}{I} \sum_{p=0}^{M} |b_p(kT)|^2 \tag{A.60}$$

Thus, for the rate 1/2 coded binary PSK system, the combiner output SNR, ρ_{ok}, equals E_b/N_o when the channel measurement is perfect, all paths of significant strength are combined, and self noise is negligible. This is exactly the SNR that would exist at the BPSK demodulator output for the AWGN (additive white Gaussian noise) channel. Consequently, the ideal Rake modem performance with coding is identical to that for the AWGN channel, *independent of the channel impulse response shape* for a given value of E_b/N_o. Of course for E_b/N_o to be fixed, the energy in the impulse response, $\sum |b_r(kT)|^2$, must remain fixed. For non-overlapping, purely dispersive propagation modes, this energy will fluctuate slowly enough that a quasi-stationary performance analysis should be adequate. An experimental determination of the statistics of $\sum |b_p(kT)|^2$ and the noise power I will then allow a calculation of the statistics of $(E_b/N_o)_k$ and a prediction of the cumulative distribution of minimum error rate achievable with the coded Rake system.

In practice, the combiner output SNR will be less than $(E_b/N_o)_k$ due to tap excision, noisy and mismatched tap weights (e.g., due to Doppler shift), and possibly self noise. An increase in $(E_b/N_o)_k$ is required to bring the combiner output SNR to a value that will achieve the same error rate as the ideal system. Assuming that the combiner output SNR can be determined as a function of the input E_b/N_o, the quasi-stationary approach can be extended to the case of imperfect combining. Thus, if $\rho(\cdot)$ relates the combiner output SNR to the input value of E_b/N_o and $p(\cdot)$ relates the error rate of the rate 1/2 coded AWGN channel to E_b/N_o, the quasi-stationary error rate of the Rake system is $p(\rho(E_b/N_o))$. In estimating the cumulative distribution of p, however, we need to consider all the channel and Rake parameters affecting the combiner output

SNR. For example, for a fixed number of Rake taps and a fixed integration time for the tap weight filter, a prime determinant of ρ will be the Doppler shifts associated with the non-overlapping dispersive modes. Thus, in addition to collection of the statistics of impulse response energy, and excisor output noise power, one must collect statistics of mode Doppler shift.

Note that the availability of the function $p(\rho(E_b/N_o))$ allows one to estimate the input value of E_b/N_o required to achieve a desired error rate for a fixed value of impulse response energy. Thus, a rate 1/2, constraint length 7, convolutional code with 3-bit soft-decision Viterbi decoding will produce an error rate of 10^{-5} for $E_b/N_o \approx 4.3$ dB, assuming PSK transmission over the AWGN channel. The required E_b/N_o for, say, 10^{-5} error rate with realistic Rake operation can be obtained by solving the equation

$$\rho(E_b/N_o) = 10^{0.43} \tag{A.61}$$

for E_b/N_o.

When the quasi-stationary approach cannot be used, the simple procedure described above for error rate evaluation with coding cannot be used. A specific analysis is needed which models the interaction of the fluctuations of signal at the combiner output and the de-interleaving/decoding operation.

A.4.2 Output SNR Neglecting Self Noise

In the absence of self noise, the output noise term (A.46) is given by

$$N_k = Re\Big\{ \sum_{p=0}^{R} e_p(\hat{n}^*_{pk}\ n_{pk} + \hat{b}^*_{R-p}(kT - T)\ n_{pk} + d_k b_{R-p}(kT)\ \hat{n}^*_{pk}) \Big\} \tag{A.62}$$

As discussed previously, the variables n_{pk} and $\hat{n}_{pk}$ are modeled as complex Gaussian. Thus, the summations of the last two terms in (A.62) are also complex Gaussian. Using the Central Limit Theorem, the summation involving the product term $\hat{n}^*_{pk} n_{pk}$ will also be modelable as a complex Gaussian variable when the number of terms in the summation is large, as assumed here. Since the mean squared value of the real part of a complex Gaussian variable equals one-half of the mean absolute value squared for the variable, we may use

$$\overline{N_k^2} = \frac{1}{2} \overline{\Big| \sum_{p=0}^{M} e_p(\hat{n}^*_{pk}\ n_{pk} + \hat{b}^*_{R-p}(kT - T)\ n_{pk} + d_k\ b_{R-p}(kT)\ \hat{n}^*_{pk}) \Big|^2} \tag{A.63}$$

To simplify the calculation further, we note that since odd order moments of complex Gaussian variables are zero and $\hat{n}_{pk}$, n_{qk} are uncorrelated for all p and q, all cross-product terms obtained by squaring in (A.63) will vanish after averaging. Thus, (A.63) simplifies to

$$\overline{N_k^2} = \frac{1}{2}\sum_{p=0}^{R} e_p \overline{|\hat{n}_{pk}|^2\,|n_{pk}|^2} + \frac{1}{2}\sum_{p=0}^{R} e_p \overline{|n_{pk}|^2}\;|\hat{b}_{R-p}(kT-T)|^2 + \frac{1}{2}\sum_{p=0}^{M-1} e_p \overline{|\hat{n}_p k|^2}\;|b_{R-p}(kT)|^2 \tag{A.64}$$

Using (A.21) and (A.41),

$$\overline{|\hat{n}_{pk}|^2} = \frac{I}{N}\sum_{m=0}^{\infty} \alpha_m^2 \tag{A.65}$$

Thus,

$$\overline{N_k^2} = \frac{I^2}{2N^2}\Big(\sum_{0}^{\infty} \alpha_m^2\Big)\Big(\sum_{p=0}^{R} e_p\Big) + \frac{I}{2N}\sum_{p=0}^{R} e_p\;|\hat{b}_{R-p}(kT-T)|^2 + \frac{I}{2N}\sum \alpha_m^2 \sum_{p=0}^{R} e_p\;|b_{R-p}(kT)|^2 \tag{A.66}$$

Using (A.66) and (A.45) in (A.47), we obtain the general expression for output SNR*, when self noise is neglected as

$$\rho = \frac{\frac{2N}{I}\,Re^2\Big\{\sum_{p=0}^{R} e_p\;\hat{b}^*_{R-p}(kT-T)\;b_{R-p}(kT)\Big\}}{(\alpha_m^2)\Big(\frac{I}{N}\sum_{p=0}^{R} e_p + \sum_{p=0}^{R} e_p\;|b_{R-p}(kT)|^2\Big) + \sum_{p=0}^{R} e_p\;|\hat{b}_{R-p}(kT-T)|^2} \tag{A.67}$$

Consider the case in which the non-disturbed HF channel consists of distinct propagation modes each with different Doppler shifts occupying mutually exclusive time delay segments of the composite channel impulse response. Then,

$$h(t,\xi) = \sum g_n(t,\xi)\;e^{j2\pi\nu_n t} \tag{A.68}$$

*For simplicity, we drop the k subscripts on various SNRs, from this point on.

where ν_n is the Doppler shift on the n^{th} mode and $g_n(t,\xi)$ is the impulse response of the m-th* mode with the Doppler shift removed. Since we are assuming very slow fading, it is sufficient to neglect the time variation of $g_n(t,\xi)$ in the present analysis and simplify notation by using

$$h(t,\xi) = \sum g_n(\xi)\, e^{j2\pi\nu_n t} \tag{A.69}$$

From the definition of $b_p(kT)$ in (A.3),

$$b_p(kT) = \sum g_n(p\Delta)\, e^{j2\pi\nu_n kT} \tag{A.70}$$

Using (A.70) in (A.39), the signal component of the tapweight becomes

$$\hat{b}_p(kT-T) = \sum_{m=0}^{\infty} \alpha_m \sum_n g_n(p\Delta)\, e^{j2\pi\nu_n(k-m-1)T} \tag{A.71}$$

or

$$\hat{b}_p(kT-T) = \sum_n g_n(p\Delta)\, e^{j2\pi\nu_n(k-1)T}\, G(\nu_n) \tag{A.72}$$

where

$$G(f) = \int g(t)\, e^{-j2\pi ft}\, dt = \sum \alpha_m\, e^{-j2\pi fmT} \tag{A.73}$$

is the transfer function of the discrete tap weight filter (A.34).

Using the "non-overlapping" mode hypothesis, (A.71) and (A.72) lead to

$$\sum_{p=0}^{R} e_p\, \hat{b}^*_{R-p}(kT-T)\, b_{R-p}(kT) = \sum_{p=0}^{R} e_{R-p} \sum_n |g_n(p\Delta)|^2\, e^{j2\pi\nu_n T} G^*(\nu_n)$$

$$= \sum_n G^*(\nu_n)\, e^{j2\pi\nu_n T}\, E_n \tag{A.74}$$

$$\sum_{p=0}^{R} e_p\, |b_{R-p}(kT)|^2 = \sum_{p=0}^{R} e_{R-p} \sum_n |g_n(p\Delta)|^2 = \sum_n E_n \tag{A.75}$$

$$\sum_{p=0}^{R} e_p\, |\hat{b}_{R-p}(kT-T)|^2 = \sum_{p=0}^{R} e_{R-p} \sum_n |g_n(p\Delta)|^2\, |G(\nu_m)|^2 = \sum_n |G(\nu_n)|^2\, E_n \tag{A.76}$$

where

$$E_n = \sum_{p=0}^{R} e_{R-p} \, |g_n(p\Delta)|^2 \tag{A.77}$$

Then, using (A.74) through (A.76) in (A.67)

$$\rho = \frac{\frac{2N}{I}\Big(\sum E_n \; Re\Big\{G^*(\nu_n) \; e^{j2\pi\nu_n T}\Big\}\Big)^2}{\Big(\sum \alpha_m^2\Big)\Big(\frac{I}{N}\sum_{p=0}^{R} e_p + \sum_n E_n\Big) + \sum_n |G(\nu_n)|^2 \; E_n} \tag{A.78}$$

Note that with the non-overlapping, purely dispersive channel the output SNR is independent of time (k).

For a single propagation model, (A.78) simplifies further to

$$\rho = \frac{\frac{2N}{I} Re^2\Big\{G^*(\nu) \; e^{j2\pi\nu T}\Big\}\Big(\sum_{p=0}^{R} e_{R-p}|g(p\Delta)|^2\Big)^2}{(\sum \alpha_m^2)\Big(\frac{I}{N}\sum_{p=0}^{R} e_{R-p} + \sum_{p=0}^{R} e_{R-p}|g(p\Delta|^2\Big) + |G(\nu)|^2 \sum_{p=0}^{R} e_{R-p}|g(p\Delta)|^2} \tag{A.79}$$

where we have dropped the n subscript. ρ may also be represented in the form

$$\rho = \frac{Re^2\left(G^*(\nu) \; e^{j2\pi\nu T}\right) \; \rho_0}{(\sum \alpha_m^2)(1 + \frac{2N_T}{\rho_0}) + |G(\nu)|^2} \tag{A.80}$$

where it will be recalled (see (A.58) without k subscript) that ρ_0 is the output SNR for perfect channel measurement, and

$$N_T = \sum_{p=0}^{R} \; e_{R-p} \; = \sum_{p=0}^{R} \; e_p \; \leq \; R+1 \tag{A.81}$$

is the total number of "active" Rake taps.

In the event that no tap excision is used and M = R (see (A.60))

$$\rho_0 = E_b/N_o \tag{A.82}$$

and

$$\rho = \frac{Re^2\left(G^*(\nu)\ e^{j2\pi\nu T}\right)\ E_b/N_o}{\left(\sum \alpha_m^2\right)\left(\dfrac{2(R+1)}{E_b/N_o}\ +1\right) + |G(\nu)|^2} \tag{A.83}$$

For the exponential filter (A.35)

$$\sum_0^\infty \alpha_m^2 = (1-\alpha)^2 \sum_0^\infty \alpha^{2m} = \frac{1-\alpha}{1+\alpha} \tag{A.84}$$

$$G(\nu) = (1-\alpha) \sum_{M=0}^{\infty} \alpha^m\ e^{-j2\pi\nu mT} = \frac{1-\alpha}{1-\alpha\ e^{-j2\pi\nu T}} \tag{A.85}$$

and for the boxcar filter (A.36)

$$\sum_0^\infty \alpha_m^2 = \frac{1}{N_F} \tag{A.86}$$

$$G(\nu) = e^{-j\pi\nu(N_F-1)T}\frac{\sin \pi\nu N_F T}{N_F \sin \pi\nu T} \approx e^{-j\pi\nu(N_F-1)T}\ \operatorname{sinc} \nu N_F T; \quad \nu T << 1 \tag{A.87}$$

Either filter will adequately reduce the noise level on the tap weight process. However, note that the boxcar filter has a linear phase characteristic corresponding to a delay $(N_F-1)T/2$, whereas the exponential filter has a nonlinear phase characteristic which is approximately linear only over a small enough bandwidth. This latter phase shift can be modeled by a group delay around zero frequency. Because of the existence of these delays, plus the delay of T shown in the tap weights branch, the Doppler shift produces a spurious phase shift in the tap weight that does not exist on the signal at the I&D output. This phase error will produce an SNR degradation at the coherent detector output. If a compensating delay could be introduced in the signal path ahead of the tap weight multiplication, the same spurious phase shift would be introduced on the signal component. Then the weighting process will remove the phase shift effect since the I&D output is multiplied by the complex conjugate of the tap weight.

Figure A.3 shows a method for introducing such a delay compensation in a decision-directed coherent Rake modem. Separate weighting and combining circuits are used for decision-directed data cancellation and delay-compensated data combining. Assuming the phase shift of the tap weight filter is adequately modeled by the group delay at zero frequency, the net effect of delay compensation is to remove the phase shift in the argument of the real parts in (A.78), yielding the result

$$\rho = \frac{\dfrac{2N}{I}\Big(\sum_n |G(\nu)|\ E_n\Big)^2}{\left(\sum \alpha_m^2\right)\left(\dfrac{I}{N}N_T + \sum_n E_n\right) + \sum_n |G(\nu_n)|^2 E_n} \tag{A.88}$$

for multiple modes, and

$$\rho = \frac{|G(\nu)|^2 \rho_0}{\left(\sum \alpha_m^2\right)\left(\frac{2N_T}{\rho_0} + 1\right) + |G(\nu)|^2} \tag{A.89}$$

For a single mode, equation (A.89) becomes

$$\rho = \frac{|G(\nu)|^2 \; E_b/N_o}{(\sum \alpha_n^2)\left(\frac{2(R+1)}{E_b/N_o} + 1\right) + |G(\nu)|^2} \tag{A.90}$$

when no tap excision is used.

In the simplest cases, (A.83) and (A.90), it is possible to solve explicitly for the E_b/N_o required to achieve a specific ρ, e.g., $\rho = 4.3$ dB. Thus in the case of no delay compensation, equation (A.83), the E_b/N_o required to achieve a desired ρ is found to be

$$(E_b/N_o)_{req} = \frac{\left(\sum \alpha_m^2 + |G(\nu)|^2\right)\rho}{2\,Re^2\,\{G(\nu)e^{j2\pi\nu T}\}} \; + \; \frac{\sqrt{(\sum \alpha_m^2 + |G(\nu)|^2)^{\,2}\,\rho^2 + 8\,(\sum \alpha_m^2)\,(R+1)\rho\,Re^2\,\{G^*(\nu)e^{j2\pi\nu T}\}}}{2\,Re^2\,\{G(\nu)e^{j2\pi\nu T}\}} \tag{A.91}$$

In the case of the boxcar filter, use of (A.86) and (A.87) in (A.91) produces the result

$$(E_b/N_o)_{req} = \frac{\left(\frac{1}{P} + \mathrm{sinc}^2\,\nu N_F T\right)\rho_o}{(2\,\mathrm{sinc}^2\,\nu N_F T)(cos^2\pi\nu(N_F+1)T)} \; + \; \frac{\sqrt{\left(\frac{1}{N_F} + \mathrm{sinc}^2\,\nu N_F T\right)^2 \rho^2 + 8(R+1)(\rho/N_F)(\mathrm{sinc}^2\,\nu N_F T)\cos^2\pi\nu(N_F+1)T}}{(2\,\mathrm{sinc}^2\,\nu PT)(cos^2\pi\nu(P+1)T)} \tag{A.92}$$

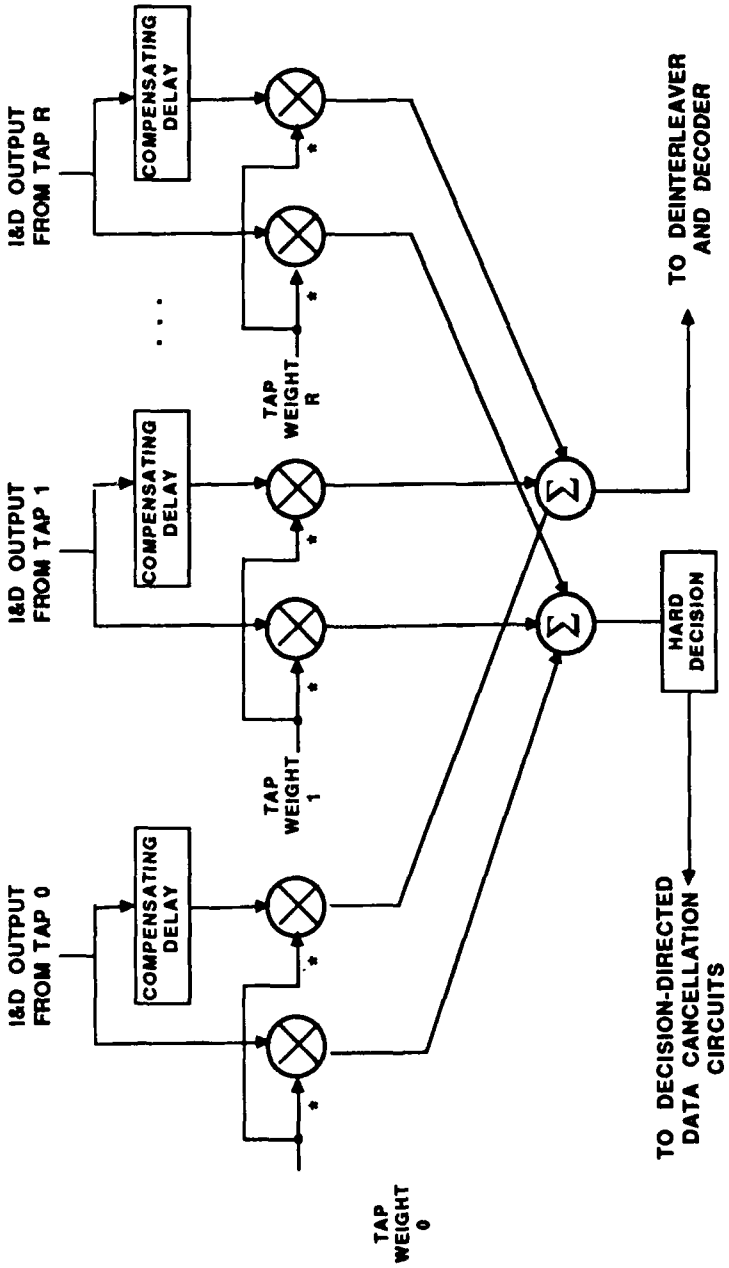

Figure A.3. Use of Compensating Delay In Decision-Directed Coherent Rake Operation

With group delay compensation

$$(E_b/N_o)_{req} = \frac{\left(\sum \alpha_m^2 + |G(\nu)|^2\right)\rho}{2\,|G(\nu)|^2\,\cos^2\left(\theta(\nu) - 2\pi\nu\tau_G\right)} +$$

$$\frac{\sqrt{\left(\sum \alpha_m^2 + |G(\nu)|^2\right)^2 \rho^2 + 8\left(\sum \alpha_m^2\right)(R+1)\rho\,|G(\nu)|^2\cos^2\left(\theta(\nu) - 2\pi\nu\tau_G\right)}}{2\,|G(\nu)|^2\,\cos^2\left(\theta(\nu) - 2\pi\nu\tau_G\right)} \quad \text{(A.93)}$$

where $\theta(\nu)$ is the phase of $G(\nu)$ and τ_G is the group delay of the tap weight filter at zero frequency. As mentioned previously, for the boxcar filter we are able to make the argument of the cosine vanish for all ν, while for the exponential filter we can only make the argument negligible for ν sufficiently small. Thus, for the boxcar filter we can write,

$$(E_b/N_o)_{req} =$$

$$\frac{\left(\frac{1}{P} + \text{sinc}^2\,\nu N_F T\right)\rho + \sqrt{\left(\frac{1}{N_F} + \text{sinc}^2\,\nu N_F T\right)^2 \rho^2 + 8(R+1)(\rho/N_F)\,\text{sinc}^2\,\nu N_F T}}{2\,\text{sinc}^2\,\nu N_F T} \quad \text{(A.94)}$$

A.4.3 Output SNR Including Self Noise But Neglecting Doppler Shift

The expression for noise at the combiner output after coherent detection, including self noise, is given by equation (A.46). Evaluation of the strength of the noise is considerably more involved when self noise is present. While, with self noise absent, we were able to argue that the complex combiner output was nearly a complex Gaussian variable for a large number of taps combined, we may not always do so in the present case.* Thus, identifying Z_k as the complex combiner output noise, we cannot use (A.53) as was done in the absence of self noise. Instead, we must use the identity

$$\overline{N_k^2} = \overline{R_e^2(Z_k)} = \frac{1}{2}\,\overline{|Z_k|^2} + \frac{1}{2}\,Re\{\overline{Z_k^2}\} \quad \text{(A.95)}$$

for computation of noise power.

In the case of complex Gaussian variables

$$\overline{Z_k^2} = 0 \quad \text{(A.96)}$$

*Specifically, when the DSPN chip modulation and data modulation are real, e.g., ± 1, a large number of Rake taps, N_T, will only guarantee that the real and imaginary parts of the self noise are individually approximatable by Gaussian variables.

and only the first term in (A.95) need be computed, as in the previous section. Consider now the summation representing Z_k (see equation (A.46)),

$$Z_k = \sum_{p=0}^{R} e_p \Big(\hat{x}^*_{pk} x_{pk} + \hat{b}^*_{R-p}(kT - T)\, x_{pk} + b_{R-p}(kT) d_k \hat{x}^*_{pk} + x_{pk} \hat{n}^*_{pk} + \hat{x}^*_{pk} n_{pk} + \hat{n}^*_{pk} n_{pk} + \hat{b}^*_{R-p}(kT - T)\, n_{pk} + b_{R-p}(kT) d_k \hat{n}^*_{pk} \Big) \quad \text{(A.97)}$$

Formulation of $\overline{|Z_k|^2}$ or $\overline{Z_k^2}$ yields a large number of cross-product averages. However, most of these averages are zero. It was already pointed out in section A.4.2 that averages of odd numbers of additive noise terms vanish. It is also true that averages of odd number of self noise terms vanish. In addition, the self noise terms and additive noise terms are zero mean and there is statistical independence between the self noise and additive noise terms. As a result, the only possible non-zero average cross-products in computation of $\overline{|Z_k|^2}$ are cross-products of the second and third terms or the seventh and eighth terms in (A.97). However we have already noted in section A.4.2 that this latter cross-product has a zero average. We will also argue that the former cross-product averages may be neglected.

The self noise terms x_{pk} and $\hat{x}_{qk}$ are each weighted sums of finite-time averages or cross-correlations between DSPN sequences. (See (A.30) and (A.40), respectively.) However, while the duration of the time average defining x_{pk} is N samples (spanning $T = N\Delta$ seconds), the duration of the time average defining $\hat{x}_{qk}$ is, by hypothesis, a large multiple of N samples (spanning a time interval equal to the time constant of the tap gain filter). Thus, only a very small fraction of the DSPN chip modulations entering into the finite-time averages defining $\hat{x}_{qk}$ will be functionally related to those entering into the finite-time averages defining x_{pk}. Consequently, the correlation coefficient between x_{pk} and $\hat{x}_{qk}$ must be quite small and will be neglected in the subsequent analysis.

As a result of the above considerations, each of the eight terms in (A.97) will be regarded as zero mean and uncorrelated with all other terms for all values of p of interest. Thus,

$$\frac{1}{2}\overline{|Z_k|^2} = \frac{1}{2}\sum_{p=0}^{R}\sum_{q=0}^{R} e_p e_q \Big[\overline{\hat{x}^*_{pk}\hat{x}_{qk}} \cdot \overline{x_{pk}x^*_{qk}} + \hat{b}^*_{R-p}(kT - T)\hat{b}_{R-q}(kT - T) \cdot \overline{x_{pk}x^*_{qk}} + b_{R-p}(kT) b^*_{R-q}(kT) \cdot \overline{\hat{x}^*_{pk}x_{qk}} + \overline{|x_{pk}|^2} \cdot \frac{I}{N}(\sum \alpha_m^2)\delta_{pq} + \overline{|\hat{x}_{pk}|^2} \cdot \frac{I}{N}\delta_{pq} \Big] + \left(\overline{N_k^2}\right)_0 \quad \text{(A.98)}$$

where

$$\left(\overline{N_k^2}\right)_0 = \frac{I^2}{2N^2}\left(\sum \alpha_m^2\right)\left(\sum_{p=0}^{R} e_p\right) + \frac{I}{2N}\sum_{p=0}^{R} e_p|\hat{b}_{R-p}(kT-T)|^2 + \frac{I}{2N}\left(\sum \alpha_m^2\right)\sum_{p=0}^{R} e_p|b_{R-p}(kT)|^2 \quad \text{(A.99)}$$

is the combiner output noise strength when self noise is neglected (right side of equation (A.65)) and use has been made of (A.20), (A.21), and (A.64).

The other component of $\left(\overline{N_k^2}\right)_0$ is somewhat simpler,

$$\frac{1}{2}(Z_k^2) = \frac{1}{2}Re\left\{\sum_{p=0}^{R}\sum_{q=0}^{R} e_p e_q \left[\overline{\hat{x}_{pk}^*\hat{x}_{qk}^*} \cdot \overline{x_{pk}x_{qk}} + \hat{b}_{R-p}^*(kT-T)\hat{b}_{R-q}^*(kT-T) \cdot \overline{\hat{x}_{pk}\hat{x}_{qk}} + b_{R-p}(kT)b_{R-q}(kT)\cdot\overline{\hat{x}_{pk}^*\hat{x}_{qk}^*}\right]\right\} \quad \text{(A.100)}$$

We consider in turn the evaluation of each of the averages in (A.98) and (A.100). Using (A.40),

$$\overline{\hat{x}_{pk}^*\hat{x}_{qk}} = \sum_m\sum_n \alpha_m\alpha_n \overline{d_{k-m-1}\, x_{p,k-m-1}^*\, d_{k-n-1}^*\, x_{q,k-n-1}} \quad \text{(A.101)}$$

With the definition of x_{pk} in (A.30) plus the definition of d_k in (A.1), (A.101) may be expressed in the form

$$\overline{\hat{x}_{pk}^*\hat{x}_{qk}} = \sum_m\sum_n \alpha_m\alpha_n \cdot \sum_{s\neq 0}\sum_{r\neq 0} b_{R-p+s}^*((k-m-1)T)\, b_{R-q+r}((k-n-1)T)\, \overline{Q_{k-m-1,s}^* Q_{k-n-1,r}} \quad \text{(A.102)}$$

where Q_{ks} is the short term autocorrelation of the transmitted data-modulated DSPN sequence

$$Q_{ks} = \frac{1}{N}\sum_{q=0}^{N-1} m_{q+kN-s}\, a_{q+kN-s}\, m_{q+kN}^*\, a_{q+kN}^* \quad \text{(A.103)}$$

For analysis purposes, the statistics of Q_{ks} will be unchanged if the data modulation is removed from (A.103) since the transmitted data stream statistics will be independent of the data modulation. Thus, to simplify notation we will use

$$Q_{ks} = \frac{1}{N} \sum_{g} A(g) a_{g+kN-s} a^*_{g+kN} \tag{A.104}$$

where

$$A(g) = \begin{cases} 1\ ; & 0 \le g \le N-1 \\ 0\ ; & \text{elsewhere.} \end{cases} \tag{A.105}$$

The required average in (A.102) can then be expressed as

$$\overline{Q^*_{ks} Q_{\ell r}} = \frac{1}{N^2} \sum_{g} \sum_{h} A(g) A(h)\ \overline{a_{g+kN-s} a^*_{g+kN} a^*_{h+\ell N-r} a_{h+\ell N}} \tag{A.106}$$

Assuming that the DSPN chip modulation is a random, unit magnitude, sequence

$$\overline{a_{g+kN-s} a^*_{g+kN} a^*_{h+\ell N-r} a_{h+\ell N}} = \begin{cases} 1\ ; & r = s \neq 0, \quad g+kN = h+\ell N \\ \left|\overline{a^2}\right|^2; & r = -s \neq 0, \quad g+kN = h+\ell N-r \\ 0\ ; & \text{elsewhere, except } r \neq 0,\ s \neq 0 \end{cases} \tag{A.107}$$

Note that if the chip modulation consists of random selections from a discrete uniformly spaced set of phases, $\overline{a^2}$ will vanish except for the case of two phases (i.e., ± 1) when $\overline{a^2}$ is unity. Using (A.107) in (A.106)

$$\overline{Q^*_{ks} Q_{\ell r}} = \frac{\delta_{sr}}{N^2} \sum_{g} A(g) A(g + (k-\ell)N) + \frac{\delta_{s,-r}}{N^2} \left|\overline{a^2}\right|^2 \sum_{g} A(g) A(g + (k-\ell)N - s) \tag{A.108}$$

Since

$$\frac{1}{N} \sum A(g) A(g + (k-\ell)N) = \begin{cases} 1\ ; & k = \ell \\ 0\ ; & k \neq \ell \end{cases} \tag{A.109}$$

$$\frac{1}{N} \sum A(g) A(g + (k-\ell)N - s) = \text{Tri}\left(\frac{s - (k-\ell)N}{N}\right) \tag{A.110}$$

where

$$\mathrm{Tri}(x) = \begin{cases} 1 - |x| \; ; & |x| \le 1 \\ 0 \quad ; & |x| > 1 \end{cases} \tag{A.111}$$

It follows that

$$\overline{Q^*_{ks} Q_{\ell r}} = \frac{\delta_{sr}\delta_{k\ell}}{N} + \frac{\delta_{s,-r}}{N} \left|\overline{a^2}\right|^2 \mathrm{Tri}\left(\frac{s-(k-\ell)N}{N}\right) \tag{A.112}$$

If (A.112) is used in (A.102), it is found that

$$\overline{\hat{x}^*_{pk}\hat{x}_{qk}} = \frac{1}{N}\sum \alpha_m^2 \sum_{s\neq 0} b^*_{R-p+s}((k-m-1)T)\, b_{R-q+s}((k-m-1)T)$$

$$+ \frac{\left|\overline{a^2}\right|^2}{N} \sum_m \sum_n \alpha_m \alpha_n \sum_{s\neq 0} b^*_{R-p+s}((k-m-1)T)\, b_{R-q-s}((k-m-1)T)$$

$$\cdot \mathrm{Tri}\left(\frac{s-(n-m)N}{N}\right) \tag{A.113}$$

In order to simplify the evaluation of (A.113), we shall ignore the possible distorting effects produced by time variations of the composite channel impulse response that are significant over a time interval of the order of the time constant of the tap gain filter. Such distorting effects must be kept to a minimum, anyway, to have high performance even in the absence of self noise. Thus, their omission in the analysis of self noise should only produce second-order errors in calculation of modem performance. The slow time variation assumption is modeled by using

$$b_p((k-m-1)T) = b_p(kT) \equiv b_p \tag{A.114}$$

in (A.113), resulting in

$$\overline{\hat{x}^*_{pk}\hat{x}_{qk}} = \frac{1}{N}\left(\sum \alpha_m^2\right)\left(\sum_{s\neq 0} b^*_{R-p+s}\, b_{R-q+s} + \left|\overline{a^2}\right|^2 \sum_{s\neq 0} \Gamma(\frac{s}{N}) b^*_{R-p+s}\, b_{R-q-s}\right) \tag{A.115}$$

where

$$\Gamma(x) = \frac{\sum_{-\infty}^{\infty} \gamma_n \;\mathrm{Tri}(x-n)}{\left(\sum \alpha_m^2\right)}$$

and

$$\gamma_n = \sum_0 \alpha_m \alpha_{m+|n|} \tag{A.116}$$

is the discrete autocorrelation function of the tap gain filter. Note that $\Gamma(\frac{s}{N})$ is a linearly interpolated and up-sampled (by a factor of N) version of the tap gain filter autocorrelation function γ_n, normalized to $\gamma_0 = \sum \alpha_m^2$. This normalization produces $\Gamma(0) = 1$.

Consider now the evaluation of $\overline{x_{pk} x_{qk}^*}$. Using (A.30), we find

$$\overline{x_{pk} x_{qk}^*} = \sum_{s \neq 0} \sum_{r \neq 0} b_{R-p+s} \, b_{R-q+r}^* \, \overline{R_{ks} R_{kr}^*} \tag{A.117}$$

where R_{ks} is given by (A.31). Proceeding as in the case of evaluation of $\overline{Q_{ks}^* Q_{\ell r}}$, we find that

$$\overline{R_{ks} R_{kr}^*} = \frac{\delta_{sr}}{N} + |\overline{a^2}|^2 \, \frac{1}{N} \, \delta_{s,-r} \, \mathrm{Tri}(\frac{s}{N}) \tag{A.118}$$

Thus,

$$\overline{x_{pk} x_{qk}^*} = \frac{1}{N} \sum_{s \neq 0} b_{R-p+s} \, b_{R-q+s}^* + |\overline{a^2}|^2 \, \frac{1}{N} \sum_{s \neq 0} \mathrm{Tri}(\frac{s}{N}) b_{R-p+s} \, b_{R-q-s}^* \tag{A.119}$$

We will use (A.115) and (A.119) to obtain a representation for the first term in the summation in (A.98), which is a self noise×self noise component of the (real part) combiner output noise power. To simplify the notation, we define

$$SN^* \times SN \equiv \frac{1}{2} \sum_{p=0}^{R} \sum_{q=0}^{R} e_p e_q \, \overline{\hat{x}_{pk}^* \hat{x}_{qk}} \cdot \overline{x_{pk} x_{qk}^*} \tag{A.120}$$

Then, substituting (A.115) and (A.119) in (A.120) and changing the summation over p and q to simplify notation,

$$SN^* \times SN = \frac{\sum \alpha_m^2}{2N^2} \sum_{p=0}^{R} \sum_{q=0}^{R} e_{R-p} e_{R-q} \Big[\sum_{s \neq 0} b_{p+s}^* \Big(b_{q+s} + |\overline{a^2}|^2 \Gamma(\frac{s}{N}) \, b_{q-s} \Big) \Big]$$
$$\times \Big[\sum_{s \neq 0} b_{p+s} \Big(b_{q+s}^* + |\overline{a^2}|^2 \, \mathrm{Tri}(\frac{s}{N}) \, b_{q-s}^* \Big) \Big] \tag{A.121}$$

We turn now to the first term in (A.100), which is the remaining part of the self noise×self noise term. Analogous to (A.102), we find

$$\overline{\hat{x}_{pk}^* \hat{x}_{qk}^*} = \sum_{m} \sum_{n} \alpha_m \alpha_n \sum_{s \neq 0} \sum_{r \neq 0} b_{R-p-s}^* b_{R-q+r}^* \, \overline{Q_{k-m-1,s}^* Q_{k-n-1,r}^*} \tag{A.122}$$

where the required average in (A.122) can be expressed as

$$\overline{Q^*_{ks}Q^*_{\ell r}} = \frac{1}{N^2}\sum_g\sum_h A(g)A(h)\,\overline{a_{g+kN-s}a^*_{g+kN}a_{h+\ell N-r}a^*_{h+\ell N}} \tag{A.123}$$

Instead of (A.107), we have

$$\overline{a_{g+kN-s}a^*_{g+kN}a_{h+\ell N-r}a^*_{h+\ell N}} = \begin{cases} |\overline{a^2}|^2; & r=s\neq 0\ ,\ g+kN=h+\ell N \\ 1 \ ; & r=-s,\ g+kN=h+\ell N-r \\ 0 \ ; & \text{elsewhere, except } r\neq 0, s\neq 0 \end{cases} \tag{A.124}$$

Use of (A.124) in (A.123) results in

$$\overline{Q^*_{ks}Q^*_{\ell r}} = |\overline{a^2}|^2\ \frac{\delta_{sr}\delta_{k\ell}}{N} + \frac{\delta_{s,-r}}{N}\ \mathrm{Tri}(\frac{s-(k-\ell)N}{N}) \tag{A.125}$$

Thus, (A.122) can be represented in the form

$$\overline{\hat{x}^*_{pk}\hat{x}^*_{qk}} = \frac{1}{N}(\sum\alpha_m^2)\Big(|\overline{a^2}|^2\sum_{s\neq 0}b^*_{R-p+s}b^*_{R-q+s} + \sum_{s\neq 0}\Gamma(\frac{s}{N})\,b^*_{R-p+s}b^*_{R-q-s}\Big) \tag{A.126}$$

Consider now the evaluation of

$$\overline{x_{pk}x_{qk}} = \sum_{s\neq 0}\sum_{r\neq 0} b_{R-p+s}\,b_{R-q+r}\,\overline{R_{ks}R_{kr}} \tag{A.127}$$

Proceeding in an analogous fashion to the evaluation of $\overline{Q_{ks}Q_{\ell,r}}$,

$$\overline{R_{ks}R_{kr}} = |\overline{a^2}|^2\ \cdot\ \frac{\delta_{sr}}{N} + \frac{1}{N}\,\delta_{s,-r}\ \mathrm{Tri}(\frac{s}{N}) \tag{A.128}$$

which leads to

$$\overline{x_{pk}x_{qk}} = \frac{|\overline{a^2}|^2}{N}\sum_{s\neq 0} b_{R-p+s}\,b_{R-q+s} + \frac{1}{N}\sum_{s\neq 0}\mathrm{Tri}(\frac{s}{N})\,b_{R-p+s}\,b_{R-q-s} \tag{A.129}$$

To simplify notation, we define the remaining portion of the self noise×self noise term as

$$SN\times SN = \frac{1}{2}\,Re\Big\{\sum_{p=0}^{R}\sum_{q=0}^{R} e_pe_q\,\overline{\hat{x}^*_{pk}\hat{x}^*_{qk}}\ \cdot\ \overline{x_{pk}x_{qk}}\Big\} \tag{A.130}$$

Substituting (A.126) and (A.129) in (A.130) and changing the summations over p and q to simplify notation,

$$SN \times SN =$$

$$\frac{\sum \alpha_m^2}{2N^2} \sum_{p=0}^{R} \sum_{q=0}^{R} e_{R-p} e_{R-q} \; Re\Big\{ \Big[\sum_{s \neq 0} b_{p+s}^* \left(|\overline{a^2}|^2 \, b_{q+s}^* + \Gamma(\frac{s}{N}) b_{q-s}^* \right) \Big] \times \Big[\sum_{s \neq 0} b_{p+s} \left(|\overline{a^2}|^2 \, b_{q+s} + \mathrm{Tri}(\frac{s}{N}) \, b_{q-s} \right) \Big] \Big\} \qquad \text{(A.131)}$$

We consider now the evaluation of the remaining terms in (A.98) and (A.100). These are included as special cases in our previous evaluations, in particular (A.115), (A.119), (A.126), and (A.129). The second and third terms in (A.98) and (A.100) are signal×self noise terms. We use the notation

$$S^* \times SN = \frac{1}{2} \sum_{p=0}^{R} \sum_{q=0}^{R} e_p e_q \Big\{ b_{R-p}^* b_{R-q} \; \overline{x_{pk} x_{qk}^*} + b_{R-p} b_{R-q}^* \; \overline{\hat{x}_{pk}^* \hat{x}_{qk}} \Big\} \qquad \text{(A.132)}$$

$$S \times SN = \frac{1}{2} \sum_{p=0}^{R} \sum_{q=0}^{R} e_p e_q \, Re\Big\{ b_{R-p}^* b_{R-q}^* \; \overline{x}_{pk} \overline{x_{qk}} + b_{R-p} b_{R-q} \; \overline{\hat{x}_{pk}^* \hat{x}_{qk}^*} \Big\} \qquad \text{(A.133)}$$

In (A.132) and (A.133) we have used

$$\hat{b}_r(kT - T) = b_r(kT) \qquad \text{(A.134)}$$

as a consequence of the slow channel time variation assumption.

Using (A.115) and (A.119) in (A.132) and changing the summation over p and q,

$$S^* \times SN = \frac{1}{2N} \sum_{p=0}^{R} \sum_{q=0}^{R} e_{R-p} e_{R-q} \Big\{ b_p^* b_q \Big[\sum_{s \neq 0} b_{p+s} \left(b_{q+s}^* + |\overline{a^2}|^2 \; \mathrm{Tri}(\frac{s}{N}) b_{q-s}^* \right) \Big] + (\textstyle\sum \alpha_m^2) b_p b_q^* \Big[\sum_{s \neq 0} b_{p+s}^* \left(b_{q+s} + |\overline{a^2}|^2 \, \Gamma(\frac{s}{N}) \, b_{q-s} \right) \Big] \Big\} \qquad \text{(A.135)}$$

while using (A.126) and (A.129) in (A.133), we obtain

$$S \times SN = \frac{1}{2N} \sum_{p=0}^{R} \sum_{q=0}^{R} e_{R-p} e_{R-q} \, Re\Big\{ b_p^* b_q^* \Big[\sum_{s \neq 0} b_{p+s} \left(|\overline{a^2}|^2 b_{q+s} + \mathrm{Tri}(\frac{s}{N}) b_{q-s} \right) \Big] + (\textstyle\sum \alpha_m^2) b_p b_q \Big[\sum_{s \neq 0} b_{p+s}^* \left(|\overline{a^2}|^2 b_{q+s}^* + \Gamma(\frac{s}{N}) b_{q-s}^* \right) \Big] \Big\} \qquad \text{(A.136)}$$

The fourth and fifth terms in (A.98) are noise×self noise terms. Using the definition

$$N^* \times SN = \frac{I}{2N} \sum_{p=0}^{R} e_p \left[(\sum \alpha_m^2) \overline{|x_{pk}|^2} + \overline{|\hat{x}_{pk}|^2} \right] \tag{A.137}$$

we find from (A.115) and (A.119) that

$$N^* \times SN = \frac{I(\sum \alpha_m^2)}{2N^2} \sum_{p=0}^{R} e_{R-p} \Bigg[\sum_{s \neq 0} b_{p+s} (b_{p+s}^* + |\overline{a^2}|^2 \, \mathrm{Tri}(\tfrac{s}{N}) \, b_{p-s}^*) + \sum_{s \neq 0} b_{p+s}^* (b_{p+s} + |\overline{a^2}|^2 \, \Gamma(\tfrac{s}{N}) \, b_{p-s}) \Bigg] \tag{A.138}$$

A.4.3.1 Binary PSK Data and Chip Modulation

The special case in which both the data and chip modulation are binary PSK results in

$$|\overline{a^2}|^2 = 1 \tag{A.139}$$

We shall rewrite the terms SN*×SN and SN×SN using (A.139) and replacing $\Gamma(\frac{s}{N})$ and $\mathrm{Tri}(\frac{s}{N})$ by

$$\Gamma(\frac{s}{N}) = 1 - \Gamma_c(\frac{s}{N}) \tag{A.140}$$

$$\mathrm{Tri}(\frac{s}{N}) = 1 - \mathrm{Tri}_c(\frac{s}{N}) \tag{A.141}$$

To simplify notation, we define an alternate tap excision variable*

$$f_p = e_{R-p} \tag{A.142}$$

Using (A.139)-(A.142) in (A.121),

$$SN^* \times SN = \frac{\sum \alpha_m^2}{2N^2} \sum_{p=0}^{R} \sum_{q=0}^{R} f_p f_q \Big[\sum_{s \neq 0} \Big(b_{p+s}^* \, c_{qs} - \Gamma(\tfrac{s}{N}) \, b_{p+s}^* b_{q-s} \Big) \Big] \times \Big[\sum_{r \neq 0} \Big(b_{p+r} \, c_{qr}^* - \mathrm{Tri}_c(\tfrac{r}{N}) \, b_{p+r} b_{q-r}^* \Big) \Big] \tag{A.143}$$

*In this alternate definition, the taps are numbered backwards from the end of the tapped delay line.

where

$$c_{ps} = b_{p+s} + b_{p-s} \tag{A.144}$$

Since

$$\sum_{s\neq 0} h_s = \sum_{s=1}^{\infty} (h_s + h_{-s}) \tag{A.145}$$

for any $\{h_s\}$, and

$$c_{ps} = c_{p,-s} \tag{A.146}$$

$$\Gamma(\frac{s}{N}) = \Gamma(\frac{-s}{N}) \tag{A.147}$$

$$\mathrm{Tri}(\frac{s}{N}) = \mathrm{Tri}(\frac{-s}{N}) \tag{A.148}$$

We can convert (A.143) to

$$SN^* \times SN = \frac{\sum \alpha_m^2}{2N^2} \sum_{p=0}^{R} \sum_{q=0}^{R} f_p f_q \Big[\sum_{s=0}^{\infty} c_{ps}^* c_{qs} - \Gamma_c(\frac{s}{N}) \Big(b_{p+s}^* b_{q-s} + b_{p-s}^* b_{q+s} \Big) \Big]$$
$$\times \Big[\sum_{r=0}^{\infty} c_{pr}\, c_{qr}^* - \mathrm{Tri}_c(\frac{s}{N}) \Big(b_{p+r}\, b_{q-r}^* + b_{p-r}\, b_{q+r}^* \Big) \Big] \tag{A.149}$$

Upon carrying out the multiplications of the bracketed terms in (A.149) and reversing the order of summations, we obtain

$$SN^* \times SN = \frac{\sum \alpha_m^2}{N^2} \Big(\frac{1}{2} \sum_{s=1}^{\infty} \sum_{r=1}^{\infty} \Big| \sum_{p=0}^{R} f_p\, c_{ps}^* c_{pr} \Big|^2$$
$$- \sum_{s=1}^{\infty} \sum_{r=1}^{\infty} \Big[\Gamma_c(\frac{s}{N}) + \mathrm{Tri}_c(\frac{s}{N}) \Big] \; Re \Big\{ \sum_{p=0}^{R} f_p\, b_{p+s}^* c_{pr} \sum_{q=0}^{R} f_q\, b_{q-s} c_{qr}^* \Big\}$$
$$+ \sum_{s=1}^{\infty} \sum_{r=1}^{\infty} \Gamma_c(\frac{s}{N})\; \mathrm{Tri}_c(\frac{r}{N})\; Re \Big\{ \sum_{p=0}^{R} f_p\, b_{p+s}^* b_{p+r} \sum_{q=0}^{R} f_q\, b_{q-s} b_{q-r}^*$$
$$+ \sum_{p=0}^{R} f_p\, b_{p+s}^* b_{p-r} \sum_{q=0}^{R} f_q\, b_{q-s} b_{q+r}^* \Big\} \Big) \tag{A.150}$$

An analogous set of manipulations produces the representation

$$SN \times SN = \frac{\sum \alpha_m^2}{N^2}\Bigg(\frac{1}{2}\sum_{s=1}^{\infty}\sum_{r=1}^{\infty} Re^2\Big\{\sum_{p=0}^{R} f_p\, c_{ps}^* c_{pr}\Big\}$$
$$-\sum_{s=1}^{\infty}\sum_{r=1}^{\infty}\Big[\Gamma_c(\frac{s}{N})+\mathrm{Tri}_c(\frac{s}{N})\Big]\, Re\Big\{\sum_{p=0}^{R} f_p\, b_{p+s}^* c_{pr}\sum_{q=0}^{R} f_q\, b_{q-s}^* c_{qr}\Big\}$$
$$+\sum_{s=1}^{\infty}\sum_{r=1}^{\infty}\Gamma_c(\frac{s}{N})\,\mathrm{Tri}_c(\frac{r}{N})\, Re\Big\{\sum_{p=0}^{R} f_p\, b_{p+s}^* b_{p+r}\sum_{q=0}^{R} f_q\, b_{q-s}^* b_{p-r}$$
$$+\sum_{p=0}^{R} f_p\, b_{p+s}^* b_{p-r}\sum_{q=0}^{R} f_q\, b_{q-s}^* b_{q+r}\Big\}\Bigg) \quad \text{(A.151)}$$

Upon combining (A.150) and (A.151), we obtain

$$SN^* \times SN \;+\; SN \times SN = \frac{\sum \alpha_m^2}{N^2}\Bigg[\sum_{s=1}^{\infty}\sum_{r=1}^{\infty} Re^2\Big\{\sum_{p=0}^{R} f_p\, c_{ps}^* c_{pr}\Big\}$$
$$-2\sum_{s=1}^{\infty}\sum_{r=1}^{\infty}\Big[\Gamma_c(\frac{s}{N})+\mathrm{Tri}_c(\frac{s}{N})\Big]\sum_{p=0}^{R} f_p\, Re\Big\{b_{p+s}^* c_{pr}\Big\}\sum_{q=0}^{R} f_q\, Re\Big\{b_{q-s}^* c_{qr}\Big\}$$
$$+2\sum_{s=1}^{\infty}\sum_{r=1}^{\infty}\Gamma_c(\frac{s}{N})\,\mathrm{Tri}_c(\frac{s}{N})\Big(\sum_{p=0}^{R} f_p\, Re\Big\{b_{p+r} b_{p+s}^*\Big\}\sum_{q=0}^{R} f_q\, Re\Big\{b_{q-s} b_{q-r}^*\Big\}$$
$$+\sum_{p=0}^{R} f_p\, Re\Big\{b_{p-r} b_{p+s}^*\Big\}\sum_{q=0}^{R} f_q\, Re\Big\{b_{q-s} b_{q-r}^*\Big\}\Big)\Bigg] \quad \text{(A.152)}$$

Consider now the $S^* \times SN$ term. Using (A.139)-(A.142) and (A.144) in (A.135),

$$S^* \times SN = \frac{1}{2N}\sum_{p=0}^{R}\sum_{q=0}^{R} f_p\, f_q\Bigg(b_p^* b_q\Big[\sum_{s\neq 0}\Big(b_{p+s}\, c_{qs}^* - \mathrm{Tri}_c(\frac{s}{N}) b_{p+s} b_{q-s}^*\Big)\Big]$$
$$+(\sum \alpha_m^2) b_p\, b_q^*\Big[\sum_{s\neq 0}\Big(b_{p+s}\, c_{qs}^* - \Gamma_c(\frac{s}{N}) b_{p+s}^* b_{q-s}\Big)\Big]\Bigg) \quad \text{(A.153)}$$

With the symmetries (A.145)–(A.148) we can convert (A.153) to one-sided summations over s,

$$S^* \times SN = \frac{1}{2N} \sum_{p=0}^{R} \sum_{q=0}^{R} f_p f_q \left(b_p^* b_q \Big[\sum_{s=1}^{\infty} c_{ps} c_{qs}^* - \mathrm{Tri}_c(\tfrac{s}{N}) \Big(b_{p+s} b_{q-s}^* + b_{p-s} b_{q+s}^* \Big) \Big] + (\textstyle\sum \alpha_m^2) b_p b_q^* \Big[\sum_{s=1} c_{ps}^* c_{qs} - \Gamma_c(\tfrac{s}{N}) \Big(b_{p+s}^* b_{q-s} + b_{p-s}^* b_{q+s} \Big) \Big] \right) \quad \text{(A.154)}$$

After inverting the order of summations in (A.154),

$$S^* \times SN = \frac{(1 + \sum \alpha_m^2)}{2N} \sum_{s=1}^{\infty} \Big| \sum_{p=0}^{R} f_p b_p^* c_{ps} \Big|^2 - \frac{1}{N} \sum_{s=1}^{\infty} \Big[\Big(\textstyle\sum \alpha_m^2 \Big) \Gamma_c(\tfrac{s}{N}) + \mathrm{Tri}_c(\tfrac{s}{N}) \Big] Re \Big\{ \sum_{p=0}^{R} f_p b_p^* b_{p+s} \sum_{q=0}^{R} f_q b_q b_{q-s}^* \Big\} \quad \text{(A.155)}$$

An analogous development yields

$$S \times SN = \frac{1 + \sum \alpha_m^2}{2N} \sum_{s=1}^{\infty} Re \Big\{ \Big(\sum_{p=0}^{R} f_p b_p^* c_{ps} \Big)^2 \Big\} - \frac{1}{N} \sum_{s=1}^{\infty} \Big[\big(\textstyle\sum \alpha_m^2 \big) \Gamma_c(\tfrac{s}{N}) + \mathrm{Tri}_c(\tfrac{s}{N}) \Big] Re \Big\{ \sum_{p=0}^{R} f_p b_p^* b_{p+s} \sum_{q=0}^{R} b_q^* b_{q-s} \Big\} \quad \text{(A.156)}$$

Thus,

$$S^* \times SN + S \times SN = \frac{1 + \sum \alpha_m^2}{N} \sum_{s=1}^{\infty} Re^2 \Big\{ \sum_{p=0}^{R} f_p b_p^* c_{ps} \Big\} - \frac{2}{N} \sum_{s=1}^{\infty} \Big[\big(\textstyle\sum \alpha_m^2 \big) \Gamma_c(\tfrac{s}{N}) + \mathrm{Tri}_c(\tfrac{s}{N}) \Big] Re \Big\{ \sum_{p=0}^{R} f_p b_p^* b_{p+s} \Big\} Re \Big\{ \sum_{q=0}^{R} f_q b_q^* b_{q-s} \Big\} \quad \text{(A.157)}$$

We now turn our attention to the last self noise term, N*×SN. Again using (A.139)-(A.142) in (A.138),

$$N^* \times SN = \frac{I(\sum \alpha_m^2)}{2N^2} \sum_{p=0}^{R} f_p \Big[\sum_{s\neq 0} b_{p+s}\, c_{ps}^* - \sum_{s\neq 0} \mathrm{Tri}_c(\frac{s}{N})\, b_{p+s}\, b_{p-s}^* + \sum_{s\neq 0} b_{p+s}^*\, c_{ps} - \sum_{s\neq 0} \Gamma_c(\frac{s}{N})\, b_{p+s}^*\, b_{p-s} \Big] \quad \text{(A.158)}$$

Using (A.145)-(A.148) to convert (A.158) to one-sided summations over s,

$$N^* \times SN = \frac{I(\sum \alpha_m^2)}{N^2} \sum_{p=0}^{R} f_p \Big(\sum_{s=1}^{\infty} |c_{ps}|^2 - \sum_{s=1}^{\infty} \Big[\Gamma_c(\frac{s}{N}) + \mathrm{Tri}_c(\frac{s}{N}) \Big] Re\{ b_{p+s}\, b_{q-s}^* \} \Big) \quad \text{(A.159)}$$

and inverting the order of summation

$$N^* \times SN = \frac{I(\sum \alpha_m^2)}{N^2} \Big(\sum_{s=1}^{\infty} \sum_{p=0}^{R} f_p\, |c_{ps}|^2 - \sum_{s=1}^{\infty} \Big[\Gamma_c(\frac{s}{N}) + \mathrm{Tri}_c(\frac{s}{N}) \Big] \sum_{p=0}^{R} f_p\, Re\{ b_{p+s}\, b_{q-s}^* \} \Big) \quad \text{(A.160)}$$

A.4.3.2 Approximations and Bounds

The results presented in section A.4.3.2 apply to rather general composite channel impulse responses and are particularly suitable for numerical evaluations. Here we wish to simplify the results by making some reasonable assumptions on HF channel parameters, SNR parameters, and ideal synchronization and windowing of the Rake modem.

The quantities $\mathrm{Tri}(s/N)$ and $\Gamma(s/N)$ are normalized discrete correlation functions which have unity value at $s = 0$ and decrease to zero slowly with s. $\mathrm{Tri}(s/N)$ is a triangle with a base of two symbol durations (the interval (0,N) corresponds to one symbol duration), while $\Gamma(s/N)$ has a duration of the order of twice the time constant of the tap gain filter, i.e., many symbol durations. Consider a typical term in which these factors appear, using F_s to denote either $\Gamma(s/N)$ or $\mathrm{Tri}(s/N)$

$$\sigma_{pq} = \sum_{s\neq 0} b_{p+s}^{(*)}\, b_{q-s}^{(*)}\, F_s \quad \text{(A.161)}$$

where the conjugate signs are optional. If the factor $b^{(*)}_{p+s}\, b^{(*)}_{q-s}$ drops to zero over a range of s values small compared to the duration of F_s, then little error will be introduced in σ_{pq} if F_s is replaced by $F_0 = 1$. The "width" of $b^{(*)}_{p+s}(b^{(*)}_{q-s})$ vs. s varies with p,q from zero when $p = q = 0$ to a maximum of $2R$ for $p = q = R$.

It appears that in most if not all cases of interest the time constant of the tap gain filter will be much larger than the time spread of the Rake tapped delay line. It follows that $\Gamma(s/N)$ will have a width much larger than R and may be set equal to unity in our previous equations with little error. This is equivalent to setting $\Gamma_c(s/N) = 0$. With this approximation the combiner output noise variance becomes

$$\begin{aligned}
\overline{N_k^2} = (\overline{N_k^2})_o &+ \frac{\sum \alpha_m^2}{N^2} \sum_{s=1}^{\infty} \sum_{r=1}^{\infty} Re^2\Big\{ \sum_{p=0}^{R} f_p\, c^*_{ps} c_{pr} \Big\} \\
&- \frac{2\sum \alpha_m^2}{N^2} \sum_{s=1}^{\infty} \sum_{r=1}^{\infty} \mathrm{Tri}_c(\frac{s}{N}) \sum_{p=0}^{R} f_p\, Re\Big\{ b^*_{p+s}\, c_{pr} \Big\} \sum_{q=0}^{R} f_q\, Re\Big\{ b^*_{q-s}\, c_{qr} \Big\} \\
&+ \frac{1+\sum \alpha_m^2}{N} \sum_{s=1}^{\infty} Re^2\Big\{ \sum_{p=0}^{R} f_p\, b^*_p\, c_{ps} \Big\} \\
&- \frac{2}{N} \sum_{s=1}^{\infty} \mathrm{Tri}_c(\frac{s}{N}) Re\Big\{ \sum_{p=0}^{R} f_p\, b^*_p b_{p+s} \Big\} Re\Big\{ \sum_{q=0}^{R} f_q\, b^*_q b_{q-s} \Big\} \\
&+ \frac{I\sum \alpha_m^2}{N^2} \sum_{s=1}^{\infty} \sum_{p=0}^{R} f_p \left| c_{ps} \right|^2 \\
&- \frac{I\sum \alpha_m^2}{N^2} \sum_{s=1}^{\infty} \mathrm{Tri}_c(\frac{s}{N}) \sum_{p=0}^{R} f_p\, Re\Big\{ b_{p+s} b^*_{p-s} \Big\}
\end{aligned} \tag{A.162}$$

where $(\overline{N_k^2})_o$ is given by (A.99).

By the same argument, when the symbol duration is sufficiently large compared to the Rake window duration, we may set $\mathrm{Tri}(s/N) = 1$ or $\mathrm{Tri}_c(s/N) = 0$ in the above expression to obtain the further approximation

$$\begin{aligned}
\overline{N_k^2} = (\overline{N_k^2})_o &+ \frac{\sum \alpha_m^2}{N^2} \sum_{s=1}^{\infty} \sum_{r=1}^{\infty} Re^2\Big\{ \sum_{p=0}^{R} f_p\, c^*_{ps} c_{pr} \Big\} + \frac{1+\sum \alpha_m^2}{N} \\
&\sum_{s=1}^{\infty} Re^2\Big\{ \sum_{p=0}^{R} f_p\, b^*_p\, c_{ps} \Big\} + \frac{I\sum \alpha_m^2}{N^2} \sum_{s=1}^{\infty} \sum_{p=0}^{R} f_p \left| c_{ps} \right|^2
\end{aligned} \tag{A.163}$$

If the combiner output SNR is not very much larger than that necessary to provide adequate error rate performance (e.g., 10^{-5}), and the SNR performance degradations of the Rake modem are modest, the input signal-to-noise-ratio for the Rake modem, ρ_i, will be small compared to unity, assuming that the signal bandwidth, e.g., 1 MHz, is much larger than the data symbol rate. Then it is instructive to examine the self noise power levels relative to the ambient additive noise levels at the Rake system output. This will lead to a criterion for the unimportance of self noise when ρ_i is sufficiently small.

From (A.115) we determine that the strength of the p-th tap gain filter self noise is

$$\overline{|\hat{x}_{pk}|^2} = \frac{\sum \alpha_m^2}{N}\Big(\sum_{s\neq 0} |b_{R-p+s}|^2 + |\overline{a^2}|^2 \sum_{s\neq 0} \Gamma(\frac{s}{N}) b^*_{R-p+s}\, b_{R-p-s}\Big)$$

$$= \frac{\sum \alpha_m^2}{N}\Big(\sum_{k=-\infty}^{\infty} |b_k|^2 + |\overline{a^2}|^2 \sum_{k=-\infty}^{\infty} \Gamma(\frac{k-R+p}{N}) b_k^*\, b_{2(R-p)-k} - 2|b_{R-p}|^2\Big) \tag{A.164}$$

For binary chip modulation $|\overline{a^2}|^2 = 1$. The second sum vanishes for quaternary phase shift keying (QPSK) modulation ($|\overline{a^2}|^2 = 0$). The first term in the parentheses in (A.164) is simply the energy in the channel's impulse response. Ignoring the slow variation of $\Gamma(\cdot)$ with k, the second term is essentially a convolution of the channel's impulse response with its conjugate, evaluated at a time $2(R-p)$. Assuming a highly dispersive channel, it will be quite small compared to the first term and, in any case, is upper-bounded by the first term. The last term will also be small compared to the first term in the highly dispersive case, since $|b_k|^2$ will have many terms of comparable size and no one value will dominate. Thus, with little error for binary PSK chip modulation and no error for QPSK chip modulation, we can set

$$\overline{|\hat{x}_{pk}|^2} = \frac{\sum \alpha_m^2}{N} \sum |b_k|^2 \tag{A.165}$$

and, in any case

$$\overline{|\hat{x}_{pk}|^2} \leq \frac{2\sum \alpha_m^2}{N} \sum |b_k|^2 \tag{A.166}$$

From (A.119) we see that the strength of the p-th tap output self noise is given by

$$\overline{|\hat{x}_{pk}|^2} = \frac{1}{N}\Big(\sum_{s\neq 0} |b_{R-p+s}|^2 + |\overline{a^2}|^2 \sum_{s\neq 0} \mathrm{Tri}(\frac{s}{N})\, b_{R-p+s} b^*_{R-p-s}\Big)$$

$$= \frac{1}{N}\Big(\sum_{k=-\infty}^{\infty} |b_k|^2 + |\overline{a^2}|^2 \sum_{k=-\infty}^{\infty} \mathrm{Tri}(\frac{k-R+p}{N}) b_k\, b^*_{2(R-p)-k} - 2|b_{R-p}|^2\Big) \tag{A.167}$$

Using the same arguments as for the tap gain filter output self noise, with little error for BPSK and no error for QPSK chip modulation, we can write

$$\overline{|\hat{x}_{pk}|^2} = \frac{1}{N} \sum |b_k|^2 \tag{A.168}$$

and, in any case,

$$\overline{|\hat{x}_{pk}|^2} \leq \frac{2}{N} \sum |b_k|^2 \tag{A.169}$$

From (A.21) and (A.65) we know that the strengths of the corresponding noise terms are

$$\overline{|\hat{n}_{pk}|^2} = \frac{I \sum \alpha_m^2}{N} \tag{A.170}$$

$$\overline{|n_{pk}|^2} = \frac{I}{N} \tag{A.171}$$

Thus, using the approximations shown,

$$\frac{\overline{|\hat{x}_{pk}|^2}}{\overline{|n_{pk}|^2}} \approx \rho_i \tag{A.172}$$

and, in any case,

$$\frac{\overline{|\hat{x}_{pk}|^2}}{\overline{|n_{pk}|^2}} \leq 2\rho_i \tag{A.173}$$

where it will be recalled that (see (A.57))

$$\rho_i = \frac{1}{I} \sum |b_k|^2 \tag{A.174}$$

Similarly,

$$\frac{\overline{|x_{pk}|^2}}{\overline{|n_{pk}|^2}} \approx \rho_i \tag{A.175}$$

and, in any case,

$$\frac{\overline{|x_{pk}|^2}}{\overline{|n_{pk}|^2}} \leq 2\rho_i \tag{A.176}$$

Thus, when the input SNR, $\rho_i << 1$, the self noise at each tap filter and tap output will be much smaller than the corresponding additive noise. This might lead

one to conclude that the self noise can always be neglected when $\rho_i << 1$. However, this is not necessarily true, since the combining operation can build up the self noise more rapidly than the additive noise, due to the correlated nature of the self noise from tap-to-tap. However, we show first that the noise×self noise terms may be ignored by comparison to the noise×noise terms at the combiner output. Then we derive criteria under which the other self noise terms at the combiner output may be neglected.

The complex representation of the noise×self noise terms at the combiner output, $z_{N\times SN}$, are the fourth and fifth terms in (A.97), i.e.,

$$z_{N\times SN} = \sum_{p=0}^{R} e_p(x_{pk}\,\hat{n}^*_{pk} + \hat{x}^*_{pk}\,n_{pk}) \tag{A.177}$$

Using the independence of the tap weight noise variables and (A.170)-(A.176), we readily find that

$$\begin{aligned}\overline{|z_{N\times SN}|^2} &= \sum_{p=0}^{R} e_p\left(\overline{|x_{pk}|^2}\cdot\overline{|\hat{n}_{pk}|^2} + \overline{|\hat{x}_{pk}|^2}\cdot\overline{|\hat{n}_{pk}|^2}\right)\\ &\approx 2\rho_i\sum_{p=0}^{R} e_p\,\overline{|n_{pk}|^2}\cdot\overline{|\hat{n}_{pk}|^2}\end{aligned} \tag{A.178}$$

The noise×noise term complex representation $z_{N\times N}$ is

$$z_{N\times N} = \sum_{p=0}^{R} e_p\,\hat{n}^*_{pk}\,n_{pk} \tag{A.179}$$

with corresponding strength,

$$\overline{|z_{N\times N}|^2} = \sum_{p=0}^{R} e_p\,\overline{|\hat{n}^*_{pk}|^2}\cdot\overline{|n_{pk}|^2} \tag{A.180}$$

Thus,

$$\overline{|z_{N\times SN}|^2} \approx 2\rho_i\,\overline{|z_{N\times N}|^2} \tag{A.181}$$

and the noise×self noise term may be neglected when $\rho_i <<< 1$.

We now develop criteria under which the other self noise terms may be neglected. First we compare the strengths of the signal×self noise terms, $z_{S\times SN}$, with the strength of the signal×noise terms, $z_{S\times N}$, of the combiner output.

The strength of $z_{S\times SN}$ is just twice the value of the previously-defined term S*×SN as may be verified by examination of (A.132). Thus, from (A.135),

$$\overline{|z_{S\times SN}|^2} = \frac{1}{N}\sum_{p=0}^{R}\sum_{q=0}^{R} f_p\, f_q \left[b_p^* b_q \sum_{s\neq 0}\left(b_{p+s}\, b_{q+s}^* + |\overline{a^2}|^2\, b_{p+s}\, b_{q+s}^*\, \mathrm{Tri}(\frac{s}{N})\right)\right.$$
$$\left. + (\sum \alpha_m^2) b_p b_q^* \sum_{s\neq 0}\left(b_{p+s}^*\, b_{q+s} + |\overline{a^2}|^2 b_{p+s}^*\, b_{q-s}\Gamma(\frac{s}{N})\right)\right] \quad \text{(A.182)}$$

By interchanging the summation variables p and q in the second triple sum, we find

$$\overline{|z_{S\times SN}|^2} = \frac{1+\sum \alpha_m^2}{N}\sum_{p=0}^{R}\sum_{q=0}^{R} f_p\, f_q\, b_p^* b_q \sum_{s\neq 0} b_{p+s}\, b_{q+s}^*$$
$$+ \frac{|\overline{a^2}|^2}{N}\sum_{p=0}^{R}\sum_{q=0}^{R} f_p\, f_q\, b_p^* b_q \sum_{s\neq 0} b_{p+s}\, b_{q-s}^*\Big(\mathrm{Tri}(\frac{s}{N}) + (\sum \alpha_m^2)\,\Gamma(\frac{s}{N})\Big) \quad \text{(A.183)}$$

Then, changing the order of summations,

$$\overline{|z_{S\times SN}|^2} = \frac{1+\sum \alpha_m^2}{N}\sum_{s\neq 0}\Big|\sum_{p=0}^{R} f_p\, b_p^*\, b_{p+s}\Big|^2$$
$$+ \frac{|\overline{a^2}|^2}{N}\sum_{s\neq 0}\Big(\mathrm{Tri}(\frac{s}{N}) + \sum \alpha_m^2)\,\Gamma(\frac{s}{N})\Big)\Big[\sum_{p=0}^{R} f_p\, b_p^*\, b_{p+s}\Big]\Big[\sum_{p=0}^{R} f_p\, b_p^*\, b_{p-s}\Big] \quad \text{(A.184)}$$

For purposes of this analysis we assume that the number of Rake taps R are large enough and synchronization has been adjusted so that all significant energy in the impulse response is passed by the Rake combiner. Then,

$$\sum_{p=0}^{R} f_p\, b_p^*\, b_{p+s} \approx \sum_{-\infty}^{\infty} b_p^*\, b_{p+s} = R_s = R_{-s}^* \quad \text{(A.185)}$$

where R_s is the autocorrelation function of the sampled composite channel impulse response. Thus, using (A.185),

$$\overline{|z_{S\times SN}|^2} \approx \frac{1+\sum \alpha_m^2}{N}\sum_{s\neq 0}|R_s|^2 + \frac{|\overline{a^2}|^2}{N}\sum_{s\neq 0}\Big(\mathrm{Tri}(\frac{s}{N}) + (\sum \alpha_m^2)\,\Gamma(\frac{s}{N})\Big)\,|R_s|^2 \quad \text{(A.186)}$$

The last sum is less than the first, since

$$\mathrm{Tri}(\frac{s}{N}) + (\sum \alpha_m^2)\,\Gamma(\tfrac{s}{N}) < 1 + \sum \alpha_m^2 \tag{A.187}$$

Thus,

$$\overline{|z_{S\times SN}|^2} \le \left(1 + |\overline{a^2}|^2\right) \frac{(1+\sum \alpha_m^2)}{N} \sum_{s\neq 0} |R_s|^2 \tag{A.188}$$

where the bound will be very tight if the symbol duration is much larger than the width of the impulse response autocorrelation function.

The strength of the signal×noise terms, $z_{S\times N}$, is readily found to be

$$\overline{|z_{S\times N}|^2} = \frac{1+\sum \alpha_m^2}{N}\, I \sum_{p=0}^{R} e_p |b_p|^2 \approx \frac{1+\sum \alpha_m^2}{N}\, I\, R_0 \tag{A.189}$$

where we have used the same approximation (A.185). Using (A.188) and (A.189) and the definition of ρ_i (A.174),

$$\overline{|z_{S\times SN}|^2} \le \left(1 + |\overline{a^2}|^2\right)\rho_i \left(\frac{\sum_{s\neq 0} |R_s|^2}{|R_0|^2} \right) \overline{|z_{S\times N}|^2} \tag{A.190}$$

Thus, to neglect the signal×self noise terms, it is necessary that

$$\rho_i << \left(\frac{1}{1+|\overline{a^2}|^2}\right) \frac{|R_0|^2}{\sum_{-\infty}^{\infty} |R_s|^2} \tag{A.191}$$

The ratio on the left can be converted to a frequency domain expression. With the aid of Parseval's Theorem, one may readily show that

$$\sum_{-\infty}^{\infty} |R_s|^2 = \frac{1}{\Delta^3} \int |H(f)|^4\, df \tag{A.192}$$

$$|R_0|^2 = \frac{1}{\Delta^2} \left[\int |H(f)|^2\, df \right]^2 \tag{A.193}$$

where $H(f)$ is the composite channel transfer function. Then the inequality, (A.191), becomes

$$\rho_i << \frac{1}{1+|\overline{a^2}|^2}\, w \tag{A.194}$$

where the parameter

$$w = \frac{\left[\frac{1}{W}\int_{-W/2}^{W/2} |H(f)|^2\, df\right]^2}{\frac{1}{W}\int_{-W/2}^{W/2} |H(f)|^4\, df} \tag{A.195}$$

Note (from (A.192) and (A.193)) that w is upper-bounded by unity. If the composite channel transfer function were an ideal rectangular bandpass filter with bandwidth B, then

$$w = B/W \quad ; \qquad \text{ideal channel of bandwidth } B \tag{A.196}$$

In such a case, by making B small enough, the inequality (A.194) will eventually be violated, since the self noise becomes ever larger as B is made smaller.

Assuming that the terminal equipment filter bandwidth $W = 1/\Delta$ Hz, there is no way that the composite HF channel can look like a bandpass filter of bandwidth $B << W$. In fact, for a single propagation mode of arbitrary dispersion, w will be very nearly equal to unity, and $|R_s|^2$ will drop to small values for $s \neq 0$. The described behavior is a consequence of the fact that for a single propagation mode the HF channel will have an essentially constant transfer function amplitude over the $W = 1$ MHz bandwidth, so that $|H(f)|^2$ will be determined entirely by the cascade of the terminal equipment filters and the chip pulse filter.

For multiple modes w will become smaller, but specific calculations have to be carried out. It is doubtful that w will become much smaller than unity for typical multimodal HF channel characteristics. As a consequence, the condition $\rho_i <<< 1$ should make the signal×self noise term small compared to the signal×noise term at the combiner output.

It is also of interest to compare the signal×self noise power to the desired signal power $|R_o|^2$. The result is

$$\frac{\overline{|z_{S\times SN}|^2}}{|R_0|^2} \leq (1 + |\overline{a^2}|^2)\frac{(1 + \sum(\alpha_m)^2)}{N}\frac{\sum_{s\neq 0}|R_s|^2}{|R_0|^2}$$

$$= \frac{(1 + |\overline{a^2}|^2)(1 + \sum(\alpha_m)^2)}{N\Delta w} = \frac{(1 + |\overline{a^2}|^2)(1 + \sum(\alpha_m)^2)}{Tw} \tag{A.197}$$

where $T = N\Delta$ is the duration of the integrate-and-dump. Since Δw will not be much less than unity, it is clear that the signal×self noise strength will be small compared to the signal strength whenever $N >> 1$ for the wide band HF channel. A similar conclusion was reached by Price [A.2] for analog transmission by the Rake technique.

We consider now the strength of the self noise×self noise signal, $z_{SN\times SN}$, in relation to the strength of the noise×noise, $z_{N\times N}$, at the combiner output. The strength of $z_{SN\times SN}$ is just twice the value of the term SN*×SN presented in (A.121). Thus,

$$\overline{|z_{SN\times SN}|^2} = \frac{\sum \alpha_m^2)}{N^2} \sum_{p=0}^{R} \sum_{q=0}^{R} f_p f_q \sum_{s\neq 0} \left(b^*_{p+s} b_{q+s} + |\overline{a^2}|^2 b^*_{p+s} b_{q-s} \Gamma(\frac{s}{N}) \right)$$
$$\times \sum_{s\neq 0} \left(b_{p+s} b^*_{q+s} + |\overline{a^2}|^2 b_{p+s} b^*_{q-s} \text{ Tri}(\frac{s}{N}) \right) \qquad \text{(A.198)}$$

Consider first the case of QPSK chip modulation ($|\overline{a^2}|^2 = 0$), for which (A.198) may be expressed in the form

$$\overline{|z_{SN\times SN}|^2} = \frac{\sum \alpha_m^2}{N^2} \sum_{p=0}^{R} \sum_{q=0}^{R} f_p f_q \left(R_{q-p} - b^*_p b_q\right) \left(R^*_{q-p} - b_p b^*_q\right) \qquad \text{(A.199)}$$

where we have used

$$R_{q-p} = \sum_{-\infty}^{\infty} b^*_{p+s} b_{q+s} \qquad \text{(A.200)}$$

The sequence f_p represents a set of rectangular Rake "windows" placed over individual HF propagation modes. We define the autocorrelation function of this (0,1) window sequence as

$$W_k = \sum_p f_p f_{p+k} \leq W_o = N_T \qquad \text{(A.201)}$$

where N_T was defined as the total number of taps included in all Rake windows.

Expanding (A.198) and using (A.185) and (A.201),

$$\overline{|z_{SN\times SN}|^2} = \frac{\sum \alpha_m^2}{N^2} \left(\sum_k (W_k - 2) |R_k|^2 + |R_o|^2 \right) \qquad \text{(A.202)}$$

If the inequality (A.201) is used, we obtain the bound

$$\overline{|z_{SN\times SN}|^2} \leq \frac{\sum \alpha_m^2}{N^2} \left(N_T \sum |R_k|^2 + |R_o|^2 \right) \qquad \text{(A.203)}$$

The strength of the noise×noise term is from (A.180), (A.170), and (A.171),

$$\overline{|z_{N\times N}|^2} = \frac{\sum \alpha_m^2}{N^2} I^2 N_T \qquad \text{(A.204)}$$

Using (A.204) and (A.194) in (A.203)

$$\overline{|z_{SN\times SN}|^2} \leq \frac{\rho_i^2}{w}\,\overline{|z_{N\times N}|^2} \tag{A.205}$$

assuming $N_R >> 1$. Thus, in order for the self noise×self noise term to be neglected in relation to the noise×noise term, it is necessary that

$$w >> \rho_i^2 \tag{A.206}$$

A comparison of (A.206) with inequality (A.194) reveals that satisfaction of (A.194) implies satisfaction of (A.206) when $\rho_i < 1$. Moreover, as already noted, w is upper-bounded by unity. Thus, satisfaction of (A.194) also guarantees that the noise×self noise terms may be neglected relative to the noise×noise terms. For the case of QPSK, satisfaction of the single inequality

$$w >> \rho_i \tag{A.207}$$

is sufficient to allow self noise effects to be neglected in performance analyses.

Consider now the case of BPSK chip modulation ($\left|\overline{a^2}\right|^2 = 1$). Then (A.198) can be expressed as the sum of four terms

$$\begin{aligned}\overline{|z_{SN\times SN}|^2} = \frac{\sum \alpha_m^2}{N^2}\Bigg[&\sum\sum f_p f_q \sum_{s\neq 0} b_{p+s}^* b_{q+s} \sum_{r\neq 0} b_{p+r} b_{q+r}^* \\ &+ \sum\sum f_p f_q \sum_{s\neq 0} b_{p+s}^* b_{q+s} \sum_{r\neq 0} \mathrm{Tri}(\tfrac{r}{N})\, b_{p+r} b_{q-r}^* \\ &+ \sum\sum f_p f_q \sum_{r\neq 0} b_{p+r} b_{q+r}^* \sum_{s\neq 0} \Gamma(\tfrac{s}{N})\, b_{p+s}^* b_{q-s} \\ &+ \sum\sum f_p f_q \sum_{r\neq 0} \mathrm{Tri}(\tfrac{r}{N})\, b_{p+r} b_{q-r}^* \sum_{s\neq 0} \Gamma(\tfrac{s}{N})\, b_{p+s}^* b_{q-s} \Bigg]\end{aligned} \tag{A.208}$$

Upon interchanging the order of summations, we obtain

$$\begin{aligned}\overline{|z_{SN\times SN}|^2} = \frac{\sum \alpha_m^2}{N^2}\Bigg[&\sum_{s\neq 0}\sum_{r\neq 0} |A_{sr}|^2 + \sum_{s\neq 0}\sum_{r\neq 0} \mathrm{Tri}(\tfrac{r}{N}) Re\{A_{sr}\, A_{s,-r}^*\} \\ &+ \sum_{s\neq 0}\sum_{r\neq 0} \Gamma(\tfrac{s}{N})\, Re\{A_{sr}\, A_{-s,r}^*\} \\ &+ \sum\sum\ \Gamma(\tfrac{s}{N})\ \mathrm{Tri}(\tfrac{r}{N})\ Re\{A_{s,r}\, A_{-s,-r}^*\} \Bigg]\end{aligned} \tag{A.209}$$

where

$$A_{sr} = \sum f_p \, b^*_{p+s} \, b_{p+r} \tag{A.210}$$

But it may be shown that the second, third, and fourth sums in (A.209) are individually upper-bounded by the first sum.* However, this first sum is identical to the strength of the self noise×self noise term for QPSK chip modulation. It follows from (A.202)–(A.205) that for BPSK chip modulation

$$\overline{|z_{SN\times SN}|^2} \leq \left(\frac{(2\rho_i)^2}{w}\right) \overline{|z_{N\times N}|^2} \tag{A.211}$$

assuming $N_T >> 1$. Thus, to neglect the self noise×self noise term in relation to the noise×noise term, it is necessary that

$$w >> (2\rho_i)^2 \tag{A.212}$$

However, from (A.194) we see that, provided $2\rho_i < 1$, satisfaction of (A.194) implies satisfaction of (A.212). Thus, combining the results for BPSK and QPSK chip modulation, provided $2\rho_i < 1$, we can neglect self noise contributions when

$$\rho_i << \frac{1}{1 + \left|\overline{a^2}\right|^2} \, w \tag{A.213}$$

A.4.3.3 Output SNR and Error Rate Evaluation for Binary PSK Data and Chip Modulation

We consider here the evaluation of modem performance when self noise cannot be neglected. The self noise terms derived previously ignore any degradations due to Doppler shift. This is consistent with high bit rate operation, where the tap gain filter time constant can be made small compared with the reciprocal Doppler shift and yet keep the SNR degradation due to additive noise acceptably small. We consider then the expression for ρ, (A.47), the SNR at the coherent combiner output, assuming slow fading and ignoring the effect of Doppler shift. Then, using (A.50), (A.99), and (A.162) we may express ρ in the form

$$\rho = \frac{\rho_0}{1 + \sum \alpha_m^2 \left(1 + \frac{2A_1}{N}\right) + \frac{2N_T \sum \alpha_m^2}{\rho_0} + \frac{\rho_0}{\rho_\infty}} \tag{A.214}$$

*For example, use the results in Chapter X of [A.3].

where ρ_0 is the value of ρ for perfect channel measurement (see (A.52) and (A.58)) and ρ_∞ depends on the self noise parameters A_1,B_1,C_1, given by

$$A_1 = \frac{1}{E}\left(\sum_{s=1}^{\infty}\sum_{p=0}^{R} f_p|c_{pk}|^2 - \sum_{s=1}^{\infty}\mathrm{Tri}_c(\frac{s}{N})\sum_{p=0}^{R} f_p\ Re\{b_{p+s}b_{p-s}^*\}\right) \tag{A.215}$$

$$B_1 = \frac{1}{E^2}\left(\sum_{s=1}^{\infty}\sum_{r=1}^{\infty} Re^2\Big\{\sum_{p=0}^{R} f_p c_{ps}^* c_{pr}\Big\} - 2\sum_{s=1}^{\infty}\sum_{r=1}^{\infty}\mathrm{Tri}_c(\frac{s}{N})\sum_{p=0}^{R} f_p\ Re\{b_{p+s}^* c_{pr}\}\sum_{q=0}^{R} f_q \mathrm{Re}\{b_{q-s}^* c_{qr}\}\right) \tag{A.216}$$

$$C_1 = \frac{1}{E^2}\left(\sum_{s=1}^{\infty} Re^2\Big\{\sum_{p=0}^{R} f_p b_p^* c_{ps}\Big\} - 2\sum_{s=1}^{\infty}\mathrm{Tri}_c(\frac{s}{N})Re\Big\{\sum_{p=0}^{R} f_p b_p^* b_{p+s}\Big\}Re\Big\{\sum_{q=0}^{R} f_q b_q^* b_{q-s}\Big\}\right) \tag{A.217}$$

$$E = \sum_{q=0}^{R} f_p\ |b_p|^2 \tag{A.218}$$

$$\rho_\infty = \frac{1}{\frac{\sum \alpha_m^2}{N^2}\ B_1 + \frac{1+\sum \alpha_m^2}{N}\ C_1} \tag{A.219}$$

The parameter E is proportional to the received signal power after tap excision.

Computation of the E_b/N_o required to achieve a given error rate proceeds as follows. First, the necessary value of ρ_0 is obtained by solving (A.214) for ρ_0 given the value ρ needed to achieve the desired error rate. This value of ρ has been shown to be equal to the value of E_b/N_o required to achieve the desired error rate when the modem and codec are operating over the AWGN channel. As mentioned previously, for the rate 1/2 constant length 7 coder and Viterbi decoder using three-bit soft decisions, E_b/N_o = 4.3 dB is required for 10^{-5} bit error rate assuming binary PSK. Thus, for

10^{-5} bit error rate, one would solve (A.214) for ρ_0 given $\rho = 4.3$ dB. The relationship between E_b/N_o and ρ_0 is (see (A.52) and (A.60)),

$$\frac{E_b}{N_o} = \rho_0 \frac{\sum_{p=0}^{R} |b_p|^2}{\sum_{p=0}^{R} f_p \, |b_p|^2} \tag{A.220}$$

Thus, (A.220) allows computation of the required E_b/N_o given the required value of ρ_0 to achieve the desired error rate. If very little of the multipath energy is excluded by the tap excision procedure, the required E_b/N_o will be nearly equal to the required ρ_0. In the case where there is too much multipath to be handled by the number of Rake taps available, the required E_b/N_o will exceed ρ_0.

Note from (A.214) that for a given pattern of excised taps, the self noise produces an *irreducible* error rate, since even when the transmitted power becomes arbitrarily large and $\rho_0 \to \infty$, the coherent combiner output SNR approaches the limiting value ρ_∞.

$$\lim_{\rho_0 \to \infty} \rho = \rho_\infty \tag{A.221}$$

When ρ_∞ is less than the desired value of ρ, e.g., 4.3 dB, the desired error rate performance cannot be reached for any transmitted power. However, by increasing the number of taps excised, the value of ρ_∞ can be increased at the expense of reducing E, the effective received signal power after tap excision. There will be an optimum number of taps to excise which minimizes the transmitter power required to achieve a specified performance.

A.4.4 Effect of Decision-Directed Errors

The previous analyses assume that the hard decision error rate at the Rake combiner output is small enough to have negligible effect on the tap weight generation process shown in figure A.2. However, the use of an efficient codec plus Doppler correction and long tap weight filter time constants can reduce E_b/N_o requirements to the point that the hard decision error rate can be in the 10^{-1} to 10^{-2} range, even though the decoded error rate is satisfactory, e.g., 10^{-5}. The following analysis is provided to assess the SNR degradation caused by hard decision errors.

To simplify the presentation, self noise is neglected and attention is confined to binary PSK chip and data modulation, although the analysis is readily extended to include the more general cases.

Assuming decision errors, the tap weight for the p-th tap and the k-th I&D output has the representation

$$g_{pk} = \sum_{m=0}^{\infty} \alpha_m \, \tilde{d}^*_{k-m-1} \, y_{p,k-m-1} \tag{A.222}$$

instead of (A.33), where $\tilde{d}_k$ is the raw data decision at the Rake combiner output after the k-th I&D outputs have been weighted and summed.

Using (A.32) in (A.222) and ignoring the self noise,

$$g_{pk} = \tilde{b}_{R-p}(kT - T) + \tilde{n}_{pk} \tag{A.223}$$

where $\tilde{b}_{R-p}(kT - T)$ is the signal component and $\tilde{n}_{pk}$ is the additive noise component of the tap weight process,

$$\tilde{b}_{R-p}(kT) = \sum_{m=0}^{\infty} \alpha_m \, \delta_{k-m-1} \, b_{R-p}(kT - mT) \tag{A.224}$$

$$\tilde{n}_{pk} = \sum_{m=0}^{\infty} \alpha_m \, \tilde{d}^*_{k-m-1} \, n_{p,k-m-1} \tag{A.225}$$

where the random sequence

$$\delta_k = \tilde{d}^*_k \, d_k = \begin{cases} 1\,; & \text{no hard decision error on } k\text{-th symbol} \\ -1\,; & \text{hard decision error on } k\text{-th symbol} \end{cases} \tag{A.226}$$

The mean signal is

$$\bar{\tilde{b}}_{R-p}(kT - T) = \sum_{m=0}^{\infty} \bar{\delta}_{k-m-1} \, b_{R-p}(kT - mT - T) \tag{A.227}$$

If q denotes the hard decision error probability, then

$$\bar{\delta}_k = 1 - 2q \tag{A.228}$$

and

$$\bar{\tilde{b}}_{R-p}(kT) = (1 - 2q) \, \hat{b}_{R-p}(kT) \tag{A.229}$$

where $\hat{b}_{R-p}(kT - T)$, given by (A.39), is the tap weight signal component without decision errors. *Thus, one effect of decision errors is to suppress the signal component*

at the tap weight output by a factor $(1-2q)$. Another is to introduce a fluctuating component

$$\tilde{b}_{R-p}(kT-T)-\bar{\tilde{b}}_{R-p}(kT-T)=\sum_{m=0}^{\infty}\alpha_m\,\epsilon_{k-m-1}\,b_{R-p}(kT-mT-T) \tag{A.230}$$

where

$$\epsilon_k=\delta_k-1+2q \tag{A.231}$$

Including the variation of $b_{R-p}(kT-mT-T)$ with m over the time constant of the tap weight filter in (A.230) will have, at most, a second-order effect on our final results. For convenience in the analysis, we neglect this variation and use

$$\tilde{b}_{R-p}(kT-T)-\bar{\tilde{b}}_{R-p}(kT-T)\approx\hat{b}_{R-p}(kT-T)\,\mu_k \tag{A.232}$$

where

$$\mu_k=\sum_{m=0}^{\infty}\alpha_m\,\epsilon_{k-m-1} \tag{A.233}$$

Then,

$$\tilde{b}_{R-p}(kT)=(1-2q)\;\hat{b}_{R-p}(kT)+\mu_k\;\hat{b}_{R-p}(kT) \tag{A.234}$$

The Rake combiner complex output for the k-th symbol is given by

$$C_k=\sum_{p=0}^{R}e_p\big(\tilde{b}^*_{R-p}(kT-T)+\tilde{n}^*_{pk}\big)\big(d_k\,b_{R-p}(kT)+n_{pk}\big) \tag{A.235}$$

With coherent demodulation and BPSK modulation, only the real part of C_k is important. Thus, we define

$$Re\{C_k\}=\overline{S}_k+N_k \tag{A.236}$$

where $\overline{S}_k, N_k$ are the mean signal and noise components, respectively, of the coherent demodulated combiner output. Here we assign the fluctuating portion of the signal due to previous data decision errors as part of the combiner output noise. Thus,

$$\begin{aligned}\overline{S}_k&=d_k\sum_{p=0}^{R}e_p\;\bar{\tilde{b}}^*_{R-p}(kT-T)\;b_{R-p}(kT)\\&=d_k(1-2q)\,Re\Big\{\sum_{p=0}^{R}e_p\hat{b}^*_{R-p}(kT-T)\,b_{R-p}(kT)\Big\}\end{aligned} \tag{A.237}$$

$$N_k = Re\Big\{ \sum_{p=0}^{R} e_p \tilde{n}_{pk}^* n_{pk} + (1-2q+\mu_k) \sum_{p=0}^{R} e_p \hat{b}_{R-p}^*(kT-T)\, n_{pk} + d_k \sum_{p=0}^{R} e_p b_{R-p}(kT) \tilde{n}_{pk}^* \Big\}$$

$$+ d_k \mu_k\, Re\Big\{ \sum_{p=0}^{R} e_p \hat{b}_{R-p}^*(kT-T)\, b_{R-p}(kT) \Big\} \qquad \text{(A.238)}$$

In the previous analysis without decision errors it was argued that N_k could be modeled as a normally distributed random variable via Central Limit Theorem arguments based upon the assumption that the number of non-excised Rake taps is large. Except for the last term in (A.239) the same argument applies. The randomness in the last term is due entirely to the random variable ϵ_k. As (A.230) shows, this variable is a filtered stream of ± 1 hard decision error variables with the mean value $1-2q$ removed. In order to carry out a simple analysis, we shall have to assume the filter time constant is long enough and the error rate is high enough for the Central Limit Theorem to be invoked. Then we can assume ϵ_k is also normally distributed. Computation of error rates then can be carried out if

$$\rho = \frac{|\overline{S_k}|^2}{\overline{|N_k|^2}} \qquad \text{(A.239)}$$

is determined.

Proceeding as in section A.4.2, we find

$$\overline{N_k^2} = \overline{\mu_k^2}\; Re^2\Big\{ \sum_{p=0}^{R} e_p \hat{b}_{R-p}^*(kT-T) b_{R-p}(kT) \Big\} + \frac{I^2}{2N^2} (\sum \alpha_m^2) N_T$$

$$+ \Big((1-2q)^2 + \overline{\mu_k^2} \Big)\, \frac{I}{2N} \sum_{p=0}^{R} e_p\, |\hat{b}_{R-p}(kT-T)|^2 + \frac{I}{2N} (\sum \alpha_m^2) \Big(\sum_{p=o}^{R} e_p\, |b_{R-p}(kT)|^2 \Big)$$

$$\text{(A.240)}$$

In order to complete the analysis, it is necessary to obtain an evaluation of the strength of ϵ_k. From (A.233),

$$\overline{\mu^2} = \sum_{0}^{\infty} \sum_{0}^{\infty} \alpha_m \alpha_n \overline{\epsilon_{k-m-1} \epsilon_{k-n-1}} = \sum_{-\infty}^{\infty} \gamma(m)\, R_\epsilon(m) \qquad \text{(A.241)}$$

where $\gamma(m)$ is the aperiodic autocorrelation function of the tap weight filter and $R_\epsilon(m)$ is the autocorrelation function of the sequence $\{\epsilon_k\}$. But

$$R_\epsilon(n) = 4\big(P(n) - q^2\big) \qquad \text{(A.242)}$$

where $P(n)$ is the probability that a pair of hard decision errors occur spaced n symbols apart. Clearly

$$P(0) = q \tag{A.243}$$

$$P(\infty) = q^2 \tag{A.244}$$

If we ignore the burst characteristics of $\{\epsilon_k\}$, i.e., assume ϵ_k is an uncorrelated sequence,

$$P(n) = q^2 \;\; ; \qquad n > 0 \tag{A.245}$$

and

$$\overline{\mu^2} = 4q(1-q)\sum \alpha_m^2 \tag{A.246}$$

It seems likely that such an assumption will lead to an underestimate for $\overline{\mu^2}$ and thus an underestimate of the SNR degradation caused by hard decision errors. However, note that for a long tap gain filter impulse response, $\sum \alpha_m^2 \prec\prec 1$, $\overline{\mu^2}$ will be small compared to unity and will have very little impact on the output SNR. In such a case, one need only include the $(1-2q)$ reduction in tap gain signal on the output SNR.

Using (A.246), (A.240), and (A.237) in (A.239), one may obtain an expression for ρ that depends upon q, the hard decision error probability. However, assuming that the combiner output is normally distributed, we have the relationship

$$\phi\left(\sqrt{\rho(q)}\right) = q \tag{A.247}$$

where

$$\phi(y) = \int_y^\infty \frac{1}{\sqrt{2\pi}} exp(-\frac{x^2}{2})dx \tag{A.248}$$

Thus, to actually determine q, it is necessary to solve the nonlinear equation (A.247).

We consider this solution in detail only for the case of a single propagation mode with a Doppler shift ν Hz. From (A.74)-(A.77), we determine that, without delay compensation,

$$Re^2\Big\{\sum_{p=o}^{R} e_p \hat{b}^*_{R-p}(kT-T)b_{R-p}(kT)\Big\} = Re^2\Big\{G(\nu)\, e^{-j2\pi\nu T}\Big\}\Big(\sum_{p=0}^{R} e_p|b_{R-p}(kT)|^2\Big)^2 \tag{A.249}$$

$$\sum_{p=o}^{R} e_p|\hat{b}_{R-p}(kT-T)|^2 = |G(\nu)|^2 \sum_{p=o}^{R} e_p|b_{R-p}(kT)|^2 \tag{A.250}$$

where $G(\cdot)$ is the transfer function of the tap weight filter.

The combiner output SNR for perfect channel measurement, ρ_0, is given by

$$\rho_0 = \frac{2N}{I} \sum_{p=o}^{R} e_p |b_{R-p}(kT)|^2 \tag{A.251}$$

Using (A.237), (A.240), (A.246), and (A.249)–(A.251) in (A.239), we obtain the following expression for the boxcar filter,

$$\rho = \frac{(1-2q)^2 \; Re^2\{G(\nu)\, e^{-j2\pi\nu T}\}\rho_0}{\left[(1-2q)^2 + \overline{\mu^2}\right] |G(\nu)|^2 + \frac{1}{N_F} + \frac{2N_T}{N_F\,\rho_0} + \overline{\mu^2}\,\rho_0\, Re^2\{G(\nu)\, e^{-j2\pi\nu T}\}} \tag{A.252}$$

where N_F is the duration of the tap filter impulse response in numbers of symbols. For binary PSK data modulation and a rate 1/2 code, it was shown that

$$\frac{E_b}{N_o} = \frac{2N}{I} \sum |b_p(kT)|^2 \tag{A.253}$$

so that

$$\frac{E_b}{N_o} = \rho_0 \, \frac{\sum |b_p(kT)|^2}{\sum f_p |b_p(kT)|^2} \tag{A.254}$$

Given a specific tap excision procedure, the mode Doppler shift, and the burst parameter b, it is possible to relate ρ_0 and q, or equivalently, E_b/N_o and q (using (A.254)), via the solution of the nonlinear equations (A.247) and (A.252).

Numerical evaluation of the relation between ρ_0 and q is most simply obtained as follows. Invert (A.247) to obtain

$$\rho(q) = \left[\phi^{-1}(q)\right]^2 \tag{A.255}$$

Then selection of a value of q yields a value of ρ. However, with q and ρ known, the solution of ρ_0 from (A.252) involves no more than the determination of the positive root of a quadratic equation.

When delay compensation is used via the structure shown in figure A.3, only the SNR at the combiner output for the *data path* changes from (A.252). The data path SNR becomes

$$\rho_{data} = \frac{(1-2q)^2 \, |G(\nu)|^2 \, \rho_0}{\left[(1-2q)^2 + \overline{\mu^2}\right] |G(\nu)|^2 + \frac{1}{N_F} + \frac{2N_T}{N_F\,\rho_0} + \overline{\mu^2}\,\rho_0\, |G(\nu)|^2} \tag{A.256}$$

In order to evaluate the performance of the coded system with delay compensation, it is necessary to develop a curve relating ρ_{data} to ρ_0 or E_b/N_o. The desired curve is obtained by using the previously-computed relationship between ρ_0 and q in (A.256). From this curve, the value of E_B/N_o required to achieve a desired value of ρ_{data}, e.g., 4.3 dB, may be determined.

Note that when the tap weight integration time is long, ($N_F >> 1$), $\overline{\mu^2}$ may be set to zero in (A.252) and (A.256), and $1/N_F$ may be neglected, yielding the simplified expressions

$$\rho \approx \frac{(1-2q)^2\, Re^2\{G(\nu)\, e^{-j2\pi\nu T}\}\rho_0}{(1-2q)^2\, |G(\nu)|^2 + \dfrac{2N_T}{N_F\, \rho_0}} \; ; \quad P >> 1 \tag{A.257}$$

$$\rho_{data} \approx \frac{(1-2q)^2\, |G(\nu)|^2\, \rho_0}{(1-2q)^2\, |G(\nu)|^2 + \dfrac{2N_T}{N_F\, \rho_0}} \; ; \quad P >> 1 \tag{A.258}$$

A.5 ANALYSIS OF THREE OTHER RAKE MODEMS

In this section we present performance analyses for three non-decision-directed Rake modems: the parallel-probe, serial-probe, and the DPSK Rake modems. Sections A.5.1–A.5.3 considers these modems individually.

A.5.1 The Parallel-Probe Rake Modem

In the parallel-probe Rake modem both a non-data-modulated probe DSPN sequence and a statistically independent, data-modulated DSPN sequence are transmitted. The received DSPN probe is used to estimate the tap weights for the Rake combiner. Figure A.4 presents a block diagram of the parallel-probe Rake demodulator processing. Two local PN generators are used to correlate against the received signal at each tap of the delay line. The probe correlator and the data correlator produce outputs at the I&D rate. A digital filter averages the probe I&D output to produce the tap weight as shown in figure A.4. Note that because of the absence of the decision-directed operation, the optional compensating delay may be inserted between the data I&D and the tap weighting.

Using the composite channel model, the transmitted signal $s(t)$ consists of the sum of two impulse trains

$$s(t) = \frac{1}{\sqrt{1+\gamma}} \sum m_k a_k\, \delta(t - k\Delta) + \sqrt{\frac{\gamma}{1+\gamma}} \sum a_k^{(p)}\, \delta(t - k\Delta) \tag{A.259}$$

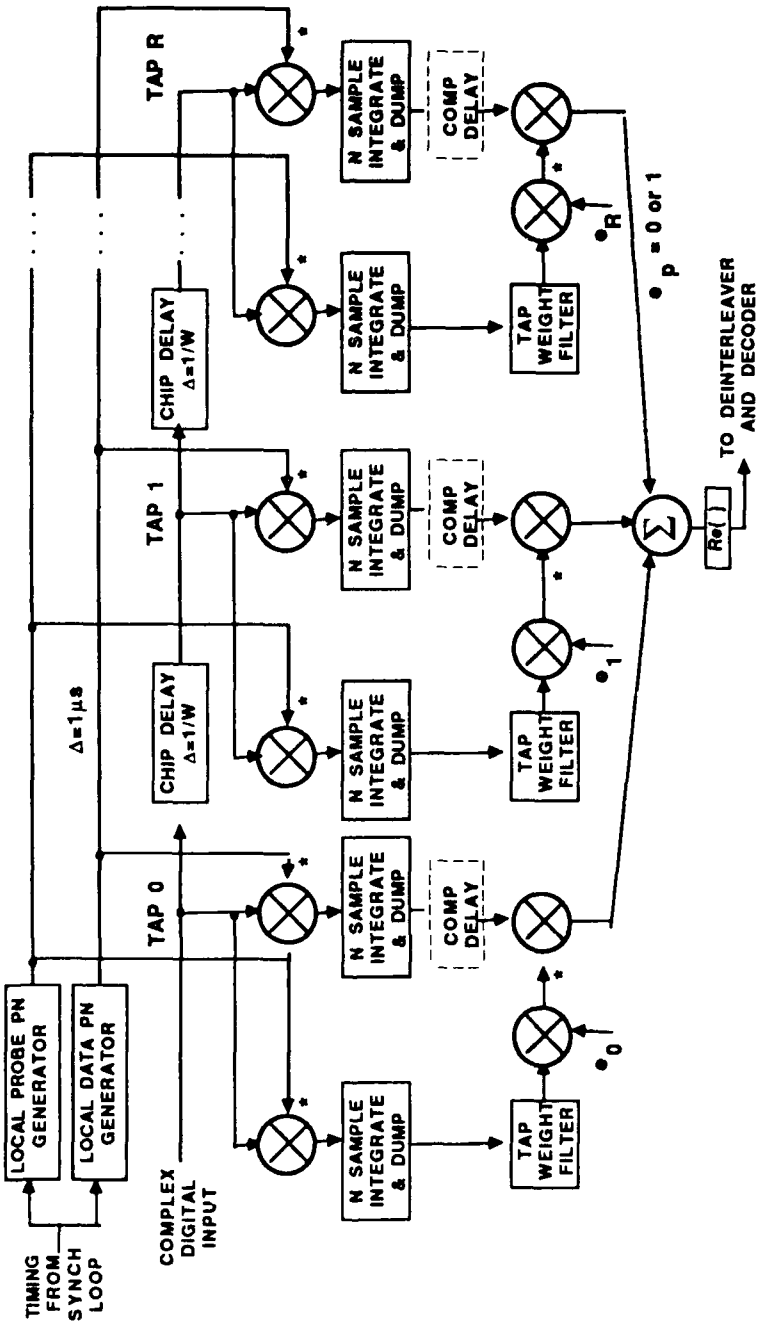

Figure A.4. A Parallel-Probe Coherent Rake Processor

where γ is the ratio of the power in the transmitted probe signal to the power in the transmitted data signal, and $a_k^{(p)}$ is the probe chip modulation. The other variables are the same as defined previously for the decision-directed system. Then the sampled signal at the input to the Rake demodulator may be represented as

$$w_k = \frac{1}{\sqrt{1+\gamma}} c_k + \sqrt{\frac{\gamma}{1+\gamma}} c_k^{(p)} + n_k \tag{A.260}$$

where c_k is identical to the sampled received signal for the decision-directed case (A.11), n_k is the sampled noise, and

$$c_\ell^{(p)} = \sum b_k(\ell\Delta)\, a_{\ell-k}^{(p)} \tag{A.261}$$

is proportional to the sampled received probe signal.

Carrying out the I&D operations and using the slow fading assumptions (c.f.(A.12)-(A.31)), it is found that the data I&D output may be represented as

$$y_{pk} = \frac{1}{\sqrt{1+\gamma}} d_k b_{R-p}(kT) + \frac{1}{\sqrt{1+\gamma}} x_{pk} + \sqrt{\frac{\gamma}{1+\gamma}} x_{pk}^{(dp)} + n_{pk} \tag{A.262}$$

where the new term in (A.262), $x_{pk}^{(dp)}$, is an additional self noise term due to the transmitter probe

$$x_{pk}^{(dp)} = \sum_s b_{R-p+s}(kT)\, R_{ks}^{(dp)} \tag{A.263}$$

in which

$$R_{ks}^{(dp)} = \frac{1}{N} \sum_{n=0}^{N-1} a_{n+kN}^{*}\, a_{n+kN-s}^{(p)} \tag{A.264}$$

The probe I&D output has the analogous form

$$y_{pk}^{(p)} = \sqrt{\frac{\gamma}{1+\gamma}} b_{R-p}(kT) + \sqrt{\frac{\gamma}{1+\gamma}} x_{pk}^{(pp)} + \frac{1}{\sqrt{1+\gamma}} x_{pk}^{(pd)} + m_{pk} \tag{A.265}$$

where

$$x_{pk}^{(pp)} = \sum_{s\neq 0} b_{R-p+s}(kT)\, R_{ks}^{(pp)} \tag{A.266}$$

in which

$$R_{ks}^{(pp)} = \frac{1}{N} \sum_{n=0}^{N-1} a_{n+kN}^{(p)*}\, a_{n+kN-s}^{(p)} \tag{A.267}$$

and

$$x_{pk}^{(pd)} = \sum_{s} b_{R-p+s}(kT)\, R_{ks}^{(pd)} \tag{A.268}$$

in which

$$R_{ks}^{(pd)} = \frac{1}{N} \sum_{n=0}^{N-1} a_{n+kN}^{(p)*}\, a_{n+kN-s} \tag{A.269}$$

The tap weight process g_{pk} is given by an average over $y_{pk}^{(p)}$, i.e.,

$$g_{pk} = \sum_{0}^{\infty} \alpha_m\, y_{p,k-m}^{(p)} \tag{A.270}$$

Thus, we may represent this process as

$$g_{pk} = \sqrt{\frac{\gamma}{1+\gamma}}\, \hat{b}_{R-p}(kT) + \sqrt{\frac{\gamma}{1+\gamma}}\, \hat{x}_{pk}^{(pp)} + \frac{1}{\sqrt{1+\gamma}}\, \hat{x}_{pk}^{(pd)} + \hat{m}_{pk} \tag{A.271}$$

where the filtered signal term $\hat{b}_{R-p}(kT)$ has been defined in (A.39) and

$$\hat{x}_{pk}^{(pp)} = \sum_{0}^{\infty} \alpha_m\, x_{p,k-m}^{(pp)} \tag{A.272}$$

$$x_{pk}^{(pd)} = \sum_{0}^{\infty} \alpha_m\, x_{p,k-m}^{(pd)} \tag{A.273}$$

$$\hat{m}_{pk} = \sum_{0}^{\infty} \alpha_m\, n_{p,k-m} \tag{A.274}$$

The Rake combiner complex output for the k-th symbol is then

$$C_k = \sum_{p=0}^{R} e_p \left(\sqrt{\frac{\gamma}{1+\gamma}}\, \hat{b}_{R-p}(kT) + \sqrt{\frac{\gamma}{1+\gamma}}\, \hat{x}_{pk}^{(pp)} + \frac{1}{\sqrt{1+\gamma}}\, \hat{x}_{pk}^{(pd)} + \hat{m}_{pk} \right)^*$$
$$\times \left(\frac{1}{\sqrt{1+\gamma}}\, d_k b_{R-p}(kT) + \frac{1}{\sqrt{1+\gamma}}\, x_{pk} + \sqrt{\frac{\gamma}{1+\gamma}}\, x_{pk}^{(dp)} + n_{pk} \right) \tag{A.275}$$

The remaining analysis neglects self noise. Then the real part of the combiner output can be expressed as

$$Re\{C_k\} = S_k + N_k \tag{A.276}$$

where the signal component is given by

$$S_k = d_k \frac{\sqrt{\gamma}}{1+\gamma} Re\Big\{ \sum_{p=0}^{R} e_p \, \hat{b}^*_{R-p}(kT) \, b_{R-p}(kT) \Big\} \tag{A.277}$$

and the noise component

$$N_k = Re\{Z_k\} \tag{A.278}$$

where

$$Z_k = \sum_{p=0}^{R} e_p \left(\frac{1}{\sqrt{1+\gamma}} d_k \, b_{R-p}(kT) \hat{m}^*_{pk} + \sqrt{\frac{\gamma}{1+\gamma}} \, \hat{b}^*_{R-p}(kT) \, n_{pk} + n_{pk} \hat{m}^*_{pk} \right) \tag{A.279}$$

is the complex noise output.

The mean squared value of N_k is found to be (c.f. (A.63)–(A.66))

$$\overline{N_k^2} = \frac{1}{2}\overline{|Z_k|^2} = \frac{I^2}{2N^2}\Big(\sum \alpha_m^2\Big) N_T + \frac{\gamma}{1+\gamma} \frac{I}{2N} \sum_{p=0}^{R} e_p \, |\hat{b}_{R-p}(kT)|^2 + \frac{1}{1+\gamma} \frac{I}{2N} \sum \alpha_m^2 \sum_{p=0}^{R} e_p \, |b_{R-p}(kT)|^2 \tag{A.280}$$

where N_T is the total number of unexcised taps. Using (A.277) and (A.280), the output SNR can be expressed in the form

$$\rho_k = \frac{\beta_k \, \rho_{ok}/(1+\gamma)}{\frac{1}{\gamma}\Big(\sum \alpha_m^2\Big)\left(\frac{2N_T}{\rho_{ok}/(1+\gamma)} + 1\right) + \chi_k} \tag{A.281}$$

where the factors β_k, χ_k depend on the channel impulse response shape and the Rake window function e_p at the k-th I&D.

$$\beta_k = \frac{Re^2\Big\{ \sum_{p=0}^{R} e_p \, \hat{b}^*_{R-p}(kT) \, b_{R-p}(kT) \Big\}}{\Big[\sum_{p=0}^{R} e_p \, |b_{R-p}(kT)|^2 \Big]^2} \tag{A.282}$$

$$\chi_k = \frac{\sum_{p=0}^{R} e_p \, |\hat{b}_{R-p}(kT)|^2}{\sum_{p=0}^{R} e_p \, |b_{R-p}(kT)|^2} \tag{A.283}$$

and it will be recalled that

$$\rho_{ok} = \frac{2N}{I} \sum_{p=0}^{R} e_p \, |b_{R-p}(kT)|^2 \tag{A.284}$$

is the combiner output SNR for ideal noise-free tap weights in the case of decision-directed operation.

Assuming $(E_b/N_o)_k$ is defined to include the energy in the probe and data

$$\rho_{ok} = (E_b/N_o)_k \left(\frac{\sum_{p=0}^{R} e_p \, |b_{R-p}(kT)|^2}{\sum_{p=0}^{M} |b_{R-p}(kT)|^2} \right) \tag{A.285}$$

which is the same relationship as for the decision-directed modem.

In terms of the simplified notation used above, the combiner output SNR for the decision-directed Rake modem operating without decision errors is

$$(\rho_k)_{dec.dir.} = \frac{\tilde{\beta}_k \, \rho_{ok}}{(\sum \alpha_m^2) \left(\frac{2N_T}{\rho_{ok} + 1} \right) + \tilde{\xi}_k} \tag{A.286}$$

where

$$\tilde{\beta}_k = \frac{R\epsilon^2 \left\{ \sum_{p=0}^{R} e_p \, \hat{b}^*_{R-p}(kT - T) \, b_{R-p}(kT) \right\}}{\left[\sum_{p=0}^{R} e_p \, |b_{R-p}(kT)|^2 \right]^2} \tag{A.287}$$

$$\tilde{\chi}_k = \frac{\sum_{p=0}^{R} e_p \, |\hat{b}_{R-p}(kT)|^2}{\sum_{p=0}^{R} e_p \, |b_{R-p}(kT)|^2} \tag{A.288}$$

However, with our basic slow fading hypothesis

$$\tilde{\beta}_k \approx \beta_k \tag{A.289}$$

$$\tilde{\chi}_k \approx \chi_k \tag{A.290}$$

Then, comparing (A.286) and (A.281) reveals that the parallel-probe modem behaves like a decision-directed modem with no decision errors in which the value of E_b/N_o has been reduced by the factor $1/(1+\gamma)$ and the tap gain filter parameter $\sum \alpha_m^2$ is divided by γ.

With delay compensation the factors β_k,γ_k become modified to

$$\beta_k = \frac{Re^2\Big\{\sum_{p=0}^{R} e_p\, \hat{b}^*_{R-p}(kT)\, b_{R-p}(kT-\tau_G)\Big\}}{\Big[\sum_{p=0}^{R} e_p\, |b_{R-p}(kT-\tau_G)|^2\Big]^2} \tag{A.291}$$

$$\chi_k = \frac{\sum_{p=0}^{R} e_p\, |\hat{b}_{R-p}(kT)|^2}{\sum_{p=0}^{R} e_p\, |b_{R-p}(kT-\tau_G)|^2} \tag{A.292}$$

where τ_G is the group delay of the tap weight filter.

Consider now the special case of the non-disturbed channel with Q Doppler-shifted, very slowly varying, non-overlapping modes (see (A.66)-(A.77) for background). In this case the factors β_k,χ_k become

$$\beta_k = \frac{\Big[\sum_{q=1}^{Q} E_q\, Re\{G(\nu_q)\}\Big]^2}{\Big[\sum_{q=1}^{Q} E_q\Big]^2} \tag{A.293}$$

$$\chi_k = \frac{\sum_{q=1}^{Q} E_q\, |G(\nu_q)|^2}{\sum_{q=1}^{Q} E_q} \tag{A.294}$$

where $G(f)$ is the transfer function of the tap weight filter, ν_q is the Doppler shift of the q-th modes, and E_q is its strength as it appears after tap excision

$$E_q = \sum_{p=0}^{R} e_{R-p} \, |g_q(p\Delta)|^2 \tag{A.295}$$

where $g_q(t)$ is the impulse response of the n-th propagation mode with the Doppler shift removed. The slow time variation of $g_n(t)$ has been suppressed.

With delay compensation the factor β_k changes to

$$\beta_k = \frac{\left[\sum_{q=1}^{Q} E_q \, Re\{G(\nu_q) \, e^{j2\pi\nu_q \tau_G}\} \right]^2}{\left[\sum_{q=1}^{Q} E_q \right]^2} \tag{A.296}$$

and χ_k stays the same. For small ν_q,

$$\beta_k \approx \frac{\left[\sum_{q=1}^{Q} E_q \, |G(\nu_q)| \right]^2}{\left[\sum_{q=1}^{Q} E_q \right]^2} \tag{A.297}$$

In the case of the boxcar filter, (A.297) becomes exact.

The simplest case is a single mode, for which

$$\beta_k = Re^2\{G(\nu)\} \tag{A.298}$$

$$\chi_k = |G(\nu)|^2 \tag{A.299}$$

With delay compensation

$$\beta_k \approx |G(\nu)|^2 \tag{A.300}$$

which is exact for the boxcar filter.

If we assume that the Rake window is expanded to include all the multipath energy ($R = M, e_p = 1$), then $\rho_{ok} = (E_b/N_o)_k$. For the single mode and a boxcar tap weight

filter using (A.87), (A.298), (A.299) in (A.281), the combiner output SNR becomes

$$\rho = \frac{\frac{1}{1+\gamma}(E_b/N_o)\cos^2 \pi\nu(N_F-1)T \left(\frac{\sin \pi\nu N_F T}{N_F \sin \pi\nu T}\right)^2}{\frac{1}{\gamma N_F}\left(\frac{2N_T}{\frac{1}{1+\gamma}(E_b/N_o)}+1\right)+\left(\frac{\sin \pi\nu N_F T}{N_F \sin \pi\nu T}\right)^2} \tag{A.301}$$

where we have removed the k subscripts for simplicity. With delay compensation the $\cos^2 \pi\nu(N_F-1)T$ factor in (A.301) would be eliminated.

There is an optimum γ, i.e., allocation of power to the probe relative to the data for a given E_b/N_o. Thus, while a large probe strength improves the quality of the tap weight, it reduces the data signal SNR at the data I&D output. This optimum will vary with propagation conditions.

A.5.2 The Serial-Probe Rake Modem

The block diagram of a serial-probe coherent Rake demodulator processing is shown in figure A.5. For this modem a data symbol subsequence known at the receiver is inserted with a period of P symbols. The tap gain measurement is conducted only with this subsequence, thus avoiding the use of decision-directed operation. Both the normal data symbol and the subsequence symbol epochs are obtained from the known starting state of the local PN generator in the same way they are obtained from the PN generator at the transmitter. An optimal compensating delay is shown inserted in the signal path to minimize the phase error in the complex tap gain produced by mean Doppler shift. Not shown is the fact that the data subsequence must be inserted after the coding and interleaving and deleted prior to deinterleaving and decoding.

The serial-probe coherent modem requires little additional hardware compared to the decision-directed coherent modem, in contrast to the parallel-probe modem which requires a substantial increase in hardware. In addition, the known data subsequence provides a means of direct measurement of raw error rates. Moreover, performance evaluations for specifications presented in section A.1 show essentially identical performances when parameters in the two cases are related properly (e.g., see (A.334) and (A.335)).

To maintain the same data rate as the previous system, it is necessary that the coded symbol rate, i.e., the I&D rate, be increased by a factor $P/(P-1)$. Thus, a new reduced symbol duration T'

$$T' = T(\frac{P-1}{P})$$

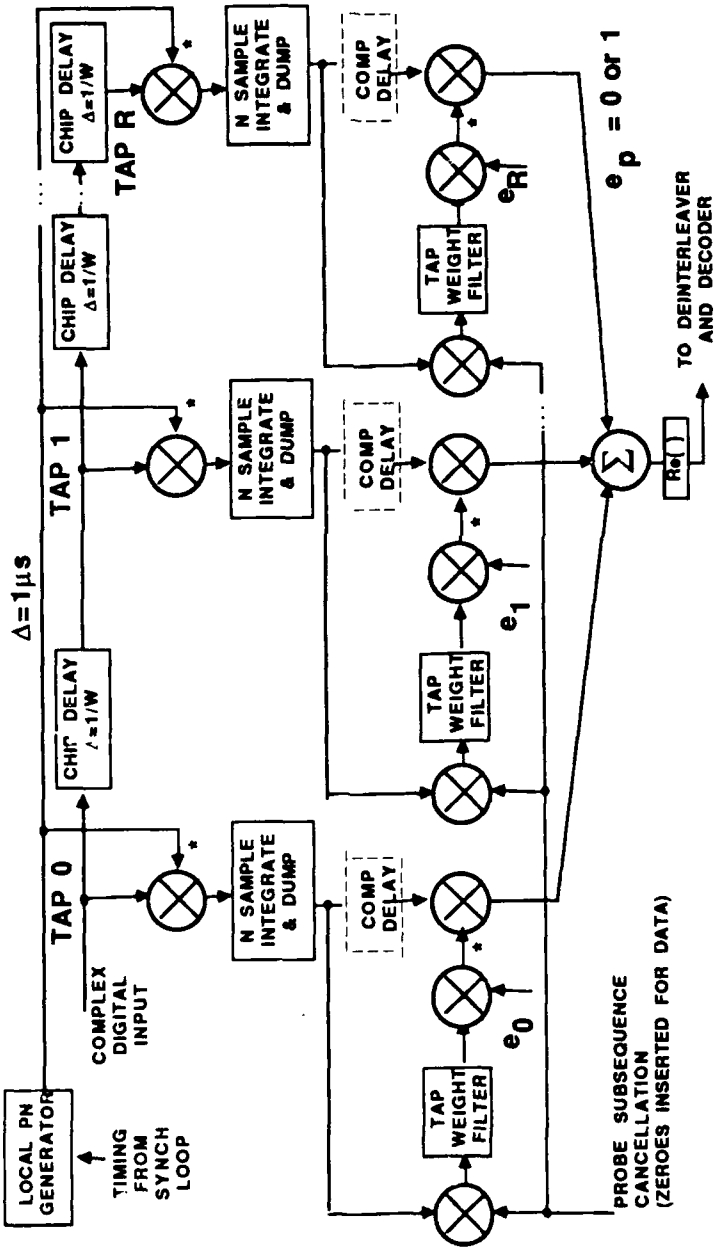

Figure A.5. A Serial-Probe Coherent Rake Processor

must be used. The number of chips in a symbol must also change if we keep the chip rate the same. Thus, the new value for the number of chips/symbol is

$$N' = \frac{N(P-1)}{P} \tag{A.302}$$

Another difference between the systems is in the tap weight filters and tap weighting. The serial-probe digital tap weight filter gets an input every PT' seconds and the same tap weight is applied to the following $(P-1)$ data symbols before it is updated. The weight will be most "out-of-date" for the last of these data symbols. Thus, if we represent the complex combiner output for the k-th I&D output as

$$C_k = \sum g^*_{pk}\, y_{pk} \tag{A.303}$$

and we assume that the probe symbols occur at $k = nP$, the combiner outputs containing data are

$$C_k = \sum g^*_{p,nP}\, y_{pk} \quad ; \tag{A.304}$$

$$k = nP+1, nP+2, \ldots, nP+P-1$$

$$n = \text{an integer}$$

where, assuming slow fading,

$$y_{pk} = d_k\, b_{R-p}(kT') + x_{pk} + n_{pk} \quad ; \quad k \neq nP \tag{A.305}$$

$$y_{pk} = b_{R-p}(kT') + x_{pk} + n_{pk} \quad ; \quad k = nP \tag{A.306}$$

$$g_{p,nP} = \tilde{b}_{R-p}(nPT') + \tilde{x}_{p,nP} + \tilde{n}_{p,nP} \tag{A.307}$$

where

$$\tilde{b}_{R-p}(nPT') = \sum_{m=0}^{\infty} b_{R-p}\big((n-m)PT'\big)\,\alpha_m \tag{A.308}$$

$$\tilde{x}_{p,nP} = \sum_{m=0}^{\infty} x_{p,nP-mP}\,\alpha_m \tag{A.309}$$

$$\tilde{n}_{p,nP} = \sum_{m=0}^{\infty} n_{p,nP-mP}\,\alpha_m \tag{A.310}$$

Using (A.305) and (A.306) in (A.304) and (A.276), and ignoring self noise

$$|S_k|^2 = Re^2\Big\{ \sum_{p=0}^{R} e_p\, \tilde{b}^*_{R-p}(nPT')\, b_{R-p}(kT') \Big\} \quad ; \tag{A.311}$$

$$k = nP+1, nP+2, \ldots, nP+P-1$$

$$n = \text{an integer}$$

$$\overline{|N_k|^2} = \frac{I^2}{2(N')^2}(\sum \alpha_m^2)N_T + \frac{I}{2N'}\sum_{p=0}^{R} e_p|\tilde{b}_{R-p}(nPT')|^2$$

$$+ \frac{I}{2N'}(\sum \alpha_m^2)\sum_{p=0}^{R} e_p|b_{R-p}(kT')|^2 \quad ; \tag{A.312}$$

$$k = nP+1, nP+2, \ldots, nP+P-1$$
$$n = \text{an integer}$$

where N' is given in (A.302). Thus the combiner output SNR can be represented as

$$\rho_k = \frac{\beta_{kN}\,\rho'_{ok}}{(\sum \alpha_m^2)\,(\frac{2N_T}{\rho'_{ok}}+1) + \chi_{kn}} \quad ; \tag{A.313}$$

$$k = nP+1, nP+2, \ldots, nP+P-1$$
$$n = \text{an integer}$$

where

$$\beta_{kN} = \frac{Re^2\Big\{\sum_{p=0}^{R} e_p\,\tilde{b}^*_{R-p}(nPT')\,b_{R-p}(kT')\Big\}}{\Big[\sum_{p=0}^{R} e_p\,|b_{R-p}(kT')|^2\Big]^2} \quad ; \tag{A.314}$$

$$k = nP+1, nP+2, \ldots, nP+P-1$$
$$n = \text{an integer}$$

$$\chi_{kN} = \frac{\sum_{p=0}^{R} e_p \, |\tilde{b}_{R-p}(nPT')|^2}{\sum_{p=0}^{R} e_p \, |b_{R-p}(kT')|^2} \quad ; \tag{A.315}$$

$$k = nP + 1, nP + 2, \ldots, nP + P - 1$$
$$n = \text{an integer}$$

where (using (A.302))

$$\rho'_{ok} = \frac{2N}{I} \sum_{p=0}^{k} e_p \, |b_{R-p}(kT')|^2 = \frac{P-1}{P} (\rho_{ok})_{T'} \tag{A.316}$$

is the combiner output SNR for ideal noise-free tap weights for the serial-probe modem and $(\rho_{ok})_{T'}$ is the combiner output SNR for the decision directed system under the same ideal conditions in the vicinity of the time kT'.

If we include the probe and data power in computing E_b/N_o at a given time instant, then this value is unchanged for all the systems analyzed (assuming the same transmitter power). Thus,

$$\left(\frac{E_b}{N_o}\right)'_k = \frac{2N}{I} \sum_{p=o}^{M} |b_{R-p}(kT')|^2 \tag{A.317}$$

is the value of E_b/N_o for the serial-probe system in the vicinity of the time $t = kT'$. Thus from (A.285) and (A.316), we see that we can set

$$\rho'_{ok} = \left(\frac{P-1}{P}\right) \left(\frac{E_b}{N_o}\right)'_k \left(\frac{\sum_{p=0}^{R} e_p \, |b_{R-p}(kT')|^2}{\sum_{p=0}^{M} |b_{R-p}(kT')|^2} \right) \tag{A.318}$$

The value of delay to use in delay compensation requires some additional consideration in the case of the serial-probe modem, because the group delay of the tap weight process is periodically time-variable due to the weight *freeze*. Thus, it is probably

best to use a compensating delay equal to the average delay of the tap weight process. This is given by the group delay of the digital filter per sé, plus half the time that the weight is frozen with the result rounded off to the nearest symbol. For computation of error rates, upper and lower bounds can be selected by choosing the particular set of data symbols for which the delay compensation is worst and best, respectively. The same bounding approach can be used when delay compensation is not used. This would entail evaluation of β_{kn} and χ_{kn} at the two sets of k values $\{k = nP + P - 1\}$ and $\{k = nP + 1\}$.

To summarize, then, without delay compensation, the upper and lower bounds on error rate may be obtained by evaluating the expressions for β_{kn} and χ_{kn} in (A.314) and (A.315), respectively, at the two values $\{k = nP + P - 1\}$ and $\{k = nP + 1\}$, respectively. With delay compensation, β_{kn} and χ_{kn} would be chosen as

$$\beta_{kn} = \frac{Re^2\Big\{\sum_{p=0}^{R} e_p\, \hat{b}^*_{R-p}(nPT')\, b_{R-p}(kT' - GT')\Big\}}{\Big[\sum_{p=0}^{R} e_p\, |b_{R-p}(kT' - GT')|^2\Big]^2} \tag{A.319}$$

$$\chi_{kN} = \frac{\sum_{p=0}^{R} e_p\, |\hat{b}_{R-p}(nPT')|^2}{\sum_{p=0}^{R} e_p\, |b_{R-p}(kT' - GT')|^2} \tag{A.320}$$

where G is the integer closest to the sum of the group delay of the tap gain filter in units of symbol duration, τ_G/T', plus $(P-1)/2$. Upper and lower bounds on error rate can be obtained by appropriate selection of k values. This will most likely be either $k = nP + 1$ or $nP + P - 1$ for the upper bound, and k somewhere halfway between these values for the lower bound.

Consider now the non-disturbed wide band HF channel with Q Doppler shifted but very slowly varying, non-overlapping nodes (see (A.66)-(A.77) for background). In this case

$$\sum_{p=0}^{R} e_p\, \tilde{b}^*_{R-p}(nPT')\, b_{R-p}(kT') = \sum_{q=1}^{Q} \hat{G}^*(\nu_q)\, e^{j2\pi\nu_q(kT' - nPT')}\, E_q \quad ; \tag{A.321}$$

$$k = nP + 1, \ldots, nP + P - 1$$

$$n = \text{an integer}$$

$$\sum_{p=0}^{R} e_p \, |b_{R-p}(kT)|^2 = \sum_{q=1}^{Q} E_q \tag{A.322}$$

$$\sum_{p=0}^{R} e_p \, |\tilde{b}^*_{R-p}(nPT')|^2 = \sum_{q=1}^{Q} |\tilde{G}(\nu_q)|^2 \, E_q \tag{A.323}$$

where E_n is given by (A.295) and $\tilde{G}(\nu)$ is the transfer function of the tap gain filter. Thus, (A.314) and (A.315) simplify to

$$\beta_{kn} = \frac{\left[\sum_{q=1}^{Q} E_q Re^2\left\{\tilde{G}^*(\nu_q)\, e^{j2\pi\nu_q(kT'-nPT')}\right\}\right]^2}{\left[\sum_{q=1}^{Q} E_q\right]^2} \quad ; \tag{A.324}$$

$$k = nP+1, \ldots, nP+P-1$$
$$n = \text{an integer}$$

$$\chi_{kN} = \frac{\sum_{q=1}^{Q} |\tilde{G}(\nu_q)|^2 \, E_q}{\sum_{q=1}^{Q} E_q} \quad ; \tag{A.325}$$

$$k = nP+1, \ldots, nP+P-1$$
$$n = \text{an integer}$$

With delay compensation χ_{kN}, (A.320), stays the same as (A.325), but β_{kN}, (A.319), becomes modified to

$$\beta_{kn} = \frac{\sum_{q=1}^{Q} E_q Re\left\{\tilde{G}^*(\nu_k)\, e^{j2\pi\nu_q(kT'-GT'-nPT')}\right\}}{\left[\sum_{q=1}^{Q} E_q\right]^2} \quad ; \tag{A.326}$$

$$k = nP+1, \ldots, nP+P-1$$
$$n = \text{an integer}$$

The previous comments about upper- and lower-bounding error rates apply to (A.324) and (A.325).

For a single mode without delay compensation

$$\beta_{kn} = Re^2\left\{\tilde{G}^*(\nu)\, e^{j2\pi\nu(kT'-nPT')}\right\} \quad ; \tag{A.327}$$

$$k = nP+1, nP+2, \ldots, nP+P-1$$
$$n = \text{an integer}$$

$$\chi_{kN} = |G(\nu)|^2 \tag{A.328}$$

and with delay compensation

$$\beta_{kn} = Re^2\left\{\tilde{G}^*(\nu)\, e^{j2\pi\nu(kT'-GT-nPT')}\right\} \quad ; \tag{A.329}$$

$$k = nP+1, nP+2, \ldots, nP+P-1$$
$$n = \text{an integer}$$

and χ_{kn} is the same as (A.328).

The expression for $\tilde{G}(f)$ in the case of a boxcar filter is given by (c.f. (A.87))

$$G(\nu) = e^{-j\pi\nu(N_F-1)PT'} \frac{\sin \pi\nu N_F PT'}{N_F' \sin \pi\nu PT'} \tag{A.330}$$

where N_F' is the memory of the boxcar filter. This must be distinguished from the impulse response duration of the tap weight filter $N_F'PT'$. Without delay compensation, the lowest combiner output SNR (which also upper-bounds the error rate) is given by

(A.327), with $k = nP + P - 1$. If, in addition, we assume that the Rake window includes all the multipath energy ($R = M, e_p = 1$), (see (A.319)), then

$$\rho'_{ok} = \left(\frac{P-1}{P}\right)\left(\frac{E_b}{N_o}\right)'_k \tag{A.331}$$

and the combiner output SNR becomes

$$\rho = \frac{\left(\frac{P-1}{P}\right)\frac{E_b}{N_o}\cos^2\pi\nu T'(PN'_F + P - 2)\left(\frac{\sin\pi\nu N'_F PT'}{N'_F\sin\pi\nu PT'}\right)^2}{\frac{1}{N'_F}\left(\frac{2N_T}{\left(\frac{P-1}{P}\right)\frac{E_b}{N_o}} + 1\right) + \left(\frac{\sin\pi\nu N'_F PT'}{N'_F\sin\pi\nu PT'}\right)^2} \tag{A.332}$$

where we have removed subscripts to simplify notation. With delay compensation, the $\cos^2\pi\nu T'(PN'_F + P - 2)$ term becomes changed to $\cos^2\pi\nu T'\big((N'_F - 1)P + 2(k - nP) - 2G\big)$. If we select G to minimize the phase error and then select $k - nP = 1, 2, \ldots P - 1$ to make the resulting error as large as possible, we find that the term becomes approximately $\cos^2\pi\nu T'P$ where we have taken some liberties in rounding off which are unimportant so long as $\nu T' << 1$, as we assume.

In comparing the combiner output SNR expression for the single mode serial-probe case, (A.332), to the single mode parallel-probe case, (A.301), we find that by selecting

$$N_F = N'_F(P - 1) \tag{A.333}$$

$$\gamma = \frac{1}{P - 1} \tag{A.334}$$

the two expressions become essentially identical, assuming $\nu T << 1$. The same conclusion results for the case of delay compensation

A.5.3 The DPSK Rake Modem

The DPSK Rake modem receiver processing is shown in figure A.6. For this version of the Rake, the tap weights are simply the previous I&D outputs. No decision-directed data cancellation is necessary because the coded binary data at the transmitter is impressed as a binary phase change ($0°, 180°$) on the carrier. The analysis of this modem may be seen to be identical to a decision-directed Rake modem in which there are no decision errors and there is no tap gain filtering.

Thus, neglecting self noise, the SNR at the combiner output is given by (A.286), where now instead of (A.287) and (A.288) the terms $\tilde{\beta}_k, \tilde{\chi}_k$ are given by

$$\tilde{\beta}_k = \frac{Re^2\Big\{\sum_{p=0}^{R} e_p\, b^*_{R-p}(kT-T)\, b_{R-p}(kT)\Big\}}{\sum_{p=0}^{R} e_p\, |b_{R-p}(kT)|^2} \tag{A.335}$$

$$\tilde{\chi}_k = 1 \tag{A.336}$$

and

$$\sum \alpha_m^2 = 1 \tag{A.337}$$

For slow fading and Doppler shifts small compared to $1/T$, $\tilde{\beta}_k$ will be essentially unity. Then

$$\rho_k = \frac{\rho_{ok}}{2\left(\frac{N_T}{\rho_{ok}} + 1\right)} \tag{A.338}$$

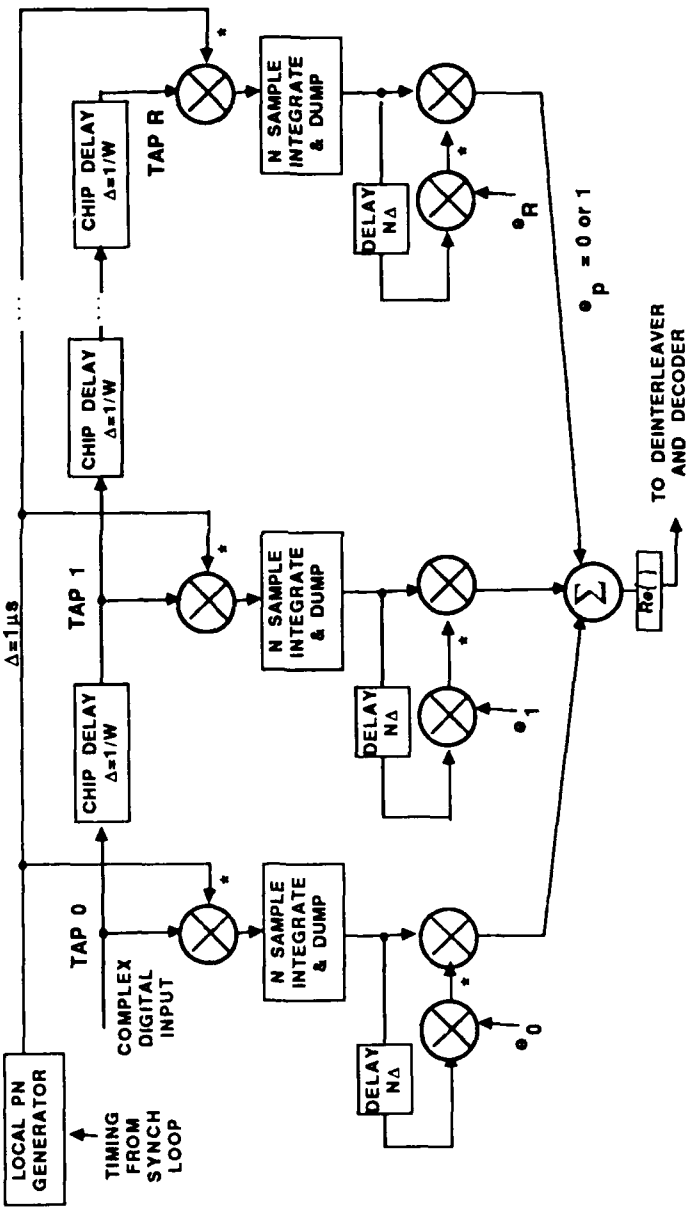

Figure A.6. A DPSK Rake Processor

LIST OF REFERENCES

A.1. P. A. Bello, "Characterization of Randomly Time-Variant Linear Channels," *IEEE Trans. on Comm. Systems* **CS-11** (December 1963).

A.2. R. Price, "Wideband Analog Communication Through Multipath by Means of a Pseudo-Noise Carrier," *Presented at the Spring Meeting, URSI, Washington, DC* (30 April - 3 May 1962).

A.3. G. H. Hardy, J. F. Littlewood, and G. Polya, *Inequalities*, Cambridge, 1957.

MISSION
of
Rome Air Development Center

RADC plans and executes research, development, test and selected acquisition programs in support of Command, Control, Communications and Intelligence (C^3I) activities. Technical and engineering support within areas of competence is provided to ESD Program Offices (POs) and other ESD elements to perform effective acquisition of C^3I systems. The areas of technical competence include communications, command and control, battle management information processing, surveillance sensors, intelligence data collection and handling, solid state sciences, electromagnetics, and propagation, and electronic reliability/maintainability and compatibility.

SUPPLEMENTARY

INFORMATION

AD-A211589

PERFORMANCE OF FOUR RAKE MODEMS OVER THE NON-DISTURBED WIDE BAND HF CHANNEL

Phillip A. Bello

RADC-TR-89-91 Interim Report
June 1989

ERRATA

Change Equation (4-2) to read as follows:

$$w = \frac{|R_o|^2}{\sum_s |R_s|^2} \tag{4-2}$$

Eliminate the reference to Equation (A.41) above Equation (A.54), as follows:

The input SNR in the bandwidth W is

$$\rho_{ik} = \frac{\frac{1}{2}\overline{|c_k|^2}}{\frac{1}{2}\overline{|n_k|^2}} \tag{A.54}$$

Change Equation (A.286) to read as follows:

$$(\rho_k)_{dec.dir.} = \frac{\tilde{\beta}_k \rho_{ok}}{(\sum \alpha_m^2)\left(\frac{2N_T}{\rho_{ok}} + 1\right) + \tilde{\chi}_k} \tag{A.286}$$

A replacement for page 8 (Figure 2) is attached.

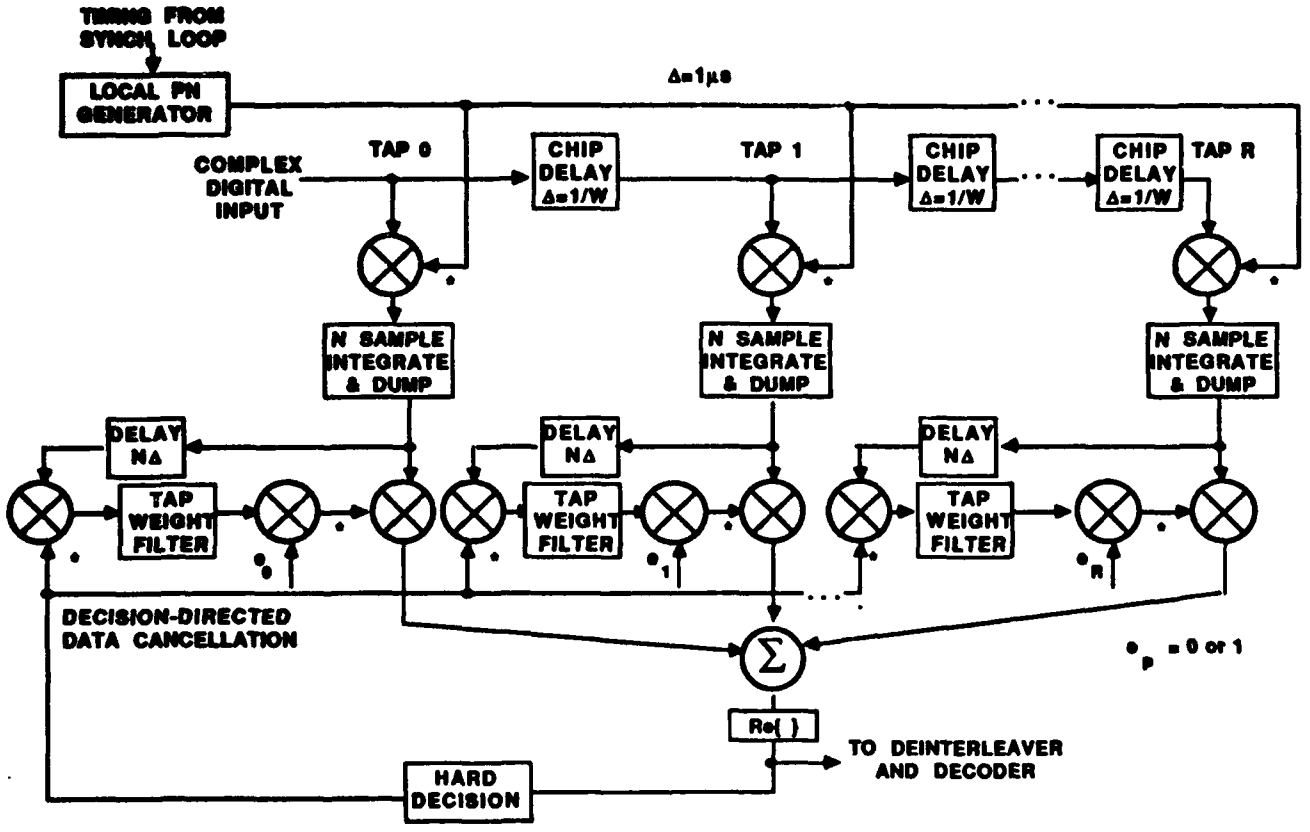

Figure 2 A Decision-Directed Coherent Rake Processor. No Delay Compensation.